SYNTHESIS OF 10, 11, 12, 12a, 12b, 13-HEXAHYDRO-5*H*-

BENZO[*f*]CYCLOPROPA[*d*]PYRIDO[1,2-*b*]

ISOQUINOLINE-5,7(9*H*)DIONE AND

RELATED COMPOUNDS

Except when reference is made to the work of others, the work described in this dissertation is my own or was done in collaboration with my advisory committee. This dissertation does not include proprietary or classified information.

_____

Joseph M. Tinkleman

Certificate of Approval:

_____	_____
C. Randall Clark Professor Pharmacal Sciences	Forrest T. Smith, Chair Associate Professor Pharmacal Sciences
_____	_____
Jack DeRuiter Professor Pharmacal Sciences	George T. Flowers Dean Graduate School

SYNTHESIS OF 10, 11, 12, 12a, 12b, 13-HEXAHYDRO-5*H*-BENZO[*f*]CYCLOPROPA[*d*]PYRIDO[1,2-*b*] ISOQUINOLINE-5,7(9*H*)DIONE AND RELATED COMPOUNDS

Joseph M. Tinkleman

A Dissertation

Submitted to

the Graduate Faculty of

Auburn University

in Partial Fulfillment of the

Requirements for the

Degree of

Doctor of Philosophy

Auburn, Alabama
May 9, 2009

SYNTHESIS OF 10, 11, 12, 12a, 12b, 13-HEXAHYDRO-5*H*-

BENZO[*f*]CYCLOPROPA[*d*]PYRIDO[1,2-*b*]

ISOQUINOLINE-5,7(9*H*)DIONE AND

RELATED COMPOUNDS

Joseph M. Tinkleman

_____
Signature of Author

_____
Date of Graduation

SYNTHESIS OF 10, 11, 12, 12a, 12b, 13-HEXAHYDRO-5*H*-

BENZO[*f*]CYCLOPROPA[*d*]PYRIDO[1,2-*b*]

ISOQUINOLINE-5,7(9*H*)DIONE AND

RELATED COMPOUNDS

Joseph M. Tinkleman

Doctor of Philosophy, May 9, 2009
(B.S., Auburn University, August 2000)

151 Typed Pages

Directed by Forrest T. Smith

Agents designed to bind with high DNA sequence selectivity offer great therapeutic opportunities in the treatment of cancer and other genetic disorders. The need for sequence selective agents arises from the fact that the administration of chemotherapeutic agents typically lead to many adverse effects due to their lack of cellular specificity. The natural products (+)-CC-1065 (**1**), Duocarmycin A (**2**), and Duocarmycin SA (**3**) have been shown to selectively alkylate AT-rich regions within the minor groove; whereas, Anthramycin (**20**) has been shown to selectively alkylate GC-rich areas. Therapeutic interest in these drugs led to the incorporation of several key structural

features into compound **28**, which was subsequently modified during the course of this dissertation. The initial target compound was identified as 10, 11, 12, 12a, 12b, 13-hexahydro-5*H*-benzo[*f*]cyclopropa[*d*]pyrido[1,2-*b*]isoquinoline-5,7(9*H*)-dione (**27**). The imine **40** was condensed with the anhydride **38** to afford the diastereomeric mixture of acids **41**, which were subsequently reduced and separated to give the pure alcohols **42**. The individual alcohols were then activated through methane sulfonate formation followed by debenzylation and cyclization to give the title compound in 50% overall yield.

The proceeding target compounds were identified as 9, 10, 11, 11a, 11b, 12-hexahydrobenzo[*f*]cyclopropa[*d*]pyrrolo[1,2-*b*]isoquinoline-5,7-dione (**28**) and 2-methyl-1, 2, 10, 10a-tetrahydrobenzo[*f*]cyclopropa[*d*]isoquinoline-3,5-dione (**98**). Analysis of both compounds revealed that the key intermediate, which could be used in both syntheses was identified as 4-bromo-1-benzyloxy-2-naphthoic acid (**92**). The bromo acid **92** was condensed with either 2-propenyl pyrrolidine (**87**) or *N*-methyl-*N*-butene (**101**) and the rest of the synthetic routes were carried out under similar conditions to afford the desired final compounds.

ACKNOWLEDGMENTS

There are many people who helped during the course of this investigation. First, I would like to thank Dr. Chandrakala Pidathala for her guidance and friendship as she mentored me during my early graduate career. Much of my lab-based knowledge was based on her excellent instruction. Next, I would like to thank my research advisor Dr. Forrest Smith for his guidance and support with his extensive knowledge. Special thanks are also extended to Dr. Randall Clark and Dr. Jack DeRuiter for their involvement in the dissertation process. Also, I would like to thank my fellow graduate students for their friendship, advice, and encouragement during the course of this dissertation. Lastly, I would like to thank my family for their love and support.

Style manual used

Journal of Medicinal Chemistry

Computer software used

Microsoft Word 2008

CS ChemDraw Std. 11.0

TABLE OF CONTENTS

LIST OF SCHEMES

LIST OF FIGURES

LIST OF TABLES

INTRODUCTION

The Center for Disease Control (CDC) currently lists cancer as the second leading cause of death in the United States.[1] Tumors are abnormal growths of cells, which may be classified as either benign or malignant. A malignant tumor, or neoplasm, is defined as an abnormal growth of cells with the capability of undergoing metastasis. There are six major types of neoplasms: carcinomas, sarcomas, leukemias, lymphomas, myelomas, and central nervous system cancers.

Figure 1 shows the typical cellular life cycle that every cell in the body must undergo in order to proliferate. The molecular events that control the cell cycle are ordered and directional; that is, each process occurs in a sequential fashion and it is impossible to "reverse" the cycle. The G_1, or Gap 1 phase, is the period between the formation of the daughter cell and the period of DNA synthesis. This is also the time when the cell may enter a quiescent period (G_0 phase) or to continue to grow and differentiate. Whether or not a cell undergoes differentiation is therefore determined during this phase. The S phase, or synthesis phase, is the time when the nuclear DNA is replicated. The G_2, or Gap 2 phase, is the period when the final preparations are performed prior to mitosis. The M phase, or mitotic phase, is the period when cellular division occurs. The G_0, or Gap 0 phase, also known as quiescence, is the period when a cell will either be destroyed if there are already enough cells present or the cell will enter

a period of hibernation. During hibernation the normal cellular activities are maintained. Cell cycle checkpoints are used by the cell to monitor and regulate the progress of the cell cycle.[2] Checkpoints prevent cell cycle progression at specific points, allowing verification of necessary phase processes and repair of DNA damage.

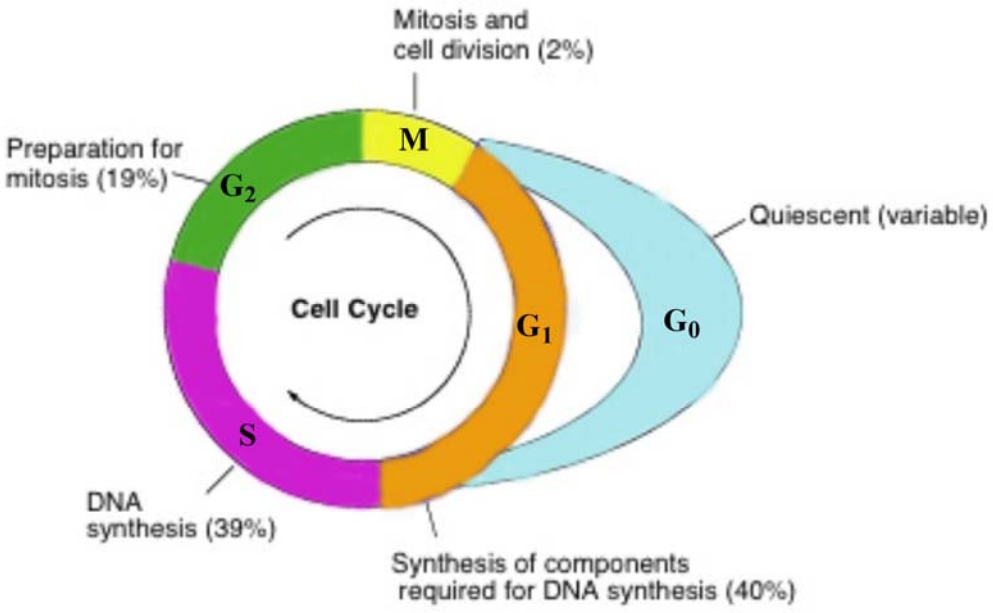

Figure 1: Cellular Life Cycle

Several checkpoints ensure that damaged or incomplete DNA is not passed on to the daughter cells. Two main checkpoints exist: the G_1/S checkpoint and the G_2/M checkpoint. G_1/S transition is a rate-limiting step in the cell cycle and is also known as a restriction point.[3] The protein p53 plays an important role in triggering the control mechanisms at both the G_1/S and G_2/M checkpoints. A disregulation of the cell cycle components may lead to tumor formation. Although the duration of the cell cycle in tumor cells is equal to or longer than that of a normal cell cycle, the proportion of cells that are in active cell division (versus quiescent cells in the G_0 phase) is much higher in

tumor cells compared to that in normal cells. Thus there is a net increase in cell numbers as the number of cells that die by apoptosis or senescence remains the same.[3]

Regulation of the cell cycle involves steps crucial to the cell, including detecting and repairing genetic damage, and provision of various checks to prevent uncontrolled cell division. Two key classes of regulatory molecules, cyclins and cyclin-dependent kinases (CDKs), determine a cell's progress through the cell cycle. Cyclins form the regulatory subunits and CDKs the catalytic subunits of an activated heterodimer; cyclins have no catalytic activity and CDKs are inactive in the absence of a partner cyclin.[3]

When activated by a bound cyclin, CDKs perform a common biochemical reaction called phosphorylation that activates or inactivates target proteins to orchestrate coordinated entry into the next phase of the cell cycle. Different cyclin-CDK combinations determine the downstream proteins targeted. CDKs are constitutively expressed in cells whereas cyclins are synthesized at specific stages of the cell cycle, in response to various molecular signals.[4]

Apoptosis, or programmed cell death, can occur when a cell is damaged beyond repair, infected with a virus, or undergoing stress conditions such as starvation. DNA damage from ionizing radiation or toxic chemicals can also induce apoptosis via the actions of the tumor-suppressing gene p53. The "decision" for apoptosis can come from the cell itself, from the surrounding tissue, or from a cell that is part of the immune system. In these cases apoptosis functions to remove the damaged cell, preventing it from sapping further nutrients from the organism, or to prevent the spread of viral infections.[4]

Apoptosis also plays a role in preventing cancer; if a cell is unable to undergo apoptosis, due to mutation or biochemical inhibition, it can continue dividing and develop

into a tumor. For example, infection by papillomaviruses causes a viral gene to interfere with the cell's p53 protein, an important member of the apoptotic pathway. This interference in the apoptotic capability of the cell plays a critical role in the development of cervical cancer.[3]

The process of apoptosis is controlled by a diverse range of cell signals, which may originate either extracellularly (extrinsic inducers) or intracellularly (intrinsic inducers). Extracellular signals may include: toxins, hormones, growth factors, nitric oxide[5] or cytokines, and therefore must either cross the plasma membrane or transduce to effect a response. These signals may positively or negatively induce apoptosis; in this context the binding and subsequent initiation of apoptosis by a molecule is termed positive, whereas the active repression of apoptosis by a molecule is termed negative.

Intracellular apoptotic signaling is initiated by a cell in response to stress, and may ultimately result in cell suicide. The binding of nuclear receptors by glucocorticoids, heat, radiation, nutrient deprivation, viral infection, hypoxia[3] and increased intracellular calcium concentrations[6] (e.g. by membrane damage) are all factors that can lead to the release of intracellular apoptotic signals by a damaged cell. A number of cellular components, such as poly ADP ribose polymerase, may also help regulate apoptosis.[7]

Before the actual process of cell death is carried out by enzymes, apoptotic signals must be connected to the actual death pathway by way of regulatory proteins. This step allows apoptotic signals to either culminate in cell death, or be aborted should the cell no longer need to die. Several proteins are involved, however two main methods of achieving regulation have been identified; targeting mitochondria functionality, or

directly transducing the signal via adapter proteins to the apoptotic mechanisms. The whole preparation process requires energy and functioning cell machinery.[3]

The tumor-suppressor protein p53 accumulates when DNA is damaged due to a chain of biochemical reactions. Part of this pathway includes alpha-interferon and beta-interferon, which induce transcription of the p53 gene and result in the increase of p53 protein levels and enhancement of cancer cell-apoptosis.[8] The protein p53 prevents the cell from replicating by stopping the cell cycle at G_1, or interphase, to give the cell time to repair itself, however it will induce apoptosis if damage is extensive and repair efforts fail. Any disruption to the regulation of the p53 or interferon genes will result in impaired apoptosis and the possible formation of tumors.[3]

Metastasis sometimes abbreviated mets, is the spread of a disease from one organ or part to another non-adjacent organ or part. Only malignant tumor cells and infections have the capacity to metastasize.[3] Cancer cells can "break away," "leak," or "spill" from a primary tumor, enter lymphatic and blood vessels, circulate through the bloodstream, and settle down to grow within normal tissues elsewhere in the body. Metastasis is one of three hallmarks of malignancy in contrast to benign tumors.[3] Most tumors and other neoplasms can metastasize, although in varying degrees (e.g., gliomas and basal cell carcinomas rarely metastasize).[3]

When tumor cells metastasize, the new tumor is called a secondary or metastatic tumor, and its cells are like those in the original tumor. This means, for example, that, if breast cancer metastasizes to the lung, the secondary tumor is made up of abnormal breast cells, not of abnormal lung cells. The tumor in the lung is then called metastatic breast cancer, not lung cancer.[4]

Metastasis is a complex series of steps in which cancer cells leave the original tumor site and migrate to other parts of the body via the bloodstream or the lymphatic system (via a process called intravasation). To do so, malignant cells break away from the primary tumor and attach to and degrade proteins that make up the surrounding extracellular matrix (ECM), which separates the tumor from adjoining tissue. By degrading these proteins, cancer cells are able to breach the ECM and escape. When oral cancers metastasize, they commonly travel through the lymph system to the lymph nodes in the neck. The body resists metastasis by a variety of mechanisms through the actions of a class of proteins known as metastasis suppressors, of which about a dozen are known.[9] Some common sites of origin for metastasis include: lung, breast, skin (e.g. melanoma), colon, kidney, prostate, and the pancreas.

Risk Factors

While cancer may affect people at any age, the elderly show a higher incidence of cancer because their regulatory processes do not function as well as younger people and the increased number of cell divisions leads to an increased chance that something abnormal may occur. Other risk factors include: tobacco, sunlight, exposure to radiation, exposure to certain chemicals, certain hormones, family history, alcohol, poor overall health (e.g. overweight, poor diet, lack of exercise), and certain viruses (e.g. HPV and HIV).[10]

Treatments

Surgery, radiation therapy, and chemotherapy are the main types of treatment. The goal of surgery is to remove as much of the tumor as possible. Surgical intervention can be used to lessen the symptoms associated with the tumor. Surgery can only be

performed during the initial stages of tumor growth and only when it is clear that part of or the entire tumor can be safely excised. Radiation therapy can also be used to treat the symptoms by shrinking or killing the tumor cell. Chemotherapy involves using drugs in order to stop or slow the growth of the cancer cells. Chemotherapeutic agents do not display high levels of selectivity towards tumor cells, and the death of healthy cells can lead to adverse effects such as myelosuppression, GI effects, and the loss of hair. While it is not unusual for a patient to undergo a single treatment regimen, almost 50% of cancer patients will undergo some combination of treatments. Other treatments include: the use of angiogenesis inhibitors, biological therapy, bone marrow transplantation, hyperthermia, gene therapy, LASER radiation, and photodynamics.[10]

DNA as a Target for Chemotherapy

Deoxyribonucleic acid (DNA) is among the most well-known and well-characterized targets for drug design. DNA is composed of four basic nucleotides, which are composed of purines and pyrimidines. The purines: adenosine (A) and guanosine (G), and the pyrimidines: cytidine (C) and thymidine (T) are the monomeric building blocks of DNA (Figure 2). The informational content of DNA resides in the sequence in which these monomers are ordered.[11] The nitrogenous bases are linked by a 3′,5′-phosphodiester bond that orients them in a linear fashion. At each terminus exists either a 5′-hydroxyl or phosphate group or a 3′-hydroxyl or phosphate functionality imparting a polarity within the molecule. A complementary strand runs in an antiparallel sequence such that one strand extends from the 5′-3′ direction and its complement runs in the 3′-5′ direction.

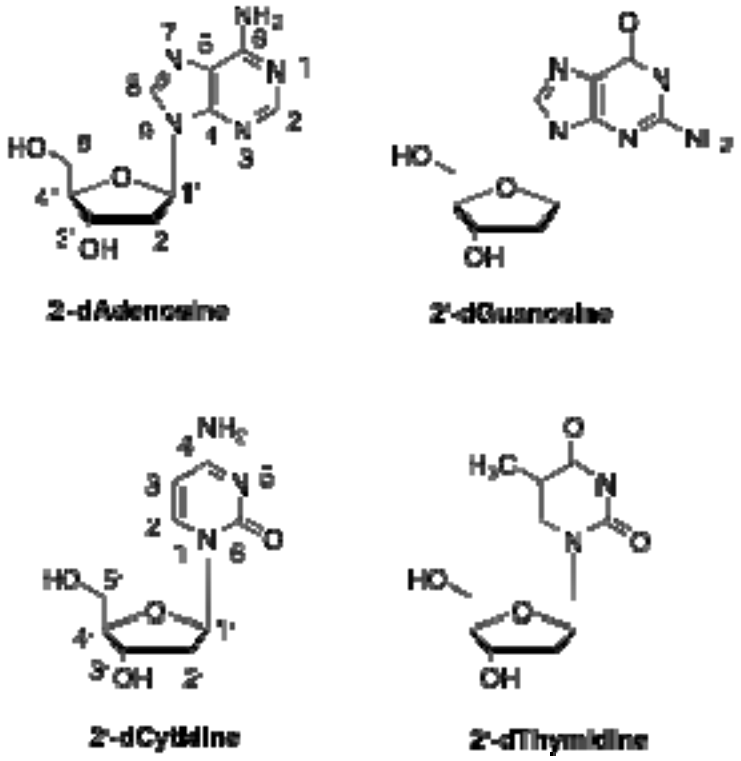

Figure 2: Monomeric Units of DNA

These two strands are held together by hydrogen bonding interactions between the purine and pyrimidine bases. The fixed anti configuration of the glycosidic linkages as well as the restricted rotation of the phosphodiester backbone allows for A to pair only with T and G to pair only with C.[11]

DNA has been shown to adopt several different conformations based on the ordering of the nucleotides and various environmental conditions. The DNA helix can assume both a right-handed twist (A and B type DNA) and a left-handed twist (Z-DNA). The difference between the A and B forms lies in the mode of sugar puckering: C3′-endo for the A type and C2′-endo for the B type. The geometrical variations of the double helices can be attributed to these various sugar-puckering modes and are expressed in the relative disposition of the base pairs as well as the size of the major and minor grooves.[11]

Under normal physiological conditions the B form is the most commonly seen. There exist 10 base pairs within a single twist of the helix, which resembles a winding staircase. Within each twist there exists both a major and a minor groove, which runs parallel to the phosphodiester backbones. Given the relative disparities in the sizes of the grooves, proteins prefer to interact within the major groove leaving the minor groove more susceptible to potential drug interactions.[12]

The Z-form of DNA forms a left-handed double helix in which the phosphodiester backbone zigzags along the molecule. Z-DNA is the least twisted helix with 12 base pairs occupying a single twist. Z-DNA can only exist under certain specific conditions such as: alternation of purine and pyrimidines bases, the presence of a high concentration of salt or specific cations like spermine, a high degree of negative supercoiling of the DNA, binding of Z-DNA specific proteins, and the methylation of C-5 of several of the deoxycytidine nucleotides. The use of chiral metal complexes can be used to differentiate Z-DNA from the A and B types.[13]

Alkylating Agents

Alkylating agents are one class of compounds used in the treatment of cancer. They generally bind in an irreversible manner to the DNA helix through the formation of a covalent bond. While many drugs such as (+)-CC-1065 (**1**), Duocarmycin A (**2**), and Duocarmycin SA (**3**) display the ability to bind to specific sequences within AT-rich regions there are only a handful of agents such as Anthramycin (**20**) which are known to selectively bind to GC-rich regions. Guanine projects its 2-amino functionality into the minor groove making this region generally less accessible for a potential alkylator. The

AT regions are much more accommodating for deep groove penetration since there is no amine functionality that projects off these bases and up into the grooves.

Cancer chemotherapeutic agents typically lack cellular specificity and as such both cancerous as well as healthy cells are killed upon administration of these drugs. The death of healthy cells can in many instances lead to adverse effects. If future agents can be designed to specifically attack the tumor cells then many if not all of these adverse effects can be obviated and/or eliminated.

Molecular and cellular studies have shown that point mutations, deletions, translocations, and other types of rearrangements in DNA may affect either the expression or the biochemical function of specific genes, such as oncogenes or tumor-suppressing genes.[14] By designing a drug capable of recognizing a specific sequence in DNA, it may be possible to specifically inhibit the expression of certain oncogenes and thereby control the development of tumor cells.[14] There is particular interest in developing ligands with GC base pair selectivity because most of the known DNA minor groove binding agents are AT specific such as compounds **1**, **2**, and **3**. This interest also stems from the observation that regions of high GC content are commonly found in genomes of mammals, including humans, and that a functional role of GC-rich sequences is suggested by their frequent occurrence in genes associated with proliferation, including a number of oncogenes.[12]

AT Specific Drugs

Initial attempts at drug design have focused on the studies of known natural products, which display high anti-neoplastic activity. (+)-CC-1065 (**1**), Duocarmycin A (**2**), and Duocarmycin SA (**3**) are members of a highly potent class of antitumor

antibiotics, which have been isolated from *Streptomyces zelensis*.[15] (+)-CC-1065 (**1**) and Duocarmycin SA (**3**) have been shown thru *in vitro* studies to inhibit the growth of L1210 cells by 50% at 0.02 ng/mL and 0.006 ng/mL respectively. These agents share similar substituted pyrrolo indole functionalities, which are linked by amide bonds. The "A" subunit contains a reactive cyclopropyl ring, which contains the only chirality in the molecules. The absolute configuration is 3b-(*R*) and 4a-(*S*).[16] All three molecules preferentially alkylate an AT-rich region of DNA within the minor groove by a stereochemically controlled addition of the N3 of adenine to the least substituted carbon on the cyclopropyl ring system.[17]

X-ray crystal analysis of compound **1** bound to SV40 DNA and T7 DNA fragments elucidated two binding sites: 5'-PuNTTA and 5'-AAAAA (Pu, purine; N, any nucleotide base).[16] Cell progression studies showed that (+)-CC-1065 (**1**) did not affect progression from mitosis to G_1 or from G_1 to S phase. Cell progression from G_2 to M phase was blocked by compound 1.[18] Cells in the G_2 and M phases are the most sensitive to **1** with cells in the S phase being more resistant. DNA synthesis is inhibited by 50% by **1** at a concentration of 7 pmol/mL.

There are several key structural features that **1** possesses which are critical for its selectivity. The cyclopropyl ring possesses the alkylating functionality required to form the covalent bond with the DNA helix, along with the natural right-handed twist, which allows for the molecule to properly follow the curve of the minor groove. The distribution of the hydrophobic and hydrophilic moieties along the edges of the molecule allow for the appropriate contacts to occur between the drug molecule and the DNA minor groove.

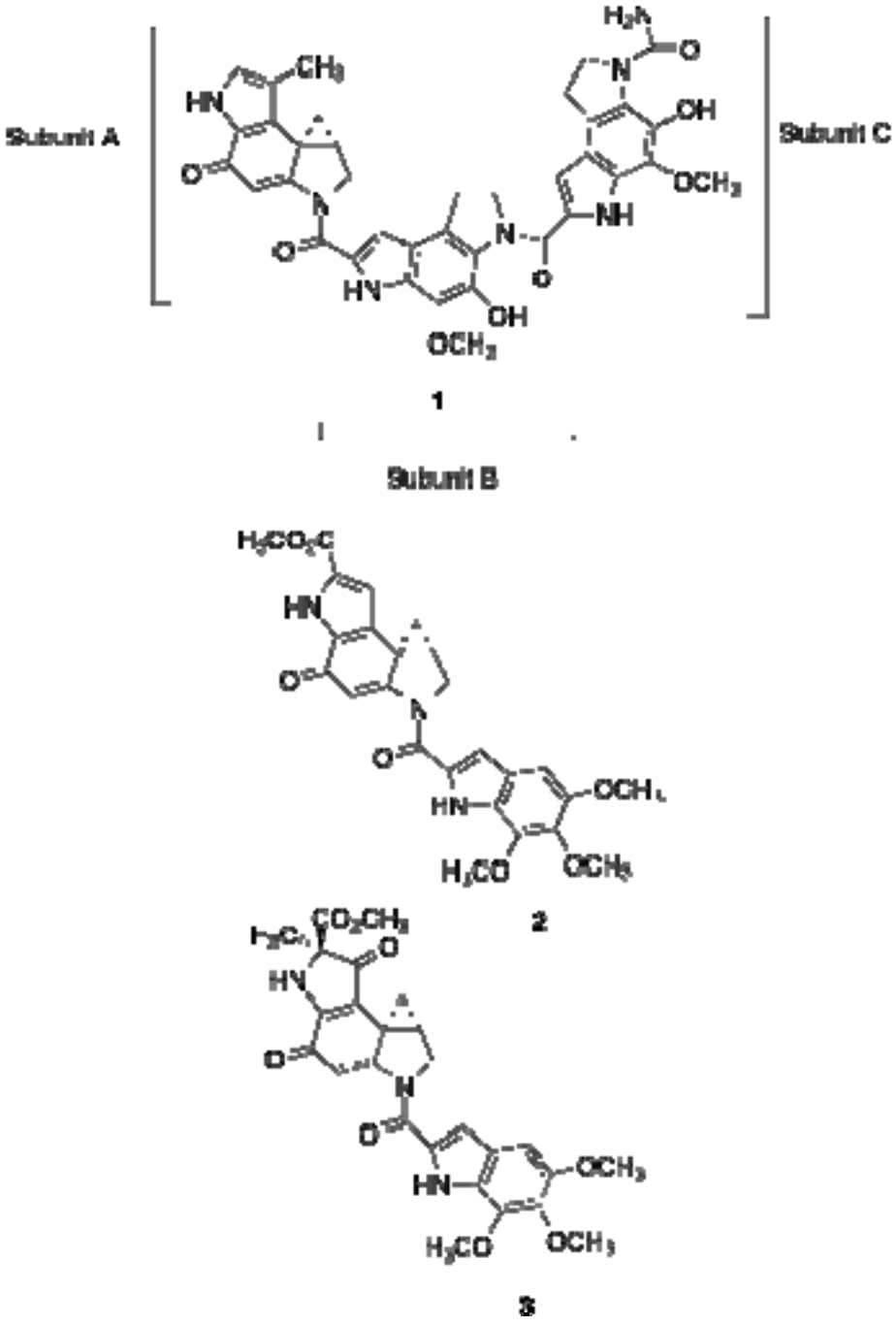

Figure 3: (+)-CC-1065 (**1**), Duocarmycin A (**2**),

and Duocarmycin SA (**3**)

Close van der Waals contacts between the drug molecule and the DNA minor groove imparts its selectivity for the AT-rich regions. (+)-CC-1065 (**1**) binding disrupts

the ability of DNA to function as a template for DNA synthesis. Also, **1** has been shown to bind only to double stranded DNA and not to RNA or proteins.[19]

X-ray studies have shown that (+)-CC-1065 (**1**) is characterized by a pronounced right-handed twist along the long axis of the drug molecule with its hydrophobic groups aligned along the inside edge while the hydrophilic groups are aligned on the outer edge. The binding site spans 5 base pairs for **1** and 4 base pairs for both of the duocarmycins **2** and **3**. Compound **1** cannot be used in humans due to its delayed toxicity resulting in death usually after 50 days of treatment as shown through animal testing models.[12] Compound **1** has been shown to stabilize the DNA helix upon its binding through melting transition studies.[20] Figure 4 shows the alkylation of compound **1** in which alkylation results in the formation of an ammonium ion, which can exist in several resonance forms.[21]

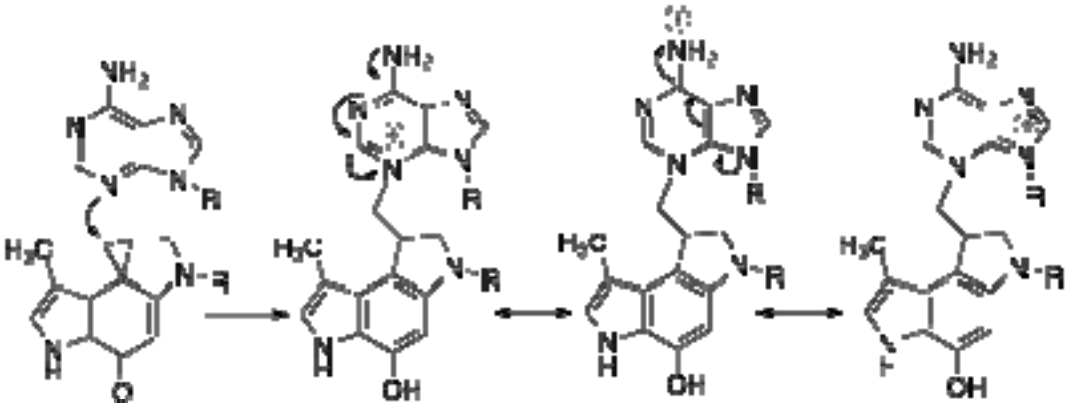

Figure 4: Alkylation of DNA by (+)-CC-1065 (**1**)

Boger *et al*. have designed a number of analogs based on the reactive "A" subunit found in the natural products **1**, **2**, and **3**.[21] The "A" subunit alone contains sufficient structural information to encode the primary molecular basis for sequence selectivity, and this subunit is essential for antitumor activity. The noncovalent binding interactions of

the “B” and “C” subunits can modulate or fine tune this sequence selectivity.[21] A key structural feature of the natural products is the alkylation subunit’s vinylogous amide and the corresponding N2 amide linkage that joins the alkylation and DNA binding subunits.[22]

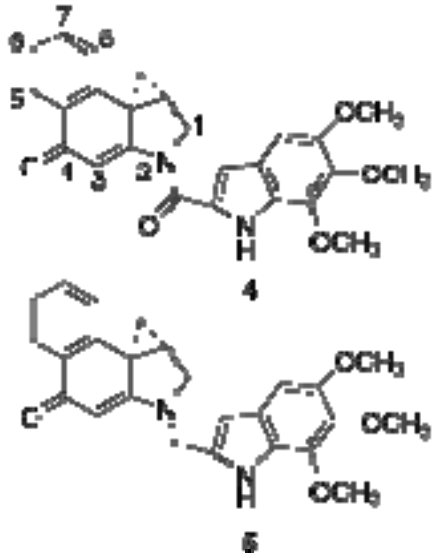

Figure 5: (+)-CBI-TMI (**4**) and its Analog **5**

Boger postulated that DNA alkylation catalysis is not derived from a long-postulated C-4 carbonyl protonation (acid catalysis) but rather from a DNA-binding induced conformational change in the agent that disrupts the cross-conjugated vinylogous amide stabilization, activating the agents for nucleophilic attack.[22] (+)-CBI-TMI (**4**) and its analog **5** were synthesized in order to determine the actual binding mechanism responsible for DNA alkylation of these agents (Figure 5). The removal of the linking amide carbonyl and its replacement with a methylene unit was expected to provide a substrate capable of full engagement of the vinylogous amide.[22] The key question was to address whether or not this would lead to increased stabilization, or by virtue of the increased basicity of the C-4 carbonyl, render the analog more susceptible to protonation

and acid-catalyzed solvolysis.[22] Compounds **4** and **5** were individually placed in three individual phosphate buffer solutions of varying pH concentrations in order to determine the solvolytic stability of each of the compounds.

The UV spectra for compounds **4** and **5** were measured over a defined time period in order to assess the rates of solvolysis. The acid-catalyzed half-life for **5** was found to be 80 hrs (pH 1), 824 hrs (pH 2), and 30,500 hrs (pH 3), with no measurable solvolysis detected above pH 3.[22]

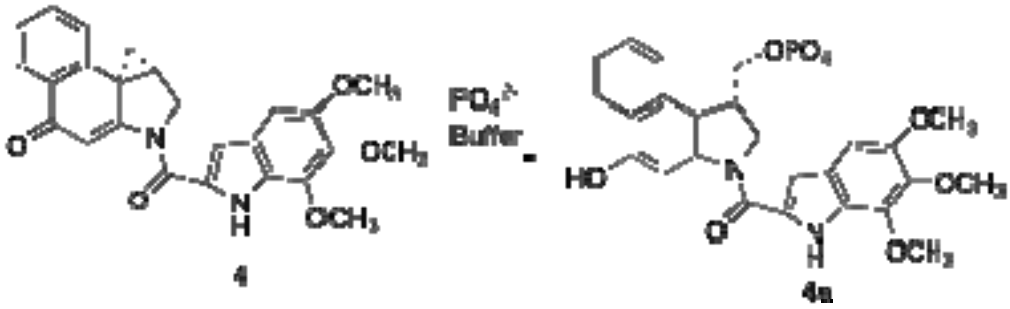

Scheme 1: Solvolysis Reaction of (+)-CBI-TMI (**4**)

Compound **4** demonstrated less solvolytic stability with half-lives reported at 12.5 hrs (pH 2) and 133 hrs (pH 3) with no data reported for pH 1. Scheme 1 shows the solvolysis reaction of compound **4**.

The removal of the linking amide did not substantially or adversely effect the noncovalent minor groove binding properties of the agent as was determined through competitive displacement studies of pre-bound ethidium bromide within an AT-rich sequence.[22] However, the removal of the linking amide did result in 10^4-10^5x reduction in cytotoxic potency. These results are consistent with the catalysis derived from a DNA binding-induced conformational change that disrupts the cross-conjugated vinylogous amide stabilization activating the agents for nucleophilic attack.

Figure 6: Substitution Analogs of (+)-*N*-Boc-CBI (**6**)

R'	K[a] [s^{-1}](pH 3)	$T_{1/2}$ [h][b]	IC_{50} (L1210)[c]
6a OMe	1.75 X 10^{-6}	110	100 nM
6 H	1.45 X 10^{-6}	133	80 nM
6b CN	9.04 X 10^{-7}	213	14 nM

Table 1: Kinetic Data for CBI Analogs **6**, **6a** and **6bzx**

a: Rate of Solvolysis per unit Time (seconds)
b: Half-Life of the Drug Molecule at pH 3
c: 50% Inhibition Concentration for Cell Line L1210

Boger *et al*. set out to determine the effects of installing a group at the C-7 position including both electron donators and electron withdrawers.[23] The cyano **6b** and the methoxy **6a** groups were successfully installed and tested along with CBI **6** in order to assess the effects. There exists a direct correlation between solvolytic stability and cytotoxic potency, with the strongest electron-withdrawing substituents providing the most stable agents (Table 1).[23] As the hydrogen at the C-7 position is substituted there is a direct effect on half-life and cytotoxicity. An electron-donating group decreases both half-life and potency while an electron-withdrawing moiety enhances both values.

The agents containing the natural (CPI **8**, DSA **3a**, or DA **7**) or modified (CI **9**, CBI **6**, or CBQ **10**) alkylation subunits attached to the same DNA binding subunits have been found to alkylate the same sites. The distinctions of the agents lie in the greater selectivity among the available sites observed with the chemically more stable agents (DSA>CBI>CPI>DA>CBQ>CI).[24]

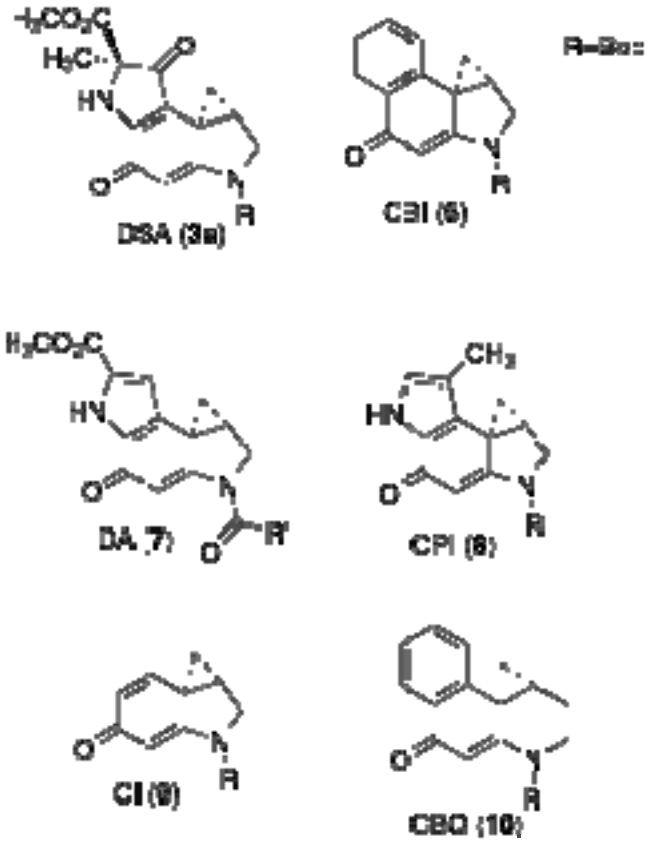

Figure 7: (+)-CC1065 (CPI **8**), Duocarmycin A (DA **7**), Duocarmycin SA (DSA **3a**) and Several Modified Analogs (**6**, **9**, and **10**)

A series of analogs (CBI **6**, CI **9**, and CBQ **10**) were synthesized in order to evaluate the effects of the removal of the pyrrolo ring **9** and the substitution of a benzene ring (**6** and **10**) system. Compound **9** was substantially more reactive than the natural

products most likely due to the loss of electron stabilization on the cyclohexadienone system by the aromatic ring. It was anticipated that the ring expansion from the 5 membered (**6**) to the 6 membered (**10**) would increase the overall chemical stability of **10** and thus decrease its reactivity by removing the ring strain.[17] However, **10** displayed a higher rate of chemical solvolysis compared with compound **6**. X-ray structure analysis revealed that the six-membered ring adopts a boat conformation and the cyclopropane is ideally conjugated with the π-system.[17] The plane defined by the cyclohexadienone perfectly bisects the cyclopropane and the bonds extending to both the secondary and tertiary cyclopropane carbons are equally aligned with the π-system.[17] The X-ray structure of the CBI subunit showed that the bent orbital of the cyclopropane bond extending to the least substituted carbon is nearly perpendicular to the plane of the cyclohexadienone and consequently overlaps nicely with the developing π-system.[17] Contrary to initial expectations, the introduction of the CBQ fused 6 versus 5 membered ring system did not diminish the reactivity. This may be attributed to the ideal conjugation and alignment of the cyclopropane with the cyclohexadienone π-system, which also results in a loss of stereoelectronic control for its cleavage.

Non-Covalent Binding Agents

Netropsin (**11**) and Distamycin A (**12**) are structurally related compounds, which are known to bind non-covalently to AT-rich regions within B-DNA (Figure 8). They share four common attributes. First, they are an overall flat molecule of thickness comparable to an organic ring, but twisted at the single bonds. Second, both of them may assume a crescent shape that allows them to fit along the floor of the minor groove. Third, they have hydrogen bond donors along the concave edge of the crescent, available

to form hydrogen bonds with the N and O atoms on the adenine and thymine base pairs. Lastly, they both display an overall positive charge, which complements the overall negative charge of the B-DNA helix.[25]

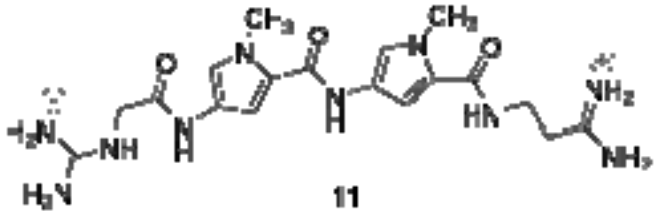

11

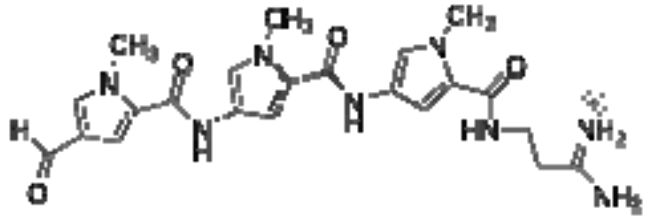

12

Figure 8: Non-Covalent Binding Agents: Netropsin (**11**) and Distamycin A (**12**)

Netropsin (**11**) binds within the minor groove by displacing the water molecules of the spine of hydration.[26] The netropsin amide NH forms hydrogen bonds to bridge DNA adenine N3 and thymine O2 atoms occurring on adjacent base pairs and opposite helix strands.[26] The narrowness of the groove forces **11** to sit symmetrically within the center of the minor groove. The natural twist of both compounds **11** and **12** favors their insertion into the minor groove of B-DNA. The AT base specificity is provided by close van der Waals contacts between adenine C-2 hydrogens and CH groups on the pyrrole rings of **11** (Figure 9).[26] Hydrogen bonds between **11** and the minor groove supply a certain amount of binding energy and provide a correct reading frame by positioning the drug molecule along the DNA molecule.[26]

Netropsin (**11**) exerts its biological activity by binding tightly to double helical B-DNA, interfering with both replication and transcription.[26] Chemical protection studies and Overhauser NMR experiments indicate that **11** does not intercalate between the base pairs, but binds within the minor groove of the intact double helix.[26]

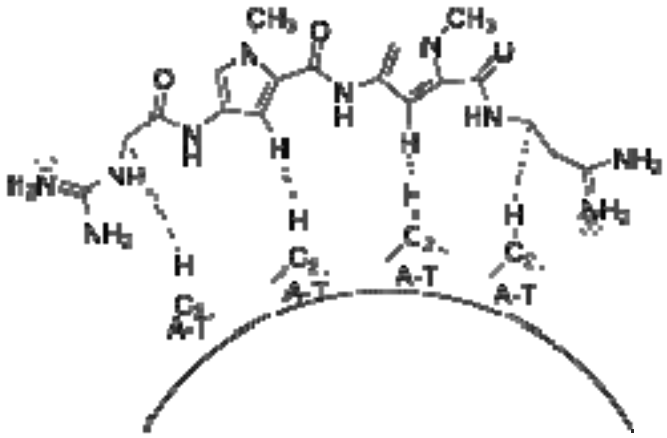

Figure 9: Non-Covalent Binding of Netropsin (**11**) to DNA

The two cationic ends form hydrogen bonds with N3 of adenine (AATT sequence). The amidinium end of the drug molecule approaches the floor of the minor groove to a greater degree than does the guanidinium moiety, perhaps as a result of the greater flexibility of its connecting ethylene chain.[26] Binding of **11** within DNA induces an angle change in the twist from 20° to 33°, and it produces no striking systematic changes in the helix rotation or in base pair stacking-but neither unwinds or elongates the double helix.[26]

Breslauer *et al*. measured the thermodynamic properties of **11** binding to two sequences of continuous fibers: poly(dA)•poly(dT) and poly(dA•dT)-poly(dA•dT).[26] The binding of netropsin to the homogeneous sequences appears to be strongly entropy driven

(10 kcal/mol) coming from an increase in disorder upon binding and only 2 kcal/mol being contributed by the energy of binding.[26]

Lown *et al*. have coined the term "lexitropsin," or information reading oligopeptides structurally related to **11** and **12**.[14] The initial focus of the work involved the substitution of the pyrrole rings with either a thiazole, triazole, pyrazole, imidazole, or oxazole heterocycle. By doing this they postulated that one could design a drug capable of binding to sequences containing one or two GC base pairs embedded within an AT sequence. Each of these groups possesses a hydrogen bond acceptor, which was expected to form hydrogen bonds with N2 of guanine.[14]

The imidazole-lexitropsins (Figure 10) displayed the most pronounced capacity for binding to GC sequences, whereas the thiazole and oxazole-lexitropsins either accept or avoid GC base pairs in their binding sites depending on the position of the S and O atoms. An alternative approach involved connecting a netropsin-like molecule with GC-recognizing elements.[14]

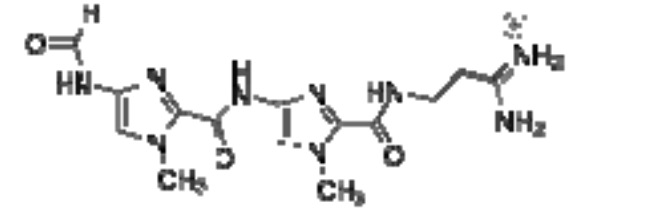

13

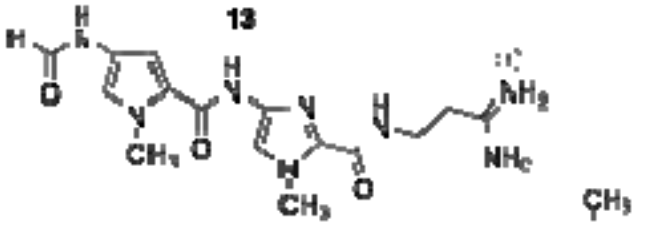

14

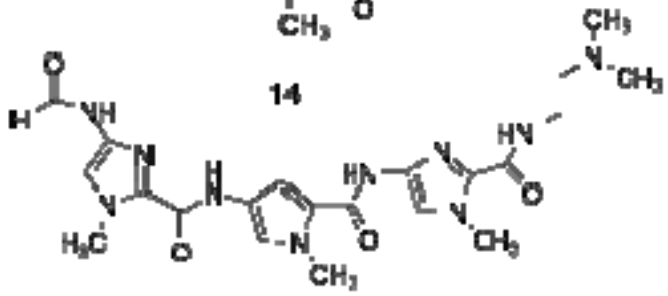

15

Figure 10: Lexitropsins (**13-15**) Developed by Lown and Co-workers

Classical alkylating agents such as the nitrogen mustards (Chlorambucil, **17**) have been shown to react within the major groove of DNA at the N7 position of guanine (Figure 11).[14] In contrast, Mitomycin C (**16**) and Anthramycin (**20**) form adducts with the exocyclic amino group of guanine within the minor groove.

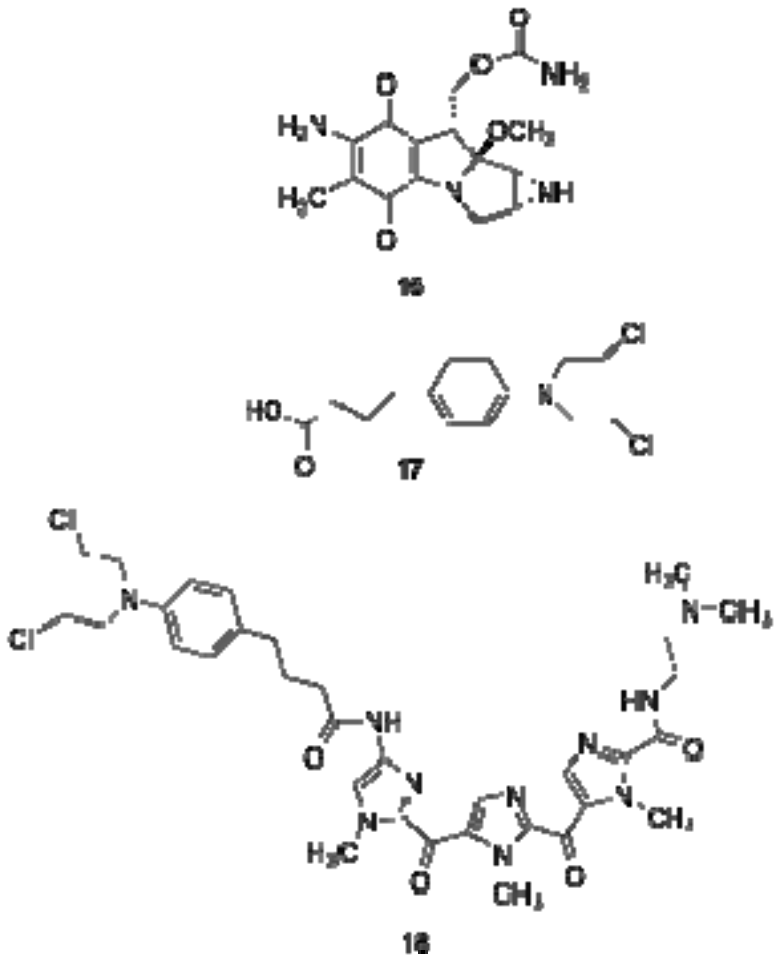

Figure 11: Mitomycin C (**16**), Chlorambucil (**17**),

and Chlorambucil-lexitropsin (**18**)

The accessibility of the major groove and the high nucleophilicity of the N7 heteroatom contribute to the preferential alkylation of guanine residues by nitrogen mustards.[14] However, the alkylation patterns of nitrogen mustards can be modified by linking **17** to a DNA reading element. Distamycin A (**12**) analogues equipped with DNA alkylating functionalities such as Chlorambucil-lexitropsin (**18**) show remarkable sequence selectivity with, in some cases, almost exclusive alkylation of adenines in the minor groove with no detectable N7 reaction.[14]

Lown and co-workers synthesized a series of cyclopropylpyrroloindole (CPI **19**) hybrids (Figure 12), which in one case was capable of exhibiting *in vitro* activity (IC_{50}=0.76 fg/L) against KB tumor cells. This compound was found to form stable covalent adducts within the minor groove.[27]

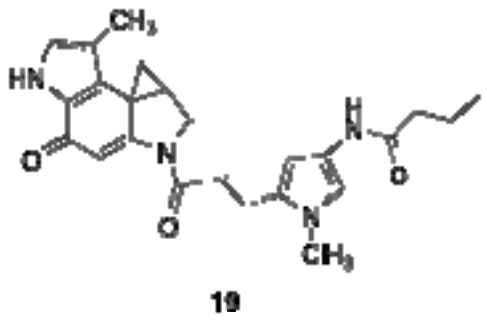

19

Figure 12: Lexitropsin (**19**) containing the "A" Subunit of (+)-CC-1065 (**1**)

GC Selective Agents

Anthramycin (**20**) is a member of the pyrrolo[1,4]benzodiazepine class of antitumor antibiotics. Other members of this class include: Tomaymycin (**21**), Neothramycin A (**22**) and B (**22a**), and Sibiromycin (**23**) (Figure 13). These drugs work by inhibiting the DNA-dependent RNA and DNA polymerase reactions by binding to the DNA template. This alkylation inhibits both the replication and transcription of DNA, but does not inhibit protein synthesis.[28,29] The stereochemistry at the two chiral carbons, C11 and C11a, is *R* and *S*, respectively.[31]

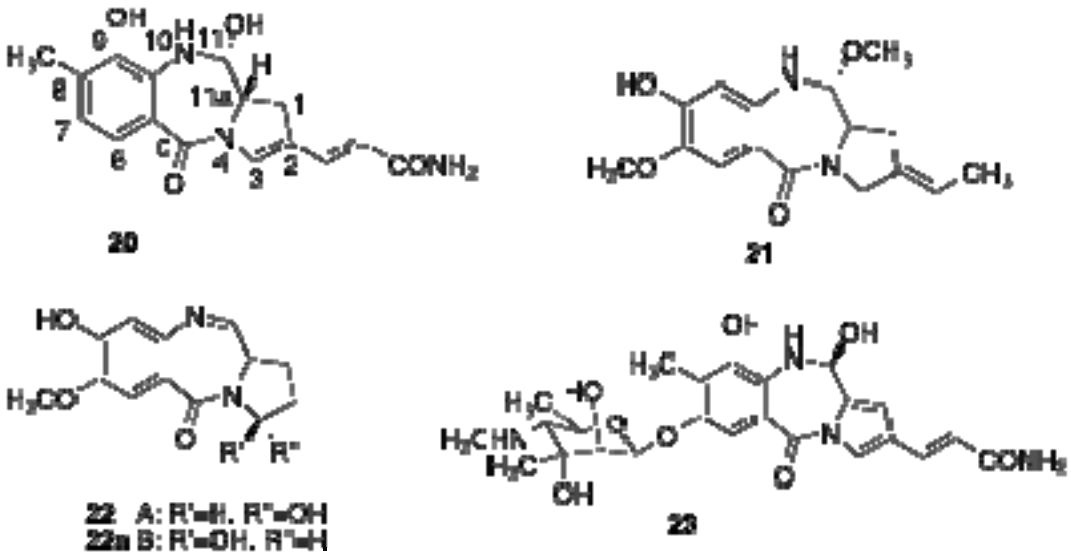

Figure 13: Members of the Pyrrolo[1,4]Benzodiazepine Class (**20**-**23**)

The amine N2 of guanine has been shown through X-ray analysis to be the group responsible for covalent bond formation, because **20** does not react with poly(dI)-poly(dC), which lacks an amine at the 2 position.[30] The preferred binding sequence is T-G-G. The drug molecule is alkylated through its C11 position to the N2 amine of the penultimate guanine of the chain. The stereochemical conformation of binding is C11*S* and C11a(*S*), which provides a 45° angle imparting a right-handed twist, which is complementary to the right-handed twist of the double helix of B-DNA.[31] This inversion of configuration must occur for the drug to properly fit within the minor groove sequence. A C11a*R* drug would only bind within a left-handed helix. The C11*S* attachment is roughly equatorial to the overall plane of the drug molecule, whereas a C11*R* configuration would result in an axial attachment to the guanine residue and would obstruct the fitting of the drug within the minor groove.[31] The origin of the specificity of **20** for three successive purine bases arises not from specific hydrogen bonding but from the low twist angles adopted by purine-purine steps in a B-DNA helix.[31] In general, A-A,

A-G, and G-G steps have smaller than average twist angles, 24-37°, whereas G-A steps are somewhat larger, 31-42°.[31] When two purines follow one another in sequence their double rings stack particularly well, and this stacking is favored by lowering the twist angle between successive base pairs.[31] This creates a good fit for the drug molecule within the minor groove.

The six membered benzo ring of **20** points towards the 3′ end of the chain to which it is bound.[31] The acrylamide tail extends back along the minor groove toward the center of the helix, binding in an analogous manner as **11** and **12**. The tail prefers AT sequences like **11** because the lack of the N2 amine of guanine makes the groove deeper and provides more room for the chain.[31]

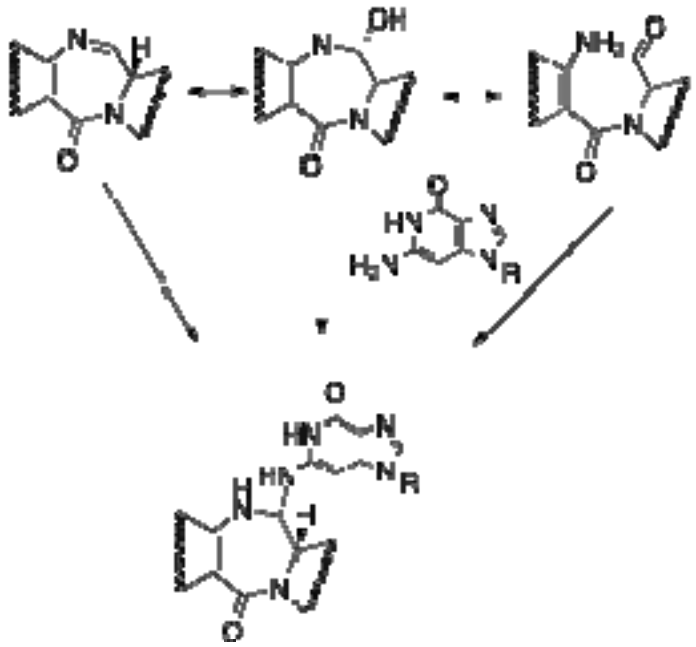

Figure 14: Alkylation of DNA by Anthramycin (**20**)

Figure 14 shows the alkylation of DNA by Anthramycin (**20**), which can occur by one of three alternate forms of the drug molecule. Compound **20** has a binding site, which

spans three base pairs and does not react with mononucleotides, polynucleotides, and RNA not containing guanine bases.[32] Competitive binding studies have shown **20** to bind covalently to N2 of guanine. When Actinomycin D was placed in a solution containing an Anthramycin-DNA complex it failed to dissociate the drug. Alcohol precipitation reactions were carried out on a sample of an Anthramycin-DNA complex and separately on an Actinomycin-DNA complex, which yielded 85% of Actinomycin after two extractions, whereas 67% of Anthramycin-DNA complex survived after four extractions.[33] These experiments verified that Anthramycin (**20**) does indeed form a stable covalent adduct with the DNA helix and cannot easily be displaced.

Designing Sequence Specific Alkylating Agents

Base pair specificity can be altered by changing the functional group(s) presented towards the floor of the minor groove.[34] Stabilizing and destabilizing interactions with the different edges of the four Watson-Crick base pairs are modulated by specific hydrogen bonds and, importantly, steric fit or shape complementarity.[34]

Dervan *et al*. have reported a series of base pairing rules that can be utilized in order to synthesize compounds that are capable of specific base pair recognition.[34-38] Initial studies involved designing sequences of polyamides linked thru amide bonds, which are capable of recognizing each of the four Watson-Crick base pairs. These base pairing rules are based on a pattern of specific hydrogen bonds between the polyamide and the edges of the Watson-Crick base pairs, as well as an ensemble of van der Waals contacts between the polyamide and the walls of the minor groove.[35]

Hairpin polyamides containing the three aromatic amino acids: 3-hydroxypyrrole (Hp, **24**), imidazole (Im, **25**), and pyrrole (Py, **26**) are synthetic ligands that bind to

specific nucleotide sequences with subnanomolar affinity (Figure 15).[34] The hairpin "locks" the individual ring pairings in a predictable cofacial manner. This allows for discrimination between the Watson-Crick base pairs by means of unsymmetrical cofacial pairs of aromatic amino acids.[34]

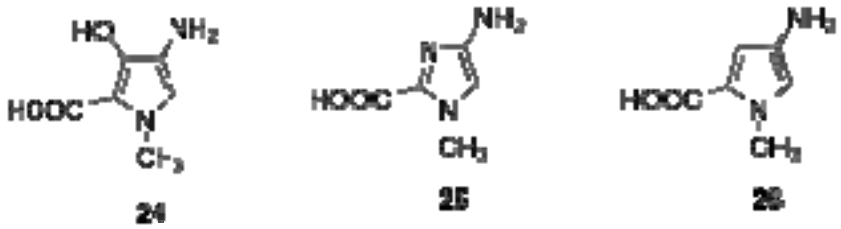

Figure 15: Dervan's Amino Acids (**24**-**26**)

It has been shown through the use of X-ray crystal structures that Hp/Py pair prefers T-A to A-T. The discrimination of TA from AT by an Hp/Py base pair arises from two discreet mechanisms: a) shape selection of an asymmetric cleft on the floor of the minor groove formed by the O-2 of thymine and C2-H of adenine, and b) formation of two specific hydrogen bonds between the 3-hydroxyl and 4-carboxamido groups of Hp with the two lone pairs on the O2 of thymine.[36]

These pairing rules have proven useful for the recognition of hundreds of DNA sequences by polyamides. However, sequence-dependent DNA structural variation such as minor groove width makes binding affinity and specificity at many DNA sequences unpredictable. Several aromatic amino acids such as, thiazole (Nt), furan (Fr), and 1H-pyrazole (Pz) have been investigated with no new selectivity uncovered.[34] These polyamides are four-ring contiguous subunits, which are π-conjugated and in turn effect their conformational flexibility. Footprinting studies have shown that by substituting the Im, Py, or Hp with the Fr, Nt, or Pz heterocycles the overall shape complementarity that

is presented to the floor of the minor groove is significant enough to disallow base pair selectivity and specificity.[34]

Drugs rarely, if ever, bind to their physiological targets with stoichiometries other than 1:1, which is a major drawback with these polyamides. Also, the hairpin polyamides also suffer from a lack of specificity when elongated to target longer dsDNA binding sites. The base pairing rules established by Dervan in order to allow small molecule recognition of specific Watson-Crick base pairs has only been shown effective when dealing with 2:1 drug-DNA complexes.[37] Further work is required to fine tune this approach so that these rules may be applied to 1:1 drug-DNA complexes.

A pairing of imidazole (Im) and *N*-methylpyrrole (Py) amino acids can be combined in antiparallel side-by-side dimeric complexes with the minor groove of DNA. A pairing of Im/Py is capable of recognizing a GC base pair, whereas a pairing of Py/Im is capable of CG selectivity. A pairing of Hp/Py is capable of recognizing TA sequences, whereas a Py/Hp pair can recognize AT base pairs.[38] Following the base pairing rules designated by Dervan *et al*.[36], the synthesis of compounds capable of recognizing specific DNA base pairs appears to be a distinct possibility.

Background Information on AutoDock 3.0

AutoDock 3.0 is a suite of three C programs: AutoTors, which facilitates the input of ligand coordinates, AutoGrid, which pre-calculates a three-dimensional grid of interaction energy based on macromolecular coordinates, and AutoDock, which performs the docking simulation.[39] AutoDock has been shown to reproduce crystallographically determined positions of ligands with up to eight degrees of torsional freedom. For molecules with more degrees, the simulated annealing search does not adequately sample

the possible conformational space. It uses a rapid grid-based lookup method for energy evaluation, but its main drawback is that the program does not allow for receptor side chain flexibility, which is allowed in other programs such as GLIDE. However, this is not a problem for DNA due to the relative rigidity of the helix. AutoDock has been shown to successfully reproduce crystallographically determined positions of ligands, which has been confirmed through the use of root mean square deviations (RMSD) between the X-ray crystal structure and the low energy docked compounds.[39-42]

Chemotherapeutic agents targeting DNA can be classified, depending on their mode of interaction, into two major classes: (i) covalent binding, and (ii) non-covalent binding, including intercalative binding and DNA major- and minor-groove binding. Until recently it was thought that AutoDock was more suited towards the evaluation of protein-ligand interactions versus DNA-ligand interactions. Sobhani *et al*. have recently reported a novel methodology for the use of AutoDock 3.0 in predicting the correct binding conformations of ligands within known DNA-ligand complexes.[43] They obtained the X-ray crystal structures of three different oligonucleotide-ligand complexes: DNA-Propamidine, DNA-Adriamycin, and DNA-Ditercalinium, from the Protein Data Bank (PDB). A series of azolyalkylquinolines (AAQ's), which have been prepared by the Sobhani lab have exhibited activity comparable to or moderately superior to Adriamycin. The primary aim of their study was to propose a binding model that would explain the mode of action of the AAQ's as DNA binding agents.

For each of the three files retrieved from the PDB all ligands and water molecules were removed. The missing hydrogens and partial atomic charges, using Amber 95, were assigned to the DNA sequence. All non-polar hydrogens, partial atomic charges, and

desolvation parameters were added to each of the three ligands. Energy minimization was performed using HyperChem. AutoDock Tools (ADT) was used to assign partial atomic charges using the Gasteiger-Marsili method. After merging the non-polar hydrogens, rotatable bonds were assigned. Forty-nine AAQ's from the Sobhani lab were designed using HyperChem and given individual files for future use.

AutoGrid, as a part of AutoDock, was used to construct gridmaps over the area of the known binding site. AutoDock 3.0 using a Lamarckian Genetic Algorithm (LGA) was used to model the interaction/binding between the DNA and the various AAQ compounds. Pseudo-Solis and Wets algorithms were then used to perform the local searches. In order to limit the computer time a standard of 50 docking runs were used for each ligand. Cluster analysis was performed using Root Mean Square (RMS) tolerance of 0.5 Å (default). These parameters were used for the docking of all 49 AAQ compounds.

Total binding free energy was empirically calibrated based on the restriction of internal rotors, global rotation, the translation, and a set of coefficient factors. All empirical methods have to use a training set, which influences the outcome of the final model. Also, AutoDock Utilities do not have certain provisions such as ADDSOL to assign partial atomic desolvation terms to the nucleic acid atoms acting as the target molecule. Consequently, the free energy change of binding (ΔG) and the corresponding inhibition constant (k_i) predicted by AutoDock 3.0 for DNA-ligand complexes may be unreliable. The program calculates a docking energy (DE) and a predicted free energy (PFE) or free docked energy (FDE), also called the binding energy (BE).

The DE includes intermolecular and intramolecular energies and are used during the docking runs. The FDE includes intermolecular energy and torsional free energy and

are only reported at the end of a given run. Because of the above mentioned limitations, the Sobhani group decided to use both the free docking energy and ΔG. The k_i was converted to ΔG using: $\Delta G=RT \ln k_i$, R is the ideal gas constant (1.987 cal K-1mol-1) and T is absolute temperature assumed to be at room temperature (298.15 K).

Morris *et al*. defines the free energy of binding (or binding energy) as the sum of dispersion/repulsion, hydrogen bonding, electrostatics, and deviations from covalent geometry (Equation 1):[39]

Equation 1: $\Delta G=\Delta G_{vdw} + \Delta G_{hbond}+ \Delta G_{elec}+ \Delta G_{conform}+ \Delta G_{tor}+ \Delta G_{sol}$

Where ΔG_{tors} models the restriction of internal rotors and global rotation and translation; and ΔG_{sol} models desolvation upon binding and the hydrophobic effect. Also, the inhibition constant (k_i) can be calculated as Sobhani *et al*. described earlier.

As was stated earlier, AutoDock calculates two different types of energies: docking energy (DE) and binding energy (BE) or free energy of binding. Docking energies are those, which include the intermolecular and intramolecular interaction energies, and are used, in the docking experiments. A global energy minimum is calculated for the ligand and the drug-receptor system and is treated as a rigid body with only the steric interactions involved between the energy minimized drug and the receptor taken into account. The second, binding energy, includes the intermolecular energy and torsional free energy and are reported at the end of the docking experiment. This binding energy is directly related to the inhibition constant (k_i).

The Sobhani group took the experimentally determined conformations and superimposed them onto the predicted conformations and calculated the root mean square deviation (RMSD). The RMSD for each of the docked ligands (Propamidine,

Adriamycin, and Ditercalinium) were reported as 1.4, 0.81, and 1.02 Å, which were considered as successfully docked. Use of the Spearman coefficient, which calculates the correlation between two sets of rankings, it became evident that the correlation between the experimentally measured k_i's and the calculated binding affinities were significant at 0.01 level.[43]

Analysis began by comparing all low energy docked conformations in relation to the location/orientation of the ligand within the active site of the oligonucleotide. If these conformers did not meet the stated requirements, then the next lowest energy conformer was chosen. Pearson correlation coefficient between the theoretically predicted and experimentally measured binding affinities indicated a significant correlation between the FDE values and the experimental binding affinities for all three ligands (Propamidine, Adriamycin, and Ditercalinium). There was no significant relationship between the predicted ΔG and the experimentally measured ΔG. This study clearly demonstrated that the FDE predicted by AutoDock was a better means for evaluating DNA-ligand interactions than the estimated free energy change of binding (ΔG).[43]

Research Objectives

Chemotherapeutic agents lack cellular specificity and as a result can lead to many adverse effects for the patient. By designing compounds capable of recognizing and alkylating specific base pair sequences within the DNA minor groove it is hoped that many if not all of these side effects can be eliminated. This lab previously reported a novel synthetic route,[44] which incorporated several key structural features from (+)-CC-1065 (**1**), Duocarmycin A (**2**), Duocarmycin SA (**3**), and Anthramycin (**20**) into a single

molecule **28** and the ring expanded molecule **27**, which was developed during the course of this dissertation.

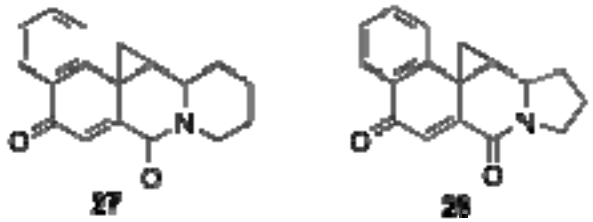

Figure 16: Compounds **27** and **28**

AutoDock 3.0 was used to model novel compounds in order to determine what modifications could be made, which would allow for greater selectivity and/or activity. The results of the modeling studies led to several promising candidates for future synthetic work. During the course of these studies it became apparent that alternate synthetic routes into these compounds would be necessary. With that in mind the initial studies began with the investigation of novel synthetic routes, which could allow for the synthesis of these agents. The focus of the modeling studies is to attempt to functionalize compound **28** with moieties that are capable of improving both selectivity and activity.

RESULTS AND DISCUSSION

Synthesis of 10, 11, 12, 12a, 12b, 13-Hexahydro-5*H* benzo[*f*]cyclopropa[*d*]pyrido[1,2-*b*]isoquinoline-5,7(9*H*)-dione (27)

All compounds were numbered and named using the autonom feature of ChemDraw 11.0, which uses an updated version of the IUPAC naming system. Retrosynthetic analysis of the cyclohexadienone **27** suggested that it could arise from a base-catalyzed intramolecular cyclization of the phenol mesylate **44**. Compound **44** was envisioned coming from the acid by selective reduction to the alcohol, which could then undergo activation to the methanesulfonate followed by debenzylation. It was thought that the acid **41** could arise from the condensation of the imine **40** with the anhydride **38**. Acid catalyzed ring closure of the diacid **37** was anticipated to afford the anhydride **38**. The diacid **37** was expected to arise from a Diels-Alder reaction between the furan **31** and the diazotized material **33**, which could lead to the epoxy intermediate **34**. At this stage it was thought that acid catalysis could open the epoxy ring system, which could then undergo standard benzylation and ester hydrolysis reactions to furnish the diacid **37**.

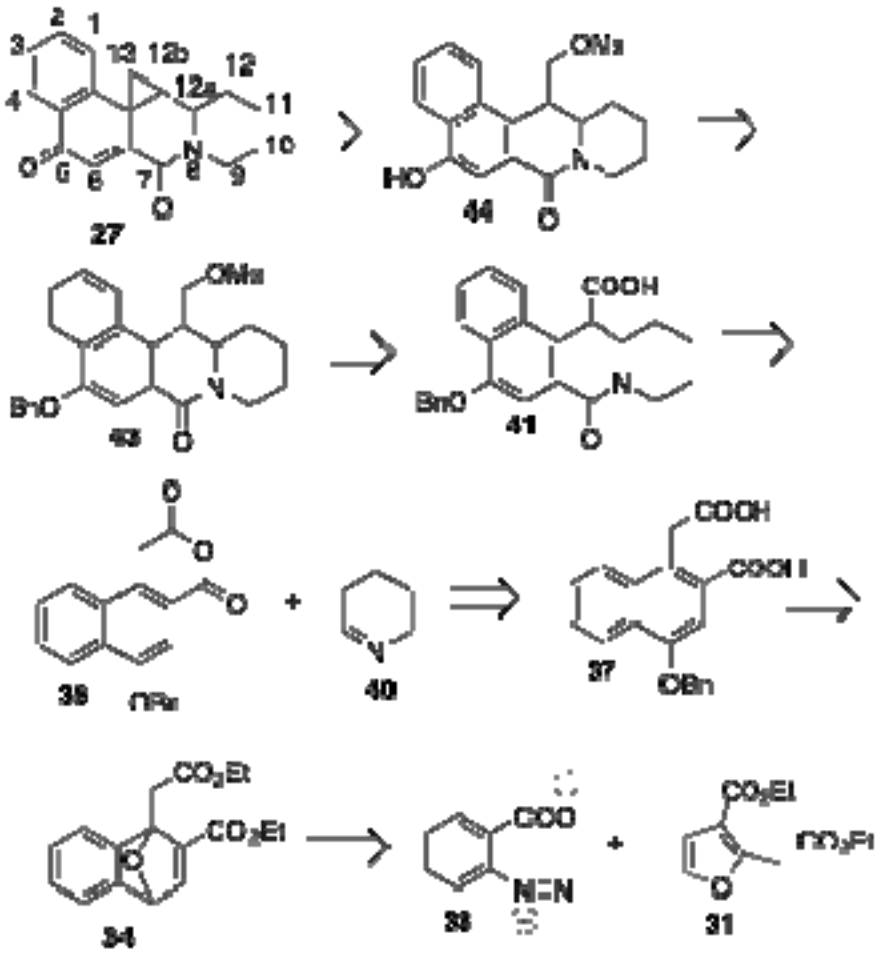

Scheme 2: Retrosynthetic Analysis of Compound **27**

Utilizing the procedure of Tada *et al*., the furan **31** was prepared by refluxing 1,3-diethylacetone dicarboxylate (**29**) with an aqueous solution of 40% chloroacetaldehyde (**30**) in dry pyridine for 24 hours. The furan **31** was purified by careful distillation so that large amounts could be prepared without the need for chromatography (Scheme 3).[45]

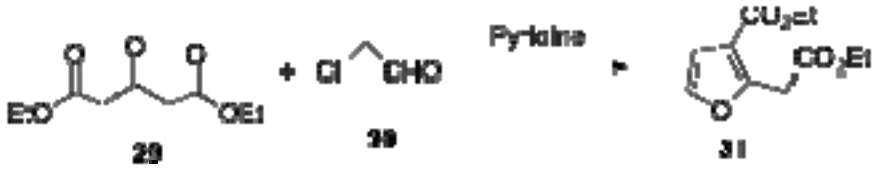

Scheme 3: Synthesis of Furan **31**

Early efforts to synthesize compound **35** involved stirring anthranilic acid (**32**) in the presence of isoamyl nitrite and compound **31** while refluxing for 45 minutes (Scheme 4). This led to the epoxy intermediate **34** in 50% yield, and subsequent purification by chromatography had to be performed immediately due to its instability. An alternate procedure was followed by Logullo *et al*., which reported a modified route for the formation of the diazotized intermediate.[46] The anthranilic acid (**32**) was allowed to stir at room temperature for 2 hours in the presence of trichloroacetic acid and isoamyl nitrite to furnish compound **34** in an 80% yield. The diazotized compound **33** could be generated and isolated prior to undergoing the Diels-Alder reaction; however, it was reported that compound **33** must remain wet to prevent explosion. The diazo zwitterion **33** was then placed in 1,2-dichloroethane and allowed to stir at reflux for 1 hour in the presence of **31** to give the epoxy material **34** in about 50% yield.

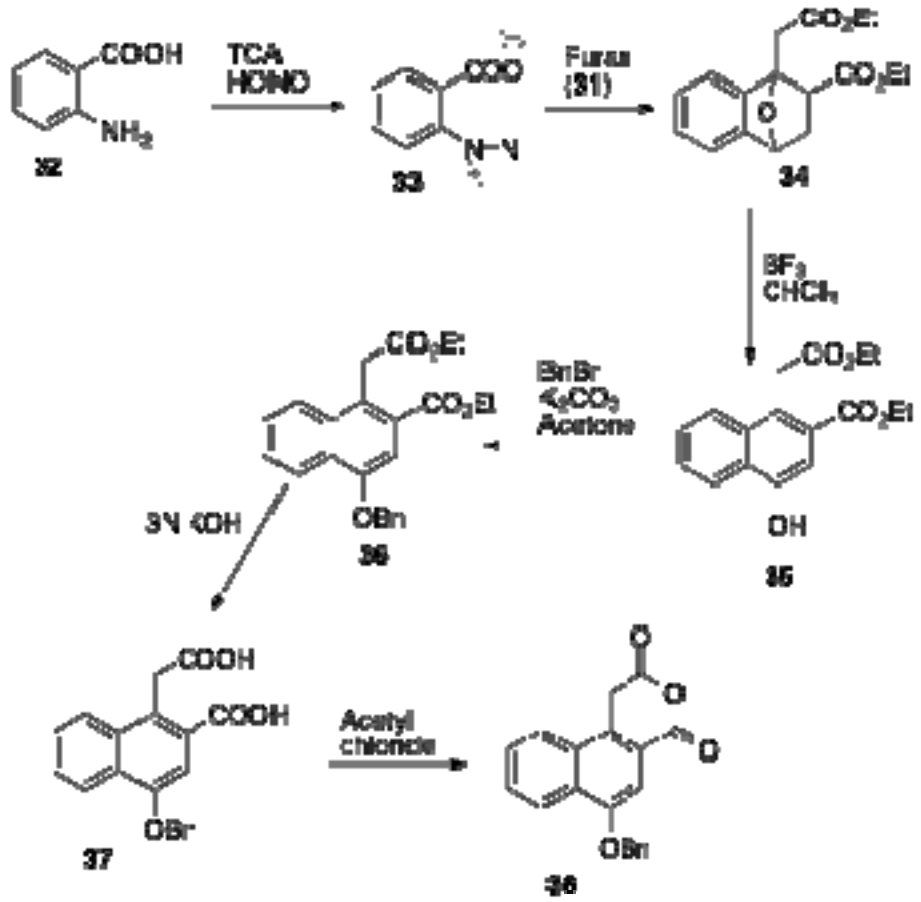

Scheme 4: Synthesis of Anhydride **38**

During the course of the investigation it was found that the acid-catalyzed ring opening of compound **34** could be achieved prior to chromatography to give compound **35** in quantitative yield. This was beneficial due to the increased stability of the phenol **35** with regards to compound **34**, which had to be treated with borontrifluoro etherate rather quickly to prevent decomposition. Compound **35** was refluxed in the presence of potassium carbonate and benzyl bromide for several hours to give the protected benzyl ether **36** in 95% yield, which was then subjected to basic hydrolysis to produce the diacid **37** in near quantitative yield. The diacid **37** was then refluxed in acetyl chloride for 24 hours to give the anhydride **38** in 95% yield (Scheme 4).

Following the procedure of Quick and Oterson, piperidine (**39**) was treated with *N*-chlorosuccinimide, which was then dehydrohalogenated in the presence of potassium hydroxide to give the imine **40** in about 50% yield (Scheme 5).[47] Formation of the *N*-chloro piperidine intermediate occurred smoothly and was verified by melting point.

Scheme 5: Synthesis of Imine **40**

The dehydrohalogenation reaction, on the other hand, proved to be more difficult. Several procedures were attempted resulting in the recapturing of starting piperidine **39**, as determined by ^{1}H and ^{13}C NMR.

Condensation of the anhydride **38** with the imine **40** led to a diastereomeric mixture of the acids **41** (Scheme 6). The condensation occurred in quantitative yield to give a 50:50 mixture of *cis* and *trans* isomers, which were fully characterized using ^{1}H and ^{13}C NMR. Although it was previously reported that the diastereomers of the pyrrolo series could be fractionally recrystallized[42] this process was not successful for compound **41**. Chromatographic separation of compound **41** gave one diastereomeric pure fraction as determined both by ^{1}H NMR and TLC.

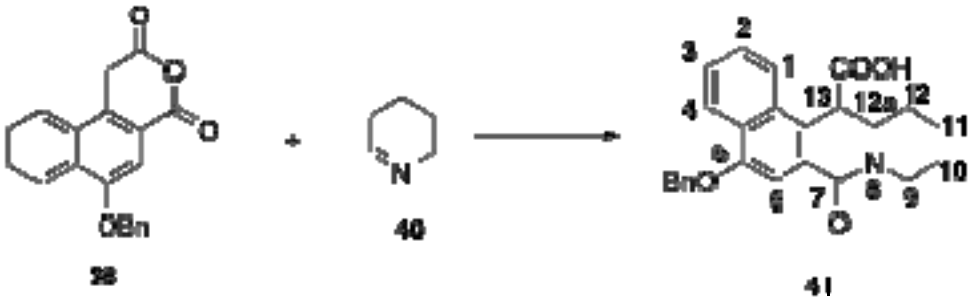

Scheme 6: Condensation of Anhydride **38** with Imine **41**

This isomer was determined to be the *trans* isomer and was assigned by the coupling constant between the C13-H and C12a-H protons. In the *cis* isomer, the C13-H proton (4.40 ppm) had a coupling constant of 5.0 Hz while the coupling constant for the *trans* C-13 proton (4.59 ppm), was 14.0 Hz.

Conversion of the acid **41** to its acid chloride followed by reduction utilizing sodium borohydride gave the desired alcohols **42** in 65% yield. An alternate method was investigated, which involved the conversion of the acid **41** to its mixed anhydride utilizing ethyl chloroformate and triethylamine followed by subsequent reduction using sodium borohydride to give compound **42** also in 65% yield (Scheme 7). This route was shown to give the same moderate yields but shorter reaction times; however, it did result in a slightly dirtier product. Once the alcohols **42** were obtained, they could be easily separated chromatographically and the rest of the synthetic sequence could be carried out on the individual diastereomers.

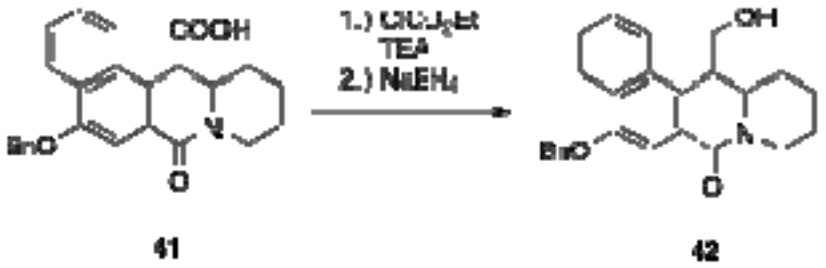

Scheme 7: Synthesis of Primary Alcohol **42**

Attempts were also made to condense the anhydride **38** with the seven- membered imine **45** (Scheme 8). TLC data initially suggested the cyclization occurred due to the similarity in two closely eluting fluorescent bands of higher R_f than compound **41**, which was run in the same mobile phase. However, upon inspection of the ^1H NMR there was a lack of signals in the region of 1-2 ppm indicating that the seven-membered imine **45** had not been condensed. Multiple attempts to synthesize compound **46** were not successful so this route was not pursued further.

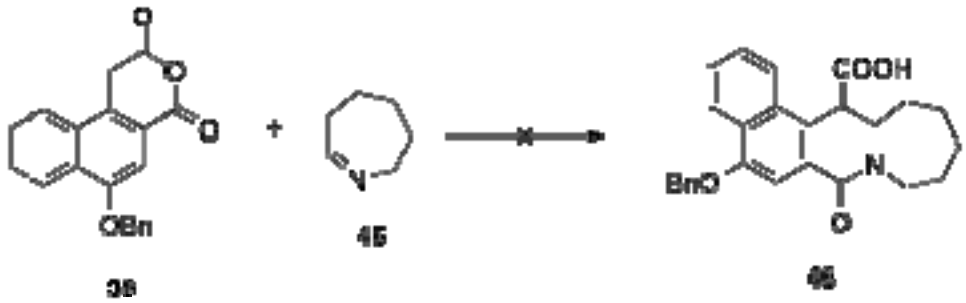

Scheme 8: Attempted Condensation with Compound **45**

The alcohol **42** was then activated for intramolecular cyclization by conversion to the mesylate **43**. Debenzylation occurred smoothly under catalytic hydrogenation conditions to furnish the phenol **44** in 90% yield. The final compound **27** was then obtained through carefully controlled conditions utilizing sodium hydride in anhydrous tetrahydrofuran and quenching with sodium phosphate buffer at pH 7.0 (Scheme 9).

Purification was performed using a freshly prepared alumina chromatotron plate as well as freshly distilled solvents. Both diastereomers of compound **27** were identified using ^{1}H and ^{13}C NMR as well as high resolution MS. The methanesulfonyl methyl group, which appeared as a singlet in the *cis* (2.82 ppm) and *trans* (2.99 ppm) phenols was absent.

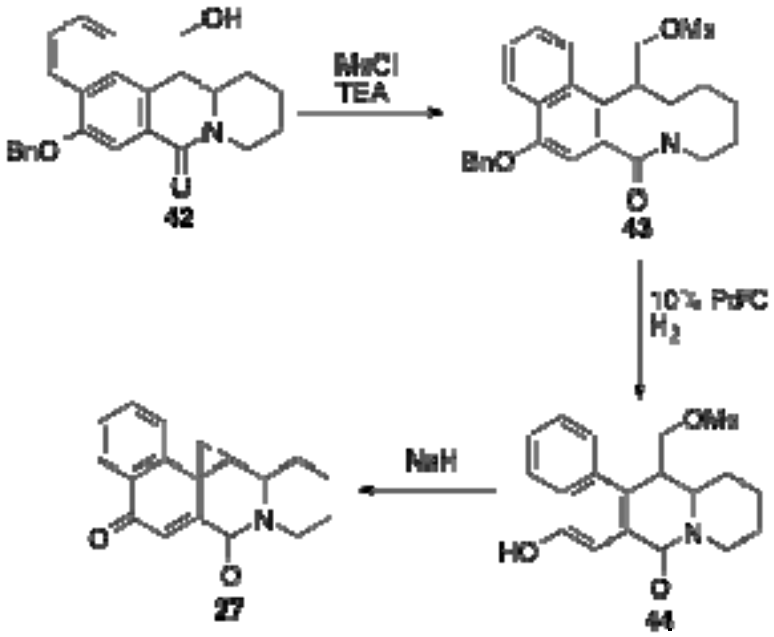

Scheme 9: Formation of Final Compound **27**

The cyclopropyl methylene protons appeared as multiplets at 2.04 ppm (*trans*) and 2.06 ppm (*cis*). The signals for the C12b protons were shifted upfield to 4.66 ppm (*cis*) and 4.78 ppm (*trans*). In the ^{13}C NMR (Figures 16 and 17), the signals for the methyl group of methanesulfonyl group were absent. The C6 proton, which appeared as a singlet at 8.27 (*trans*) and 7.97 (*cis*) ppm, was shifted upfield to 7.36 (*trans*) and 7.32 (*cis*) ppm, respectively. The cyclopropyl methylene carbon appeared at 34.9 ppm (*trans*) and 33.4 ppm (*cis*). Also, the signal for C13 appeared at 26.8 ppm (*trans*) and 26.9 ppm (*cis*), and the signal for the newly generated ketone appeared at 185 ppm for both isomers.

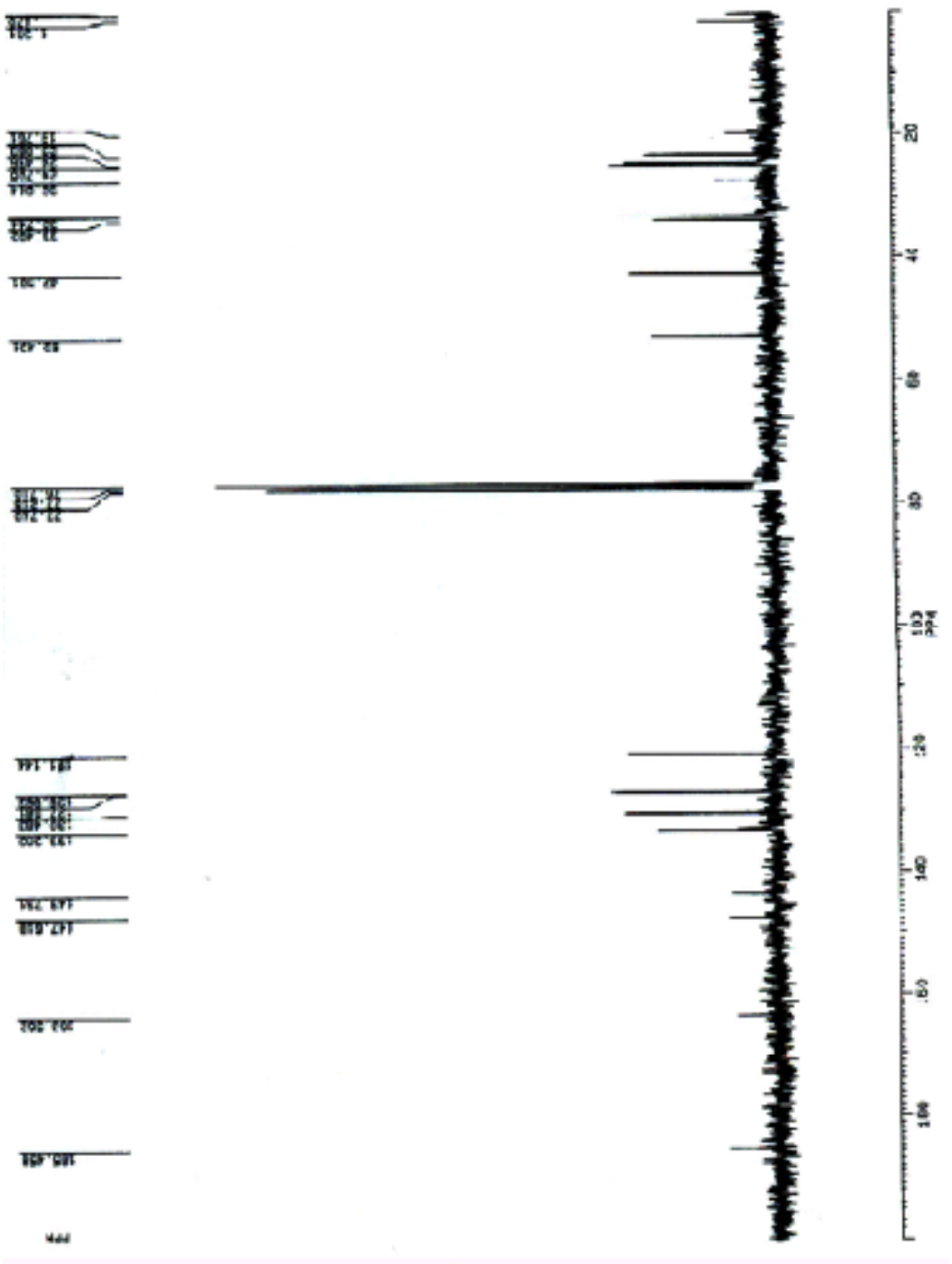

Figure 17: ^{13}C NMR *Cis* Final Compound **27**

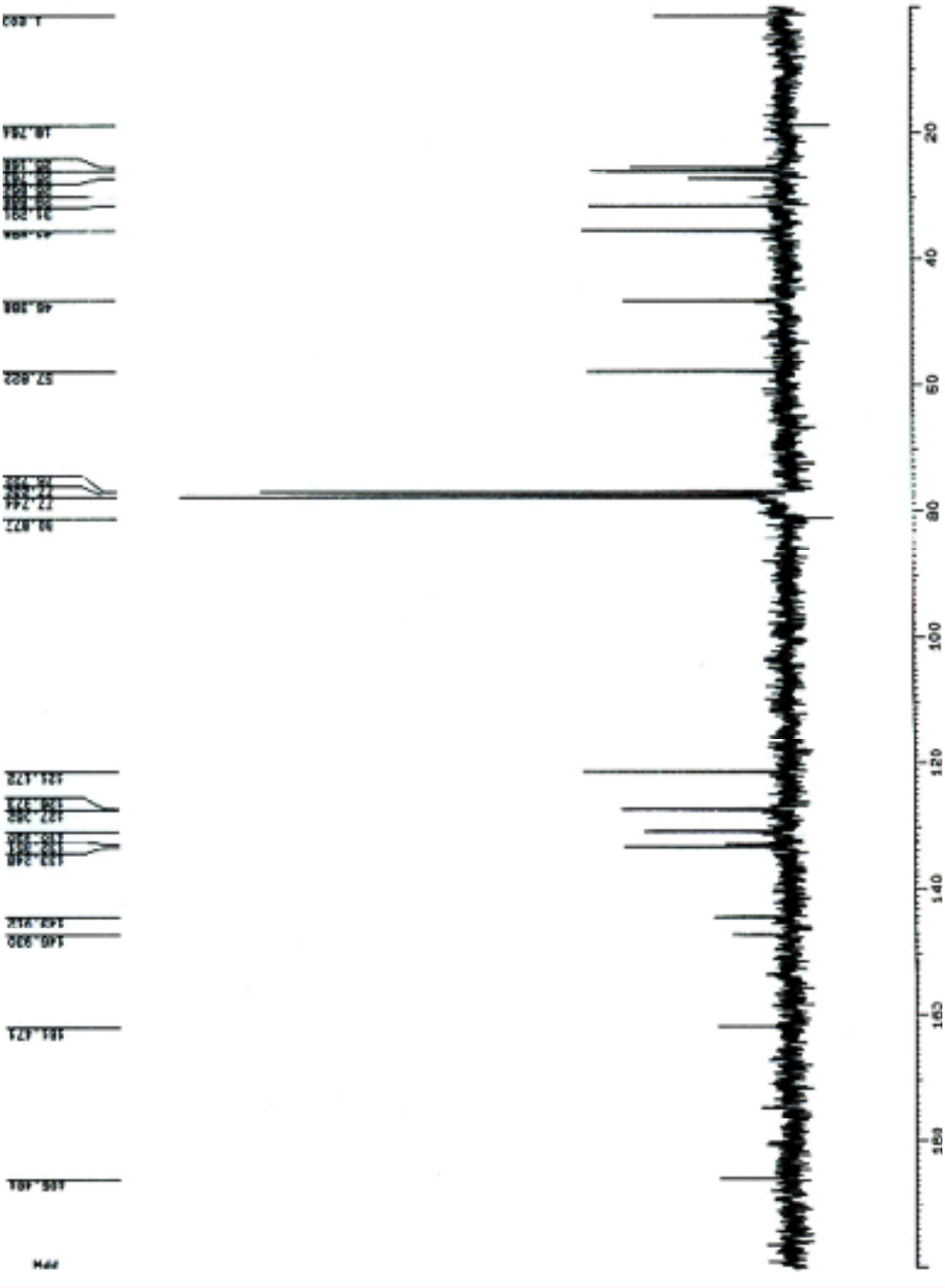

Figure 18: ^{13}C NMR *Trans* Final Compound **27**

Antitumor Activity of 27

Upon completion of the synthesis of the individual diastereomers of **27** they were sent to the National Cancer Institute (NCI) to be tested in a 60 cell-line anti-tumor panel. The screening is a two-stage (*in vitro*) process beginning with the evaluation of all compounds against a 60 cell-line at a single concentration of 10 μM. The drug is introduced into wells of varying cell concentrations and incubated for a period of 48 hours. Upon work-up, a cell counter is used to determine the GI_{50} values, which measures the concentration of drug required to inhibit new cell growth by 50%.[48]

As will be discussed later, compound **27** displayed moderately low GI_{50} values. Several of the more active cell lines have been marked in bold and the < sign indicates that the compounds displayed activity lower than the testing parameters were designed to measure. The results listed in Table 2 show that as an overall trend the *trans* isomer was more active than the *cis* isomer; however, closer inspection of the individual tumor cell lines shows that the *trans* isomer shows remarkably greater activity on the order of 10 - 100x difference on several of the cell lines. The HOP-62 cell line (Non-Small Cell) and the K-562 (Leukemia) are two examples of this difference. As a result of these studies the *trans* isomer was chosen by NCI for further testing. The *trans* isomer was one of less then 1% of all compounds tested to be selected to undergo a hollow fiber assay (*in vivo*).

National Cancer Institute GI_{50} Values (M)								
Panel/ Cell Line	Cis	Trans	Panel/ Cell Line	Cis	Trans	Panel/ Cell Line	Cis	Trans
Leukemia			CNS			Renal		
CCRF-CEM K-562 MOLT-4 RPMI-8226 SR	-6.26 -5.43 -6.65 -5.96 -6.74	-6.87 -6.48 **-7.03**[a] -6.88 **-7.27**	SF-268 SF-295 SF-539 SNB-19 SNB-75 U251	-5.85 -5.17 -5.61 -5.34 -4.86 -5.80	-6.59 -5.74 -6.32 -6.47 -6.04 -6.62	786-0 A498 ACHN CAKI-1 RXF-393 SN12C TK-10 UO-31	-5.84 **<-8.0** -6.48 **-7.48** -5.55 -6.15 -4.99 -5.05	-6.88 -6.61 -6.93 -6.72 -6.70 -6.88 -5.90 -5.73
None-Small Cell Lung			Melanoma			Prostate		
A549 EKVX HOP-62 HOP-92 NCI-H226 NCI-H23 NCI-H322M NCI-H460 NCI-H522	-5.78 -5.09 -5.99 -5.76 -6.04 -6.60 -5.02 -5.66 -5.44	-6.66 -5.69 **<-8.00** -6.80 -6.71 **-7.40** -6.41 -6.27 -6.01	LOX IMVI MALME-3M M14 SK-MEL-2 SK-MEL-28 SK-MEL-5 UACC-256 UACC-62	-5.69 -4.92 -5.47 -5.04 -4.67 -5.90 -5.22 -5.64	-6.74 -5.81 -6.82 -5.74 -6.50 -6.91 -6.39 -6.76	PC-3 DU-145	-5.42 -6.15	-6.41 -6.55
Colon			Ovarian			Breast		
COLO 205 HCT-15 HT 29 KM12 SW-620	-5.38 -5.73 -5.55 -4.77 -5.65	-6.29 -6.79 -6.91 -5.57 -6.30	IGROV-1 OVCAR-3 OVCAR-4 OVCAR-5 OVCAR-8 SK-OV3	-5.27 -6.31 -5.05 -5.62 -5.85 -5.26	-5.67 N/A -6.34 -6.48 -6.70 -6.52	MCF7 NCI/ADR-RES MDA-MB-231/ATCC HS 578T MDA-MB-435 BT-549	-6.17 -6.22 -5.20 -5.74 -4.86 -5.52	-6.64 -6.84 -6.27 N/A -5.71 -6.21

Table 2: NCI Data on Cis and Trans Compound **27**

a: Several highly active compounds are noted in bold face

Standard panels of 12 tumor cell lines are typically used for the hollow fiber testing. A total of three different tumor lines are prepared for each mouse then heat sealed

in a hollow fiber and injected intraperitoneally (1 of each cell line) and subcutaneously. Drug treatment begins on day 3 or 4 following implantation, and continues for four successive days. The doses of the drug are based on the maximal tolerated dose (MTD) determined during prior acute toxicity testing. The hollow fibers are collected at the end of the fourth day of treatment and examined for percent net growth for each cell line. A 50% or greater reduction in net growth in each sample is considered a positive result. Each positive result is given a score of 2 and all of the scores are totaled for a given compound. The maximum possible score for an agent is 96 (12 cell lines X 2 sites X 2 dose levels X 2 [score]). A compound is considered for xenograft testing if it has a combined ip + sc score of 20 or greater, a sc score of 8 or greater, or produces cell kill of any cell line at either dose level evaluated.[48] The results for the *trans* cyclopropyl compound **27** listed an ip score of 8 and an sc score of 16 with a combined score of 24 (ip + sc), but the compound was not selected for further testing. The results also listed the cell kill as being positive.

Table 3 lists the NCI testing data for compound **27** against other commonly used antineoplastic agents such as: Chlorambucil (**17**), 5-Fluorouracil (**47**), Procarbazine (**48**), and Actinomycin D (**49**) (Figure 19). Also used for comparison to compound **27** were the natural products (+)-CC-1065 (**1**) and Anthramycin (**20**). While compound **27** was not as cytotoxic as compounds **1**, **20**, or **49**, it was more potent than Chlorambucil (**17**) and 5-Fluorouracil (**47**).

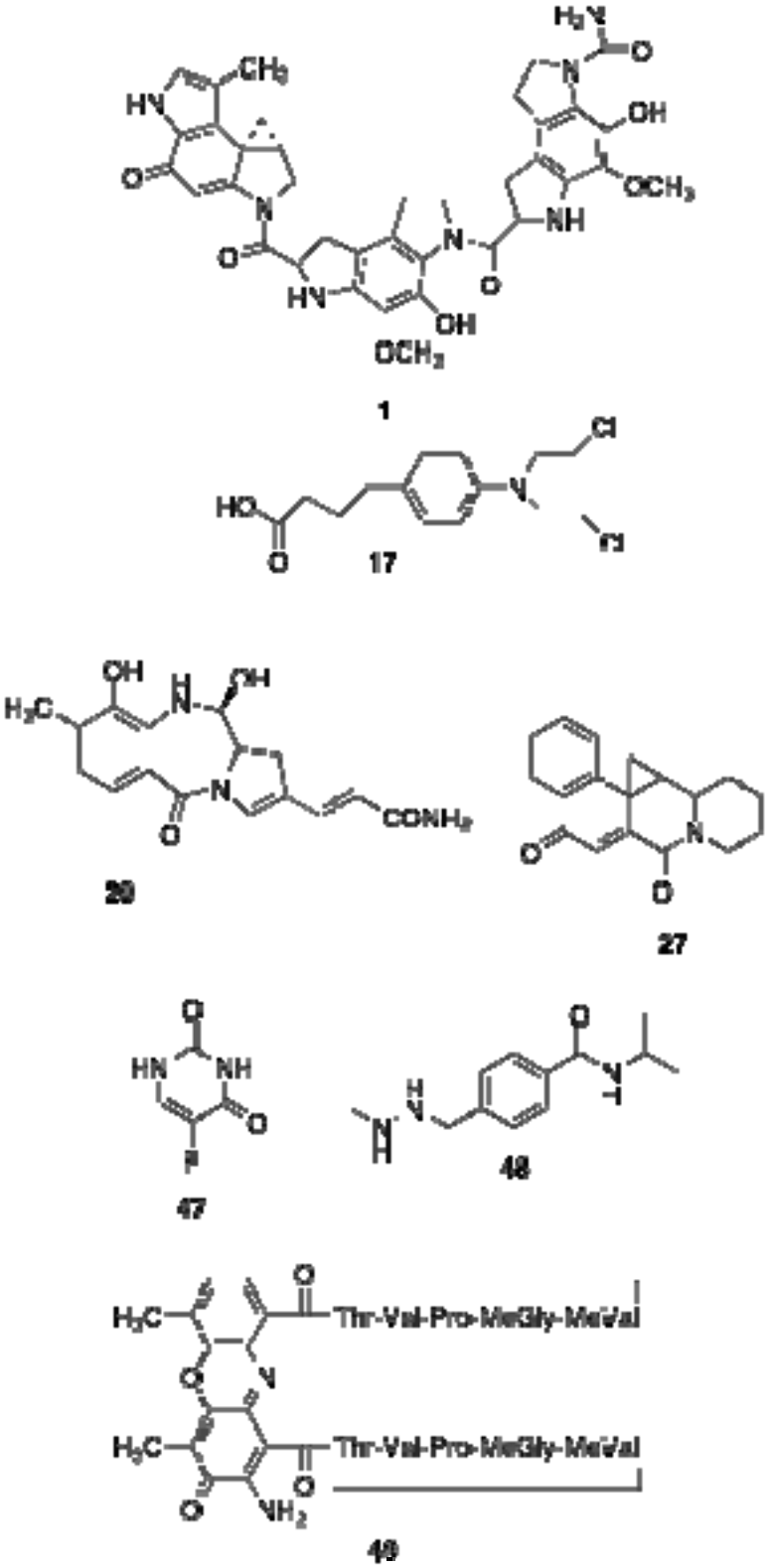

Figure 19: Structures for the Compounds Listed in Table 3

Avg. GI_{50} Values for Selected Antineoplastic Agents (M)								
	Trans 25	**Cis 25**	**1**	**17**	**20**	**47**	**48**	**49**
Leukemia	-6.91 (6.48-7.27)[b]	-6.21 (5.43-6.74)	-8.05 (7.6-8.5)	-5.63 (4.7-6.1)	-7.55 (7.4-7.7))	-6.23 (5.0-7.6)	-3.3 (3.3)[c]	-10.0 (10)
NSC[a] Lung	-6.66 (5.69-8.00)	-5.71 (5.02-6.60)	-8.72 (7.7-9.8)	-4.96 (4.6-5.7)	-7.33 (6.4-7.7)	-5.68 (4.1-7.2)	-3.4 (3.3-3.9)	-9.51 (8.7-10.0)
Colon	-6.37 (5.57-6.91)	-5.42 (4.77-5.73)	-8.54 (6.9-9.7)	-4.64 (4.5-4.9)	-7.33 (6.7-7.6)	-6.74 (6.0-7.3)	-3.33 (3.3-3.4)	-9.73 (8.1-10.0)
CNS	-6.29 (5.74-6.62)	-5.44 (4.86-5.85)	-8.67 (8.3-9.7)	-5.01 (4.7-5.3)	-7.72 (7.6-8.0)	-5.85 (4.1-7.2)	-3.34 (3.3-3.5)	-9.92 (9.5-10.0)
Melanoma	-6.46 (5.74-6.91)	-5.32 (4.67-5.90)	-8.58 (7.9-9.0)	-4.92 (4.5-5.4)	-7.68 (7.2-7.9)	-6.14 (4.2-7.3)	-3.33 (3.3-3.4)	-9.88 (9.2-10.0)
Ovarian	-6.34 (5.67-6.70)	-5.56 (5.05-6.31)	-8.5 (7.7-9.5)	-4.66 (4.5-4.8)	-7.37 (7.3-7.5)	-5.87 (4.7-7.8)	-3.33 (3.3-3.4)	-8.84 (6.3-10.0)
Renal	-6.54 (5.73-6.93)	-6.19 (4.99-8.00)	-8.66 (7.6-9.4)	-4.97 (4.5-5.4)	-7.48 (6.7-7.8)	-6.21 (5.6-7.1)	-3.36 (3.3-3.6)	-9.33 (8.2-10.0)
Prostate	-6.48 (6.41-6.55)	-5.79 (5.42-6.15)	N/A	N/A	-7.55 (7.4-7.7)	-6.0 (5.6-6.4)	-3.3 (3.3)	-9.4 (9.0-9.8)
Breast	-6.33 (5.71-6.84)	-5.62 (4.86-6.22)	N/A	N/A	-7.60 (6.3-8.0)	-5.48 (5.0-7.1)	-3.3 (3.3)	-9.23 (6.7-10.0)

Table 3: Average GI_{50} Values for Selected Cancer Cell Lines

a: NSC= Non-Small Cell
b: Numbers inside parentheses denote the range within the given panel
c: Single number indicates that all cell lines reported the same value

Analysis of Table 3 shows that while compound **27** is not quite as active as the natural products, in particular (+)-CC-1065 (**1**) and Anthramycin (**20**), they do display greater activity than both Chlorambucil (**17**) and Procarbazine (**49**), which are currently on the market. Overall, both the *cis* and *trans* isomers of compound **27** display fairly high biological activity. The general ranking of activity for all 8 compounds: **49** > **1** > **20** > *trans* **27** > **47** > *cis* **27** > **17** > **48**. Analysis of Table 3 indicates that the leukemia and non-small cell lung cancer panels are the two most susceptible to the *trans* compound **27** whereas the *cis* isomer displays its maximum activity against the leukemia and the renal panels.

Attempts at Exocyclic Functionalization of 27

An investigation towards the functionalization of the benzo ring system was undertaken, which could be used to install the linking amides that Dervan *et al*. have reported.[34-38]

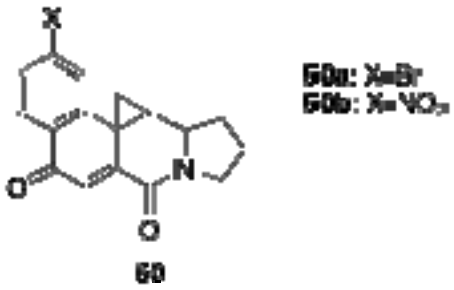

Figure 20: Functionalization of C-2 on the Benzo Ring System

With that in mind the study was focused towards the synthesis of compound **50**, which could contain either the bromo or nitro moiety at the C-2 position. Buchwald *et al*. have reported that the aryl halides can be transformed into various amines through the Buchwald-Hartwig reaction (Scheme 10).[49-50] The installation of the nitro group would

allow for a simple selective reduction of the nitro functionality to the amine moiety thereby bypassing the extra synthetic step(s).

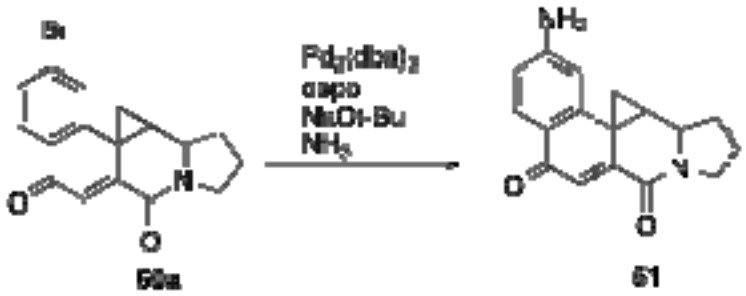

Scheme 10: General Procedure of the Buchwald-Hartwig Reaction

Installation of the amine **51** would then allow for the coupling of Dervan's agents (Py, Hp, or Im), which would hopefully impart DNA sequence selectivity as was mentioned earlier. The initial ideas into the functionalization of the benzo ring were envisioned coming from the Diels-Alder reaction between anthranilic acid **32**, which would be suitably functionalized and the furan **31** (Scheme 11).

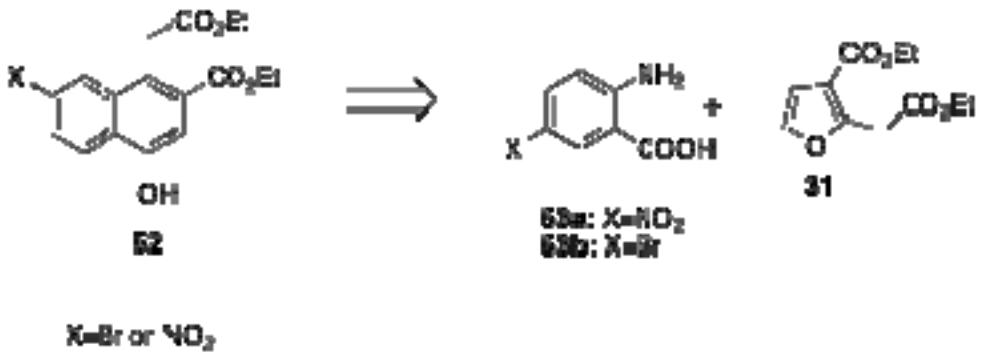

Scheme 11: Retrosynthetic Analysis of Compound **52**

Scheme 12: Bromination of Anthranilic Acid (**32**)

Following the procedure of Wheeler, anthranilic acid (**32**) was stirred in glacial acetic acid and bromine for several hours followed by several fractional recrystallizations to furnish compound **53b** (Scheme 12). Literature preparation of the 4-bromoanthranilic acid (**53b**) occurred in 50% yield.[51] The identity and purity of the bromo anthranilic acid (**53b**) was confirmed by melting point comparison to the reported value.

The nitroanthranilic acid (**53a**) was commercially available; however, it failed to undergo the Diels-Alder reaction with compound **31** (Scheme 13). This was attributed most likely to the nitro benzyne not forming or its subsequent decomposition before the reaction could take place.

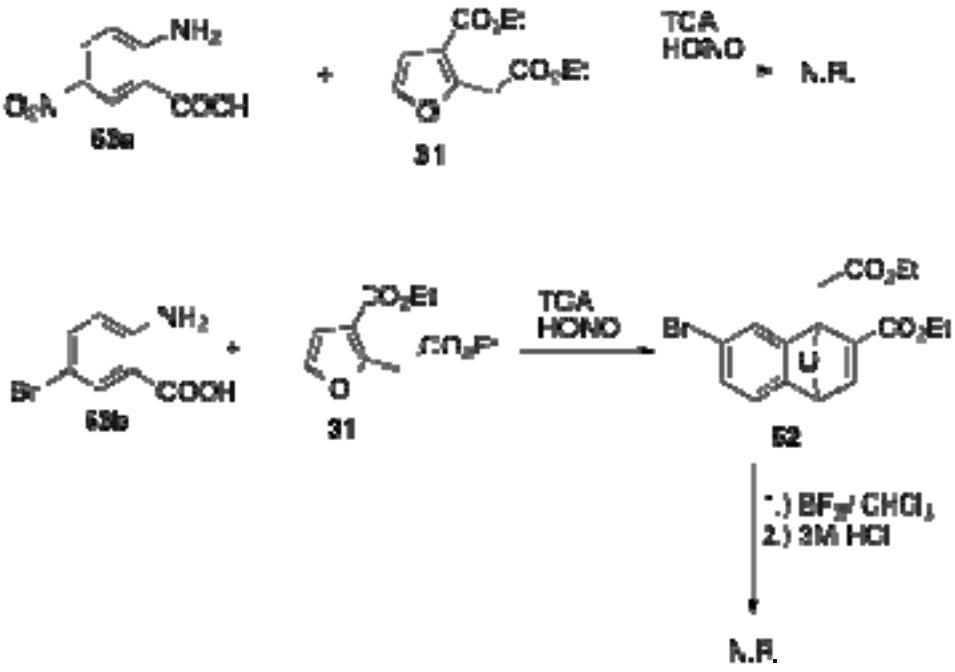

Scheme 13: Attempted Diels-Alder Reactions

Formation of the bromo benzyne appeared to occur, as the bromo epoxy intermediate **52** was isolated and characterized by ^{1}H NMR. However, several attempts (BF_3 and 3M HCl) failed to open the epoxy ring of **52** under standard conditions resulting

in the recapturing in starting material. The inability to produce the properly functionalized phenol containing either the bromo or nitro functionality by this route led to the consideration of alternate synthetic routes (*vide infra*).

AutoDock 3.0 Modeling Studies

An Octane model SGI computer using an IRIX64 operating system with a 270 MHz MIPS R12000 processor was used to perform the modeling studies. A SYBYL program was utilized to prepare all molecules and the active site prior to docking, which was performed using AutoDock 3.0. AutoDock Tools was used to visualize each of the predicted binding conformations within the Duocarmycin SA active site. Having established the validity of the AutoDock program as well as the parameters used during the course of the docking runs, the program was used to model novel compounds for possible future synthetic work.

All energies reported are from the lowest energy conformer, which may or may not be the optimal binding conformer. X-ray coordinates for Duocarmycin SA (**3**) were taken from the Brookhaven Protein Data Bank (PDB). Sybyl was used to extract the drug molecule and all water molecules from the active site. The parameters established by Sobhani *et al*. were followed in order to prepare the active site and all compounds prior to the modeling studies.[43]

Preliminary Studies

The dsDNA sequence of the receptor was 5′-G14-G13-A12-A11-A10-A9-G8-3′ to which Duocarmycin SA (**3**) preferentially alkylated at the N3 of (A12). The

Duocarmycin SA (DSA) receptor was chosen given its similarity in size to compounds **28** and **27**. The initial work focused on determining the ability of AutoDock 3.0 to accurately reproduce the X-Ray crystal structures of several natural products. The natural products Duocarmycin A (**2**), Duocarmycin SA (**3**), Netropsin (**11**) Distamycin A (**12**), and Anthramycin (**20**) were all chosen for the preliminary studies (Figure 21).

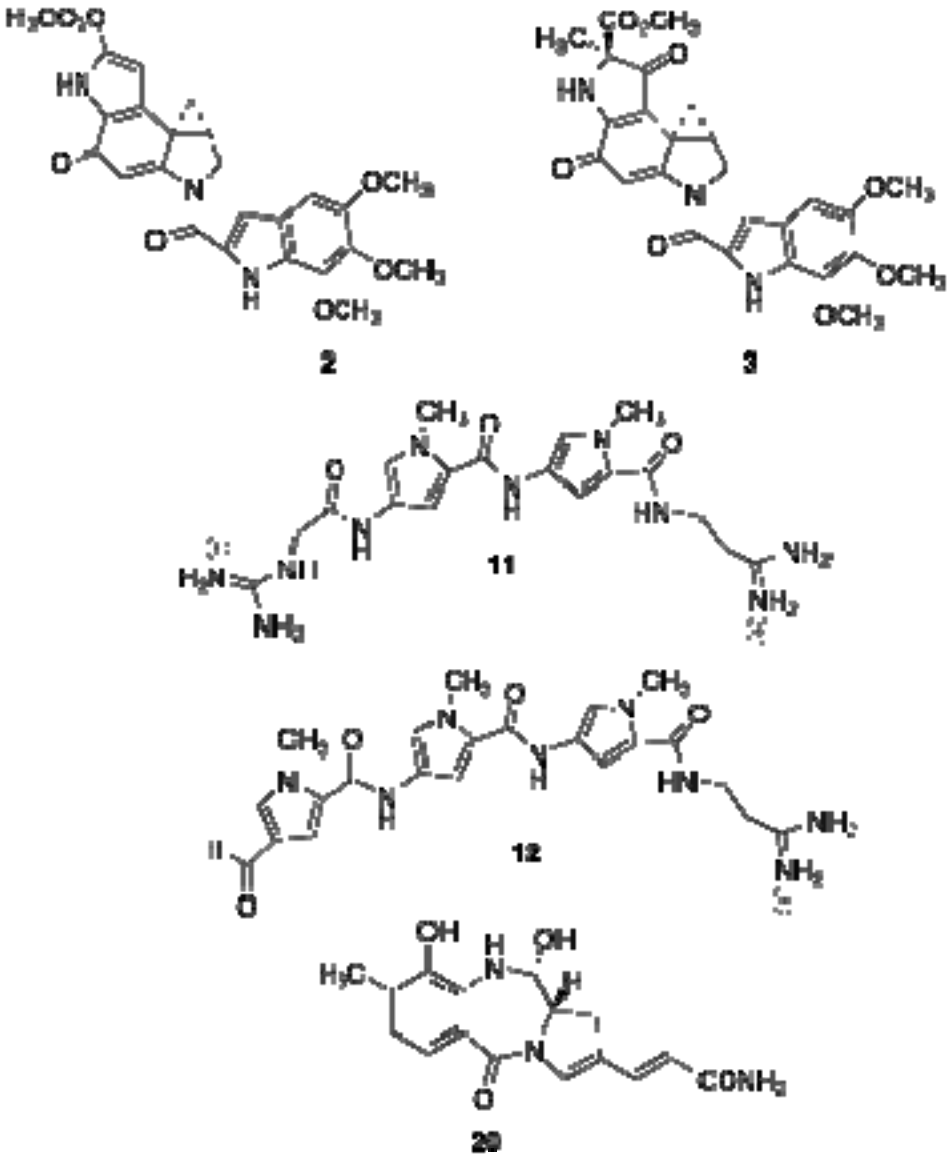

Figure 21: Natural Products

Each of the natural products were docked in the DSA receptor and the low energy conformer was then taken and overlapped with its X-Ray crystal structure, which was obtained from the PDB. Table 4 lists the root mean squared deviations (RMSD) of the natural products. The lower the RMSD values the more closely the modeled compound

matched their X-Ray crystal structures. All compounds were found to be within acceptable ranges.

Compound	RMS Calculated (Å)
Duocarmycin A (**2**)	1.102
Duocarmycin SA (**3**)	2.344
Distamycin A (**12**)	1.283
Netropsin (**11**)	2.122
Anthramycin (**20**)	1.105

Table 4: RMSD Values for Natural Products

Evaluation of Distamycin A (**12**) was chosen as a model for how accurate AutoDock was in reproducing the X-Ray crystal structure for each of the natural products. Compound **12** has been shown to recognize and bind a 5 base pair sequence of AT nucleotides. This recognition is thought to occur by close van der Waals contacts between the adenine C-2 atoms with both C-H atoms on each of the three successive pyrrole rings of the ligand. Also, the CH_2 atoms that extend between the amidine functionality and the terminal amide off the terminal pyrrole also participate in these van der Waals interactions. The hydrogen bonds provide the binding energy and correct reading frame by properly positioning the drug molecule within the minor groove, with its crescent-shape nicely following the right-handed twist of the groove.

Two of the three pyrroles projected the methyl groups away from the floor of the minor groove. The third pyrrole needed a slight rotation (about 20º) to correctly project the methyl group out of the minor groove. Also noteworthy was the similarity in which

AutoDock oriented the Distamycin A (**12**) ligand so that the hydrogen bonds and van der Waals contacts mirrored those of its X-ray crystal structure.

(+)-CC1065, Duocarmycin A, Duocarmycin SA, and their *N*-Boc Derivatives

(+) CC1065 (**1**), Duocarmycin A (DA, **2**), and Duocarmycin SA (DSA, **3**) are all known to recognize a 4-5 base pair sequence of AT-rich DNA (Figure 22); however, they irreversibly alkylate DNA unlike Distamycin A (**12**), which is a non-covalent binder.

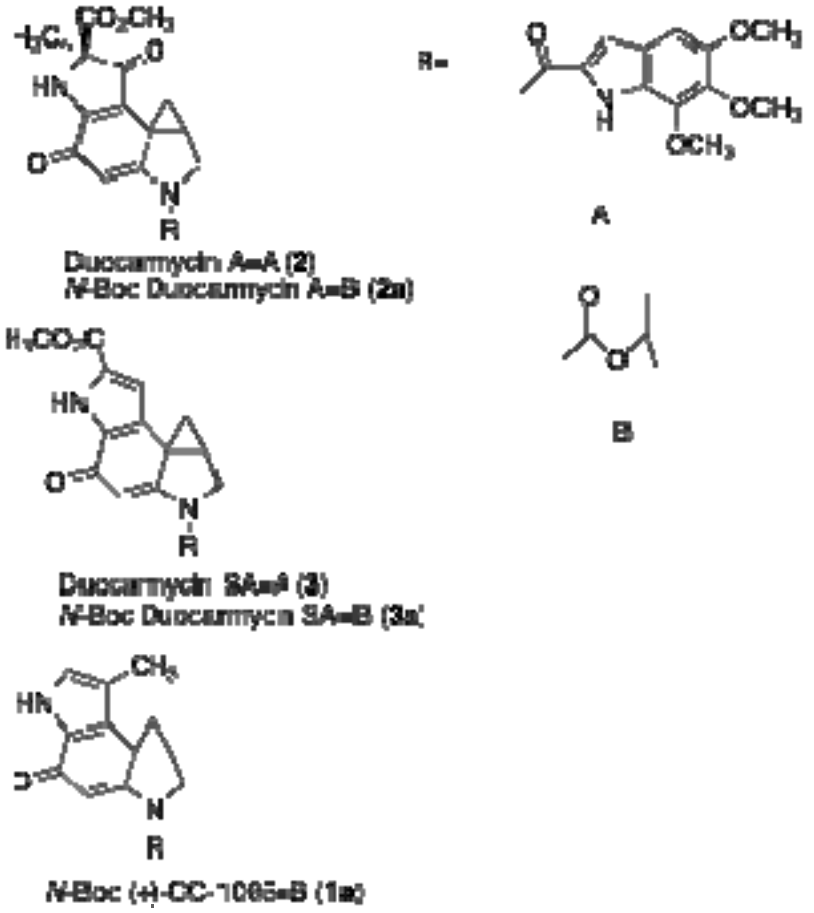

Figure 22: Natural Products and their *N*-Boc Derivatives

Each compound contains a reactive cyclopropane ring that is alkylated by a stereoelectronically-controlled addition of N3 of adenine to the least hindered carbon on

the cyclopropyl ring. The flexible amide bonds impose the necessary right-handed twist, which is required to follow the curve of the minor groove.

Kopka *et al*.[26] have reported that close van der Waals contacts between the drug molecule and the minor groove are primarily responsible for allowing the nucleotide specificity, and that the hydrogen bonds act to properly orient the molecule within the minor groove.

As was stated earlier, AutoDock calculates two different types of energies: docking energy (DE) and binding energy (BE) or free energy of binding. Docking energies are those, which include the intermolecular and intramolecular interaction energies, and are used, in the docking experiments. A global energy minimum is calculated for the ligand and the drug-receptor system and is treated as a rigid body with only the steric interactions involved between the energy minimized drug and the receptor taken into account. The second, binding energy, includes the intermolecular energy and torsional free energy and are reported at the end of the docking experiment. This binding energy is directly related to the inhibition constant (k_i). Table 5 lists the docking and binding energies as well as the predicted k_i of several natural products, their *N*-Boc derivatives and compounds **28** and **27**.

Compound	Docking Energy (kcal/mol)	Binding Energy (kcal/mol)	K_i (M) Predicted
Distamycin A (**12**)	-53.20	-50.61	8.02×10^{-38}
Duocarmycin A (**2**)	-18.32	-19.75	3.32×10^{-15}
N-Boc-Duo A (**2a**)	-13.24	-13.65	9.83×10^{-11}
Duocarmycin SA (**3**)	-16.50	-16.17	1.39×10^{-12}
N-Boc-Duo SA (**3a**)	-12.37	-13.06	2.67×10^{-10}
N-Boc-(+)-CC-1065 (**1a**)	-11.34	-12.23	1.08×10^{-9}
Anthramycin (**20**)	-14.31	-13.94	6.07×10^{-11}
5 *Cis* (**28**)	-12.34 (B Strand -11.4)	-12.34	8.97×10^{-10}
5 *Trans* (**28**)	-12.16 (A Strand -9.63) (B Strand -10.6)	-12.16	1.22×10^{-9}
6 *Trans* (**27**)	-12.77 (B Strand -11.8)	-12.77	4.34×10^{-10}

Table 5: Docking Results of Natural Products

The data reported for compounds **28** and **27** were the low energy conformers found by AutoDock; however, neither compound was oriented so as to allow for alkylation.

The program successfully docked DA **2** and DSA **3** within close proximity to their X-ray crystal structures as was determined by utilizing an atom-fitting program within SYBYL to calculate all relevant RMS values. Each of the drugs nicely followed the twist of the helix with their trimethoxy indole (TMI) subunits occupying a position that allowed for the TMI groups to project away from the floor of the minor groove. Substitution of the TMI subunit with a Boc group resulted in a noticeable drop in docking and binding energies for both Duocarmycins. However, it was seen that the replacement of the TMI with the smaller Boc group did not affect the proper orientation of the alkylation subunit into the floor of the minor groove.

Unlike the Duocarmycins (**2** and **3**); however, *N*-Boc-(+)-CC-1065 (**1a**) did not retain the proper binding orientation, which allowed the cyclopropyl ring to project deep into the groove. The cyclopropyl ring projected out of the groove with the vinylogous amide projecting towards the floor of the minor groove. A possible explanation has to do with the substitution of the pyrrole ring. On both compounds **2** and **3** there exists a bulky ester at C-7, whereas on (+)-CC-1065 (**1**) there is only hydrogen at C-7 and a relatively small methyl group at C-8. It appears that this bulk may play a pivotal role in the proper orientation of these drugs within the minor grove.

Compound	**Docking Energy (kcal/mol)**	**Renal A498**	**NSC HOP-62**	**Leukemia RPMI-8826**
(+)-CC-1065 (**1**)	N/A	-8.6	-8.7	-7.6
Anthramycin (**20**)	-14.31	-6.7	-7.7	-7.6
5 *Cis* (**28)**	-12.34	-5.91	-6.63	-N/A
5 *Trans* (**28**)	-12.16	-6.75	-6.42	-6.82
6 *Trans* (**27**)	-12.77	-6.61	<-8.0	-7.27
6 *Cis* (**27**)	N/A	<-8.0	-5.99	-6.74

Table 6: Known NCI Data for Compounds **28** and **27** and Selected Natural Products

Table 6 lists the three cancer cell panels/lines most susceptible to compounds **28** and **27** as well as the natural products **1** and **20** for comparison. Both isomers of compound **27** are more active than **28**. These results correlate with the docking energies predicted by AutoDock in which the *trans* isomer of **27** binds tighter than both isomers of **28**. While **1** and **20** display greater activity than either **28** or **27** in these particular lines it should be noted that (+)-CC-1065 (**1**) displays its greatest potency against the non-small cell panel/ line NCI-H460 with a value of -9.8. Anthramycin (**20**) displays its greatest activity against the breast cancer/ line HS578T with a value of -8.0.

Compounds 27 and 28

Docking of both compounds **28** and **27** resulted in a similar low energy binding orientation that was previously described for Anthramycin (**20**). The reactive cyclopropyl ring did not project into the groove instead allowing the amide carbonyl to situate itself

towards the floor while the fused benzene ring and cyclopropyl ring projected out of the groove. Analysis of the other docking runs performed on compounds **28** and **27** revealed two alternate binding conformations of higher energy than what is listed in Table 5. For *trans* compound **28** there were two alternate binding orientations that properly positioned the cyclopropyl ring into the minor groove. One orientation (DE=-9.63 kcal/mol) placed the drug in a manner to potentially alkylate the A strand, whereas the second orientation (DE=-10.6 kcal/mol) was capable of potentially being alkylated by the B strand. The overall energy difference between these orientations and the low energy conformer is approximately 1.66-2.53 kcal/mol. The *cis* isomer, on the other hand, only adopted one other binding conformation whereby the cyclopropyl ring was capable of being alkylated by the B strand (-11.4 kcal/mol) suggesting a preference for the *cis* versus the *trans* stereoisomer. Compound **27** only adopted one other binding orientation. The cyclopropyl ring was oriented into the minor groove on the B strand with a binding energy of -11.8 kcal/mol, which suggested that there was not a great discrepancy in how the molecule was oriented within this specific sequence of the minor groove.

External Ring Analogs Containing Linking Agents

at C-2 thru C-4, C-6, and C-10

All analogs were derived from the structure of compound **28** in order to cut down the computer time required for docking.

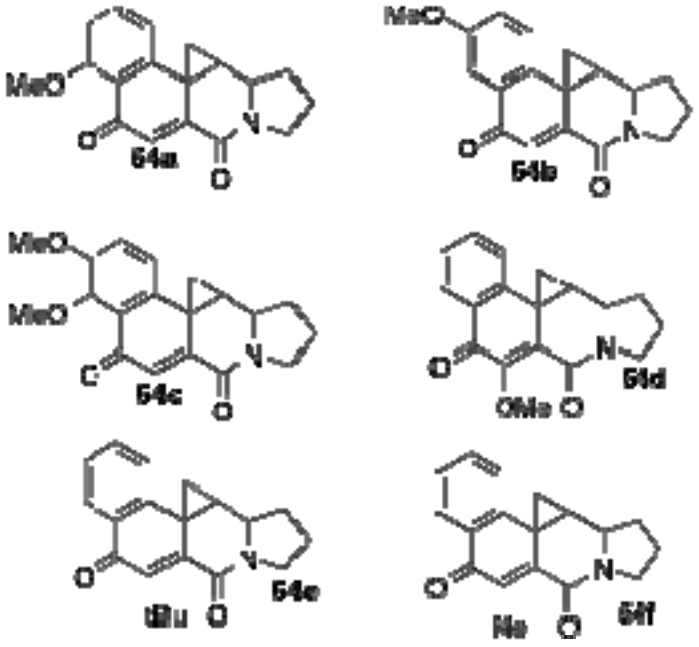

Figure 23: Bulky Substituents at C-3. C-4 and C-6 Positions

Initial analogs were proposed to see whether or not adding steric bulk could invert the molecule, which would allow for the cyclopropyl ring to be potentially alkylated. Initially, methoxy groups were added to the C-3, C-4, and C-6 positions; as well as, methyl and *t*-butyl moieties at C-6 (Figure 23).

Compound	Docking Energy (kcal/mol)	Binding Energy (kcal/mol)	K_i (M) Predicted
54a	-12.50	-12.68	5.12×10^{-10}
54b	-12.21	-12.36	8.68×10^{-10}
54c	-12.66	-12.92	3.37×10^{-10}
54d	-12.09	-12.16	1.21×10^{-9}
54e	-10.42	-11.14	6.78×10^{-9}
54f	-11.99	-11.55	3.43×10^{-9}

Table 7: Binding Data for Bulky Group Substituents

Evaluations of the results showed that **54d** was the only methoxy-containing analog that oriented the cyclopropyl ring towards the floor of the minor groove. The higher energies predicted for **54d** suggests that there are favorable enthalpic contributions

when the methoxy group is oriented into the minor groove however closer inspection did not reveal any obvious interactions. When the methoxy group was replaced with either the methyl (**54f**) or *t*-butyl groups (**54e**) at C-6 there was no loss of cyclopropyl orientation towards the floor of the minor groove and only slightly higher energies (Table 7). Also, analogs **54d**, **54e**, and **54f** were oriented in a manner that would allow for alkylation by either the T5 or T6 nucleotides. AutoDock predicted that the orientation of the cyclopropyl ring could be achieved by installing a functional group at the C-6 position with slight energy preferences for the polar methoxy moiety. The next series of analogs investigated involved the installation of various amides at the C-2 position (Figure 24).

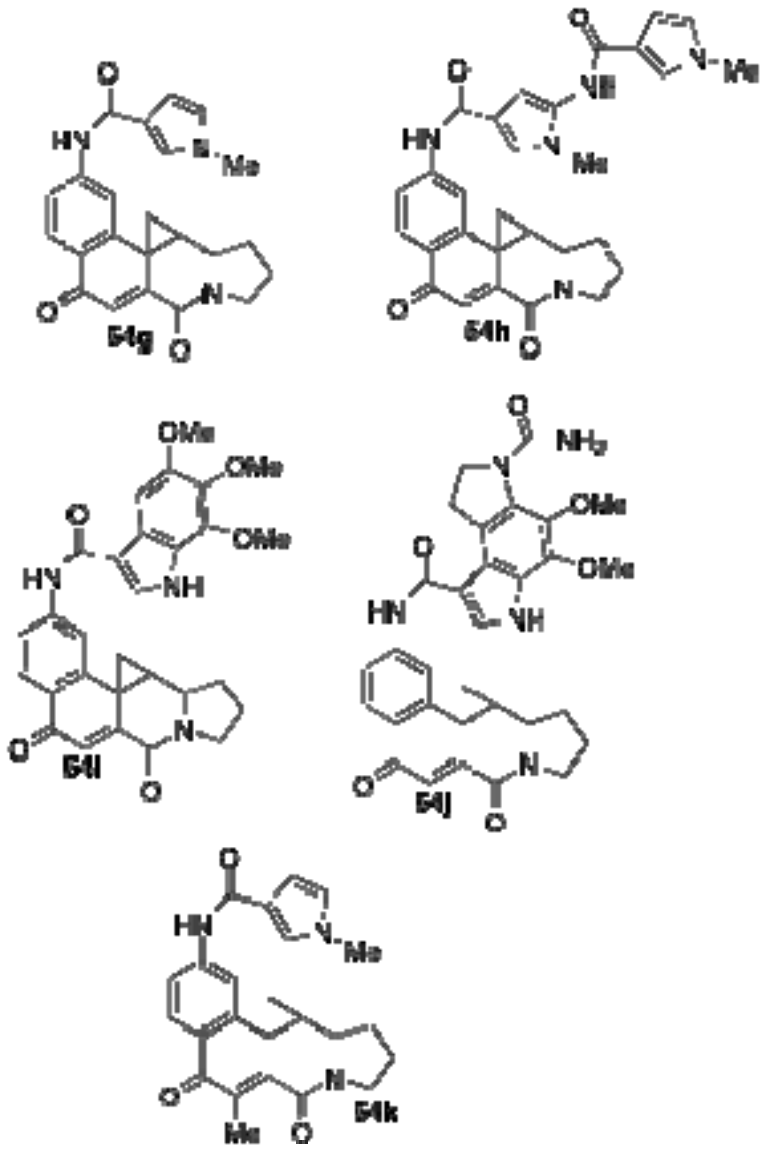

Figure 24: C-2 Exocyclic Ring Analogs

N-Methyl pyrrole, the TMI subunit from the Duocarmycins, and one of the pyrroloindole rings from (+)-CC-1065 (**1**) were used as linking groups at the C-2 position. Table 8 lists the results for each of the compounds. Every analog projected the cyclopropyl ring towards the floor of the minor groove. Analog **54k**, which contained a pyrrole linker and a methyl group at C-6, displayed the lowest energies of this series.

Compound	Docking Energy (kcal/mol)	Binding Energy (kcal/mol)	K_i (M) Predicted
54g	-13.06	-13.92	6.28 X10^{-11}
54h	-14.42	-15.41	5.08 X10^{-12}
54i	-11.57	-15.38	5.28 X10^{-12}
54j	-11.94	-15.53	4.10 X10^{-12}
54k	-15.10	-14.49	2.41 X10^{-11}

Table 8: C-2 Ring Analogs

Also, each of the analogs were positioned such that the *N*-methyl and *O*-methyl moities were projected out of the groove. Analogs **54i** and **54k** each oriented the cyclopropyl ring towards the N3 of (A11) while the other analogs projected the cyclopropyl ring to non-specific ribose oxygens within the minor groove. The functionalization of the C-10 position was subsequently investigated (Figure 25).

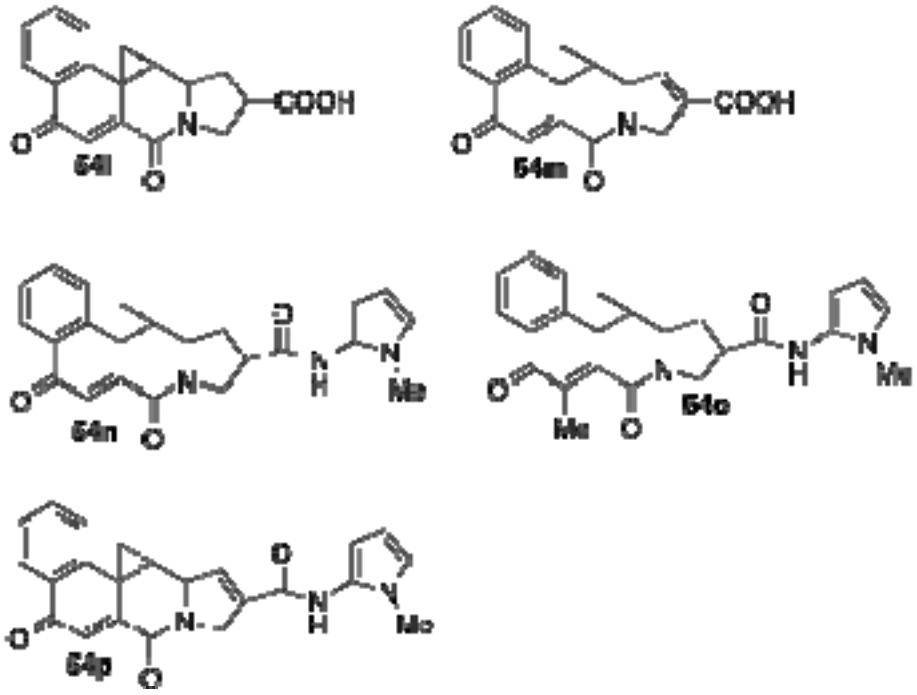

Figure 25: C-10 Exocyclic Ring Analogs

Only analogs **54m** and **54p** oriented the cyclopropyl ring with a position near T5 within the minor groove (Table 9). While the carboxylic acid functionality possesses the ability to form hydrogen bonds, the energy differences between **54l** and **54m** suggest that the double bond is not energetically favored.

Compound	**Docking Energy (kcal/mol)**	**Binding Energy (kcal/mol)**	**K_i (M) Predicted**
54l	-14.17	-14.19	3.97×10^{-11}
54m	-13.52	-13.45	1.39×10^{-10}
54n	-15.78	-15.82	2.55×10^{-12}
54o	-16.36	-15.94	2.08×10^{-12}
54p	-15.45	-15.07	9.03×10^{-12}

Table 9: C-10 Ring Analogs

The planarity that the alkene imparts in **54m** suggests that the pyrrolidine ring cannot adopt the proper orientation within the minor groove. The data suggests that the C-2 analogs are more likely to project the cyclopropyl ring within the minor groove than the C-10 analogs. The last couple of analogs in the exocyclic ring series involved the functionalization at both the C-2 and C-10 positions (Figure 26).

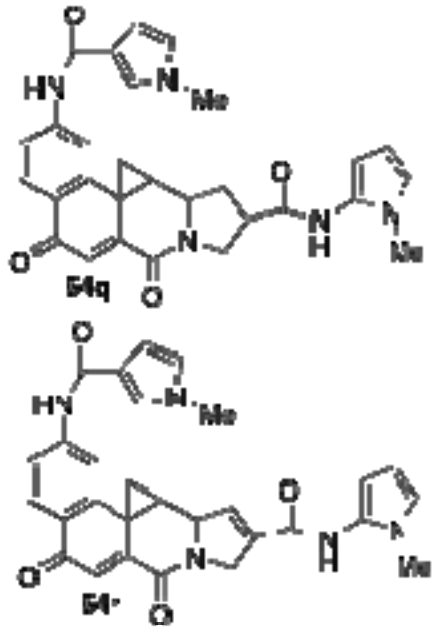

Figure 26: C-2 and C-10 Exocyclic Ring Analogs

Compound	**Docking Energy (kcal/mol)**	**Binding Energy (kcal/mol)**	**K_i (M) Predicted**
54q	-12.90	-13.03	2.79 X10^{-10}
54r	-11.82	-14.50	2.37 X10^{-11}

Table 10: C-2 and C-10 Exocyclic Ring Analogs

Neither **54q** nor **54r** were able to orient the molecule so that alkylation of the cyclopropyl ring may be achieved. This may be due to the rather large size of the molecules and their inability to "fit" within the active site. Based on the data, the most active compounds appear to have only one linking amide attached at the C-2 position with the C-10 position resulting in compounds with higher energy values (Table 10). Unlike the C-10 analog **54q**, when the pyrrolidine ring was partially planarized with the alkene (**54r**) the energy value decreased making it a tighter binder within the minor groove. This may be due to the double bond causing the *N*-methyl pyrrole to align itself more properly within the edge of the minor groove thereby minimizing any potential

steric interactions. Having completed the study on exocyclic ring analogs, the modeling was focused on installing endocyclic heteroatoms within the ring system at the C-2, C-10 and C-11 positions (Figure 27).

The quinoline nitrogen was installed at the C-1 position because it was thought that the N atom could help direct the alkylation towards the cyclopropyl ring by forming a hydrogen bond with the nucleophilic base pair within the minor groove. Also, the methoxy group was installed at the C-6 position for the reasons that were mentioned earlier. Hydrogen bond donors and acceptors were installed at the C-10 and C-11 positions in order to evaluate where and which kind of groups would be the most beneficial for increasing the binding of the agents within the minor groove. Table 11 lists the results for all 9 compounds that were modeled.

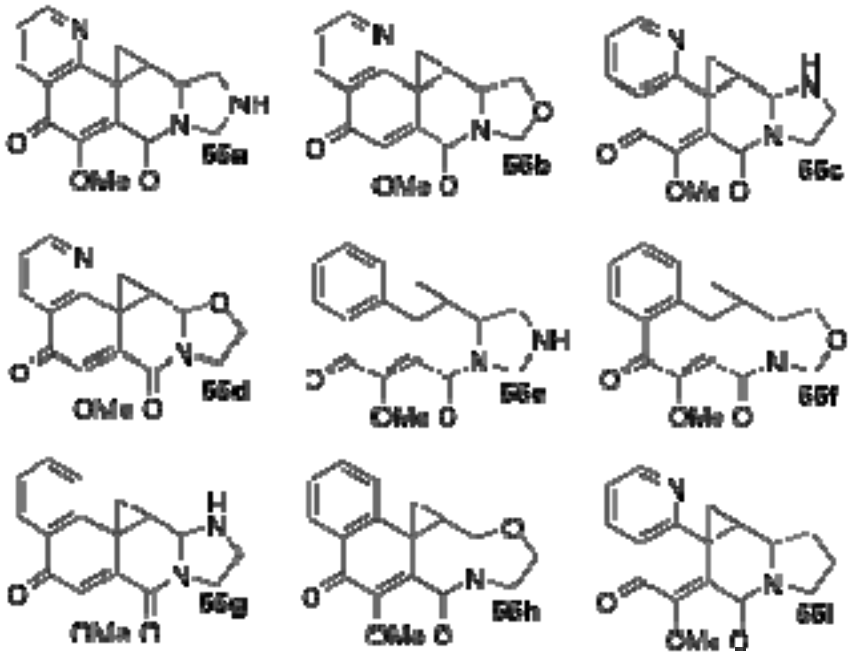

Figure 27: Endocyclic Ring Analogs

Compound	Docking Energy (kcal/mol)	Binding Energy (kcal/mol)	K_i (M) Predicted
55a	-12.25	-12.22	$1.11 X10^{-9}$
55b	-12.08	-12.08	$1.41 X10^{-9}$
55c	-13/07	-13.05	$2.70 X10^{-10}$
55d	-13.50	-13.50	$1.28 X10^{-10}$
55e	-11.99	-12.07	$1.42 X10^{-9}$
55f	-11.71	-11.66	$2.82 X10^{-9}$
55g	-12.80	-12.78	$4.28 X10^{-10}$
55h	-13.12	-13.13	$2.39 X10^{-10}$
55i	-12.09	-12.26	$1.04 X10^{-9}$

Table 11: Endocyclic Ring Analogs

Only analogs **55e** and **55i** failed to orient the cyclopropyl ring towards the floor of the minor groove. There was no base pair preference amongst any of the analogs. The quinoline nitrogen while it does have the capability of forming hydrogen bonds within the groove only contributes 0.15 kcal/mol of energy to the molecule (**55a** vs. **55e**). The placement of the heteroatom on the pyrrolidine ring appears to be critical to tighter binding. Analog **55c** contributes a binding energy (BE) of -13.05 kcal/mol whereas **55a** only displays a BE of -12.22 kcal/mol. Also, by substituting the NH for an O atom at the C-11 position (**55d**) the BE increase 0.45 kcal/mol in energy to -13.50. Analog **55d** was predicted by AutoDock to be the tightest binding agent containing the quinoline nitrogen and the O atom at the C-11 position on the pyrrolidine ring. These results are not unexpected within this active site, which mostly contains hydrogen bond acceptors from the adenine and thymine base pairs. Finally, the pyrrolidine ring was aromatized to the furan and pyrrole ring systems (Figure 28).

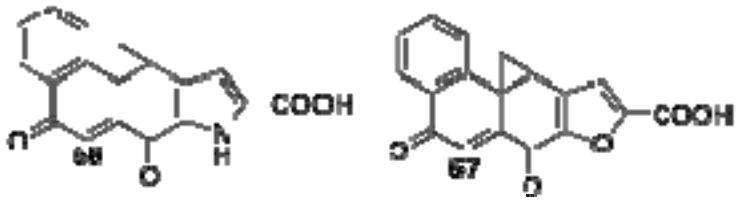

Figure 28: Aromatization of the Pyrrolidine Ring

Compound	**Docking Energy (kcal/mol)**	**Binding Energy (kcal/mol)**	**K_i (M) Predicted**
56	-13.67	-13.63	1.02×10^{-10}
57	-14.19	-14.02	5.33×10^{-11}

Table 12: Aromatized Pyrrolidine Ring Analogs

Of the two analogs only **56** oriented the cyclopropyl ring into the minor groove with the aromatic rings providing significant energetic benefits (Table 12). These analogs were modeled instead of compounds where the aromatic heteroatoms were placed at the C-11 position due to the synthetic difficulty that would be encountered should these compounds be selected for future synthesis.

GC-DNA Sequence

The next step was to determine if compounds **28** or **27** could/ or would display any selectivity for a GC base pair sequence. Utilizing SYBYL, a ten base pair double stranded sequence 5′-C-A-T-G-A-G-T-A-A-3′ was constructed. Anthramycin (**20**) was the first compound to be docked utilizing this sequence (Table 12) in order to establish a baseline for comparisons to be made. The strands of the double helix were labeled in order to simplify the discussion. Strand A contained the 5′-GAG-3′ sequence and the B strand contained the 3′-CTC-5′ sequence. Analysis of the docked runs of compound **20** revealed only one alternate binding site. Run 1 (-9.89 kcal/mol) oriented the imine

towards the N3 of adenine on the B strand. All other runs oriented the reactive imine species towards either the G4 or G6 on the A strand with very little energetic difference.

Compound	**Docking Energy (kcal/mol)**	**Binding Energy (kcal/mol)**	**K_i (M) Predicted**
Anthramycin (**20**)	-10.37	-9.88	5.77 $X10^{-8}$
5 *Trans* (**28**)	-8.19	-8.19	9.89 $X10^{-7}$
5 *Cis* (**28**)	-9.16 (B Strand -8.8)	-9.16	1.93 $X10^{-7}$
6 *Trans* (**27**)	-8.87 (A Strand –8.05)	-8.87	3.14 $X10^{-7}$
6 *Cis* (**27**)	-9.56	-9.56	9.85 $X10^{-8}$
54f	-7.81	-7.77	2.03 $X10^{-6}$
55a	-7.77	-7.78	1.99 $X10^{-6}$
55b	-7.39	-7.35	4.12 $X10^{-6}$
55c	-8.21	-8.22	9.46 $X10^{-7}$
55d	-8.18	-8.19	9.93 $X10^{-9}$
55e	-7.76	-7.71	2.24 $X10^{-6}$
55f	-7.46	-7.42	3.66 $X10^{-6}$
55g	-8.21	-8.16	1.05 $X10^{-6}$
55h	-8.19	-8.14	1.08 $X10^{-6}$
55i	-7.71	-7.66	2.41 $X10^{-6}$

Table 13: GC DNA Docked Compounds

Compound **20** followed the curve of the groove with its C-11 imine carbon approaching the ideal 180º angle for backside attack of the corresponding N2 of guanine (G6) on the A strand. Stabilizing hydrogen bonds could be seen between the phenolic hydrogen and O1 (C5, 2.2 A) with the methyl group projecting out of the groove. The acrylamide wound its way up the helix forming hydrogen bonds with O1 (C7, 2.1 A) and N2 (G4, 2.56 A). Both carbonyls correctly oriented themselves out of the groove.

Compounds **28** and **27** were then docked within this GC-rich sequence (Table 13). Both **28** and **27** projected the cyclopropyl rings towards the floor of the minor groove. Unlike the AT-rich DNA, the cyclopropyl ring was projected towards N2 of guanine. Of

the 10 docking runs that were performed on each compound eight of the conformers were found to selectively prefer guanine with a 50:50 preference for G4 versus G6. Both *cis* and *trans* isomers of the compounds **28** and **27** were docked. For the isomers of **28** there were no alternate binding orientations for the *trans*, and only one for the *cis* isomer. Run 9 of the *cis* isomer oriented the cyclopropyl ring towards cytosine on the B strand (-8.8 kcal/mol). Compound **27** was just the opposite with no alternate binding sites for the *cis*, but one for the *trans*. Run 4 showed the cyclopropyl group near N3 (A3, -8.05 kcal/mol). The overall conclusion drawn from both the 5 and 6 membered compounds were that they both preferred the guanine bases within this stretch of DNA. However, it cannot be discounted that energetically both series preferred the AT-rich versus the GC-rich by roughly 2-2.5 kcal/mol, although neither series displayed the ability to orient the cyclopropyl rings towards the floor of the minor groove. Compounds **28** and **27** each spanned a three base pair sequence with the cyclopropyl group of **27** sitting slightly further away from N2 (G4, 3.0 A) than **28** (2.8 A).

The endocyclic analogs were the only series from the previous AT-rich series to be modeled because of their ability to more frequently position the cyclopropyl ring within the minor groove. Only analog **55i** was unable to orient the cyclopropyl ring towards the floor of the minor groove. Also, the C-11 position was found to be the more energetically beneficial as was discussed earlier. However, unlike the previously described preference for the O vs. NH atoms in the pyrrolidine ring, within the GC-rich sequence it was the NH moiety, which was preferred.

Overall results for the modeling studies suggest several trends: first, the C-2 exocyclic analogs were energetically favored over the C-10 position analogs, second,

although not energetically favored the endocyclic analogs consistently projected the cyclopropyl ring in both the AT and GC-rich DNA sequences towards the floor of the minor groove. Within the endocyclic analogs, the quinoline nitrogen does not appear to contribute (energetically) as significantly as the heteroatoms on the pyrrolidine ring. The C-11 position is favored in both AT and GC-rich DNA with the O being favored in the AT regions and NH favored in the GC-rich regions.

The results of the AutoDock work led to several potential agents that could be synthesized in future work. With the results of the modeling studies it became apparent that alternate synthetic routes would be needed in order to construct these compounds.

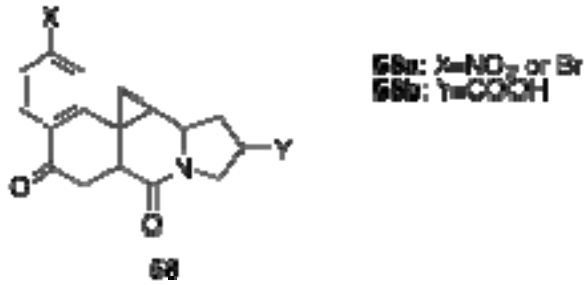

58

Figure 29: Functionalization of Compound **28** (**58**)

The design and synthesis of novel synthetic routes, which would allow for the functionalization of the aromatic ring system as well as the pyrrolo ring was the primary aim resulting from these modeling studies (Figure 29).

Following previous synthetic efforts reported by Reddy *et al.*[44] it was demonstrated that both functionalization of the benzo ring system and stereochemical control could not be achieved. Alternate methodologies were investigated to address these shortcomings. Functionalization allows for greater synthetic flexibility in either the

benzo or pyrrolo ring systems. The functionalization allows for the installation of Dervan's amino acids.

Synthetic studies towards 9, 10, 11, 11a, 11b, 12-

Hexahydrobenzo[*f*]cyclopropa[*d*]pyrrolo[1,2-*b*] isoquinoline-5,7-dione (28)

The initial retrosynthetic analysis of compound **28** suggested that it could arise from the benzyl mesylate **96** by debenzylation followed by base-catalyzed intramolecular cyclization conditions (Scheme 14).

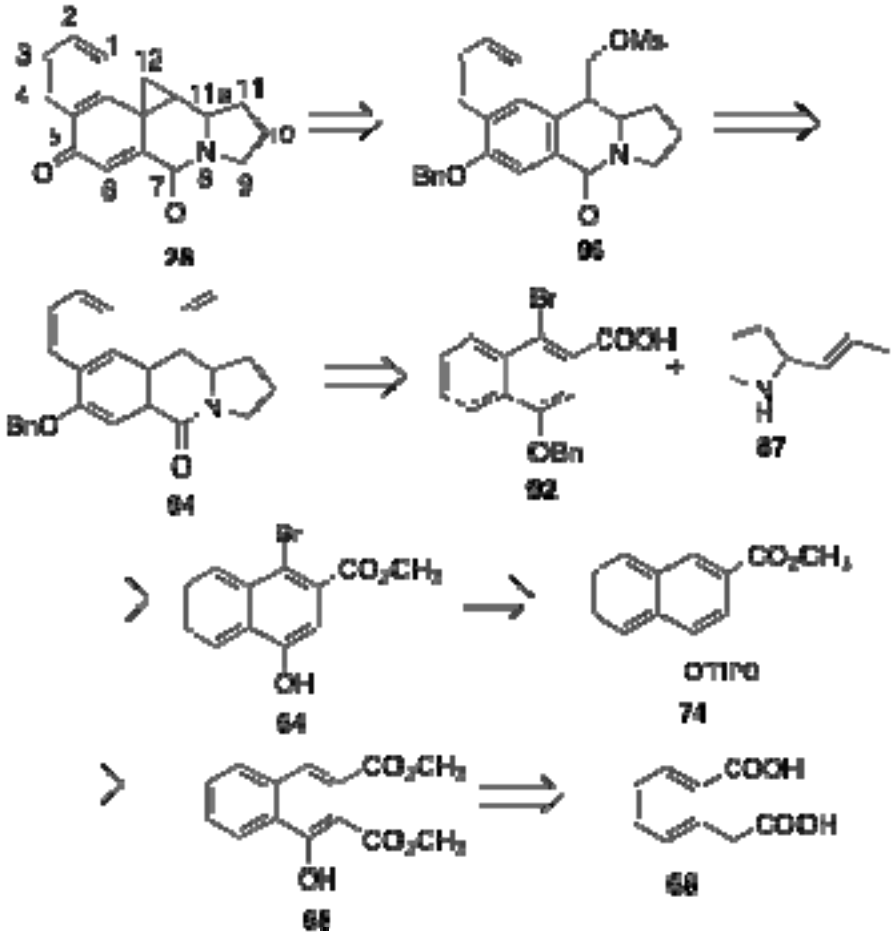

Scheme 14: Retrosynthetic Analysis of Compound **28**

It was anticipated that the mesylate **96** could arise from the vinyl pyrrolo compound **94** by undergoing an oxidative cleavage reaction followed by mesylation of the resulting alcohol. It was thought that compound **94** could be obtained through a simple condensation reaction between compound **92** and propenyl pyrrolidine **87**. The bromo acid **92** was envisioned coming from the bromo phenol **64** by undergoing benzylation followed by ester saponification under standard conditions. The bromo phenol **64** was envisioned coming from a controlled bromination of the silyl ester **74** followed by a simple desilylation reaction. Compound **74** was thought to arise from the starting dimethyl ester **68** by a simple hydrolysis and decarboxylation reaction under basic conditions followed by esterification and silyl protection by protection of the phenol **63**. Finally, compound **68** was envisioned coming from a Diels-Alder-like reaction involving homophthalic anhydride (**67**) and dimethylacetylene dicarboxylate. The homophthalic anhydride (**67**) was thought to arise by refluxing the starting homophthalic acid (**67**) in acetyl chloride for several hours.

The bromo acid **92** was identified as a key intermediate during the retrosynthetic analysis, so initial studies involved investigating the methodology for its production. Early synthetic efforts followed the procedure of Boger *et al*., which reported a synthetic route into the bromo ester **65**. (Scheme 15).[52] Starting from benzaldehyde (**59**), a Wadsworth-Horner-Emmons reaction could furnish the α,β-unsaturated ester **60** followed by acid catalyzed cleavage of the *tert*-butyl ester to afford compound **61** in 73% overall yield. Compound **61** was then stirred in acetic anhydride to give the cyclyzed acetate intermediate **62**, which was subsequently deprotected to give the phenol ester **63** in 90% yield.

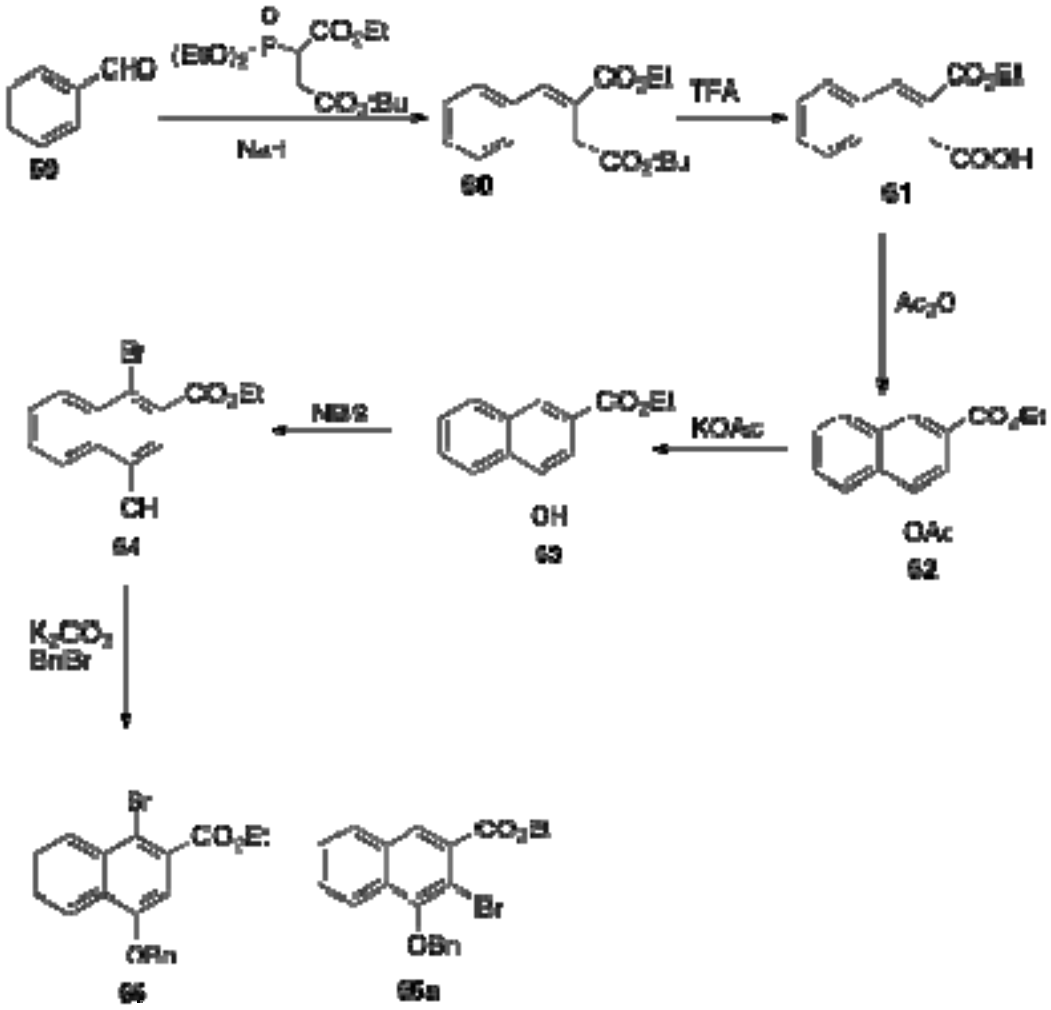

Scheme 15: Boger's Route into the Bromo Ester (**65**)

Bromination of the phenol **63** was carried out using *N*-bromosuccinimide followed by benzylation of the phenol to furnish the desired ester **65** in 74% overall yield. Boger and co-workers have reported X-Ray data for similar compounds made by alternate syntheses; however, no X-ray data was reported for this route. This led to the question of regiochemistry for the bromine atom (**65** vs. **65a**). An alternate route was investigated in order to address this question.

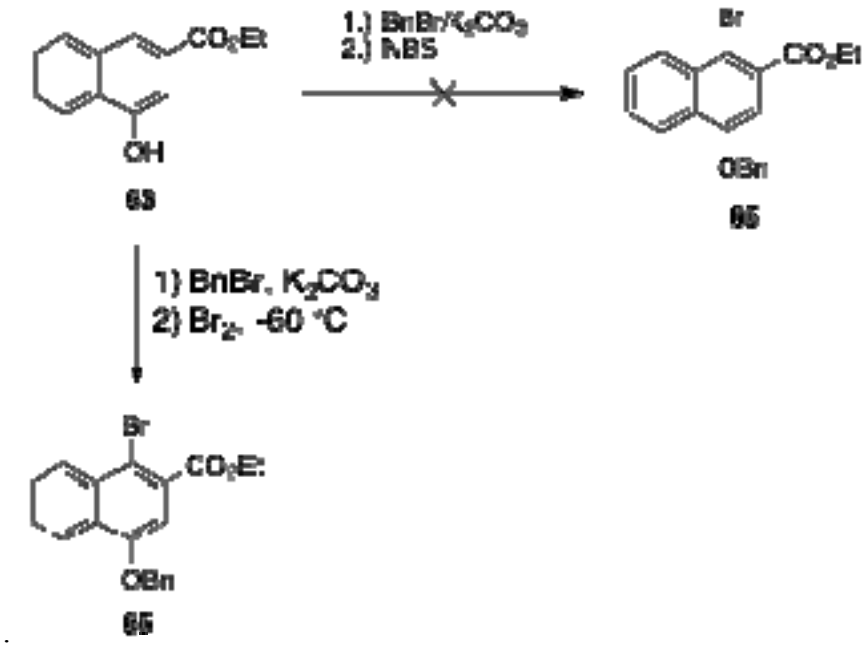

Scheme 16: Alternate Routes into Bromo Ester **65**

Benzylation of the phenol **63** followed by bromination using *N*-bromosuccinimide failed to give the desired bromo ester **65**. This was attributed to the relatively low bromine concentration that is generated using the *N*-bromosuccinimide reagent. The benzylated intermediate was then cooled to -60 °C and treated with liquid bromine, which furnished bromo ester **65** in 44% yield (Scheme 16). The moderate yield was attributed to the formation of multiple side products generated from over bromination of the naphthalene and benzyl ring systems. Figure 30 shows the ^{1}H NMR of **65a** produced in Scheme 15. The aromatic proton appeared at 7.67 ppm as a singlet with all other protons accounted for. A literature search for similar compounds was pursued so that ^{1}H NMR comparisons could be made. This led to 1,4-dihydroxy naphthoic acid (**76**), which showed a singlet at 7.01 ppm for the H-3 proton. This suggested that the bromo ester **65a** produced by Boger's route might contain the wrong regioisomer.

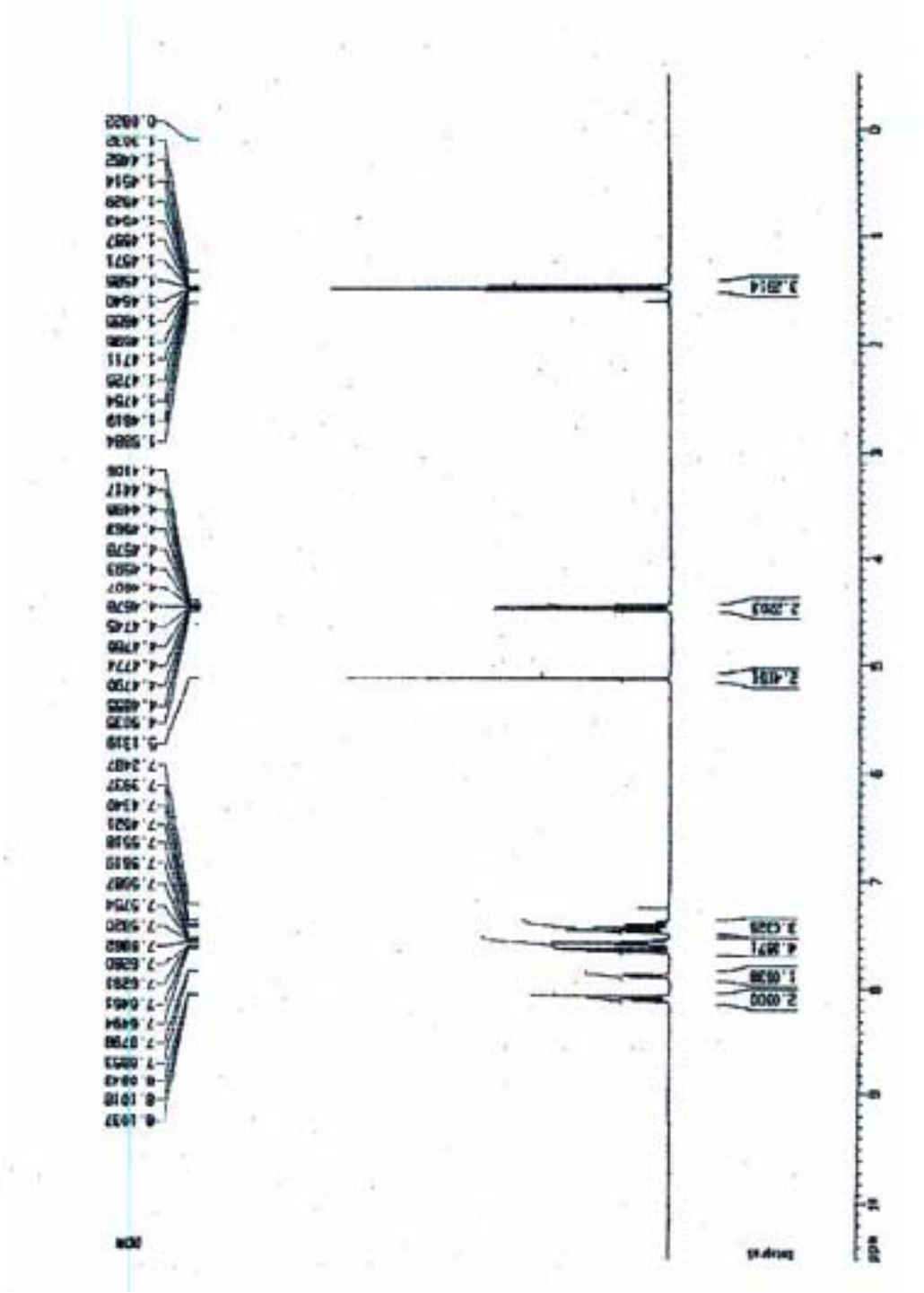

Figure 30: ^{1}H NMR of **65a**

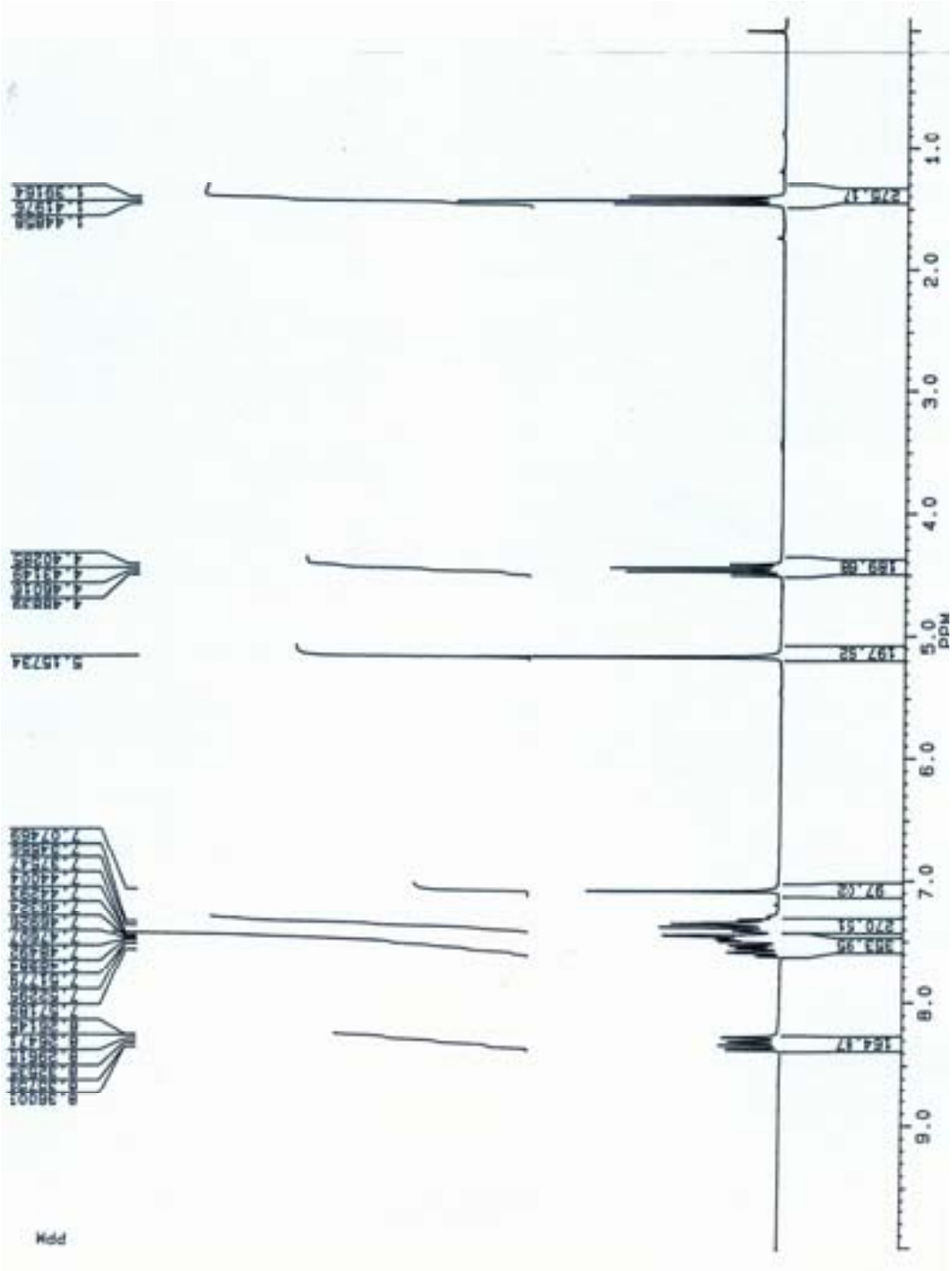

Figure 31: ^{1}H NMR of **65**

Figure 31 shows the proton spectra of compound **65**. The H-3 proton appears as a singlet at 7.07 ppm. The confirmation of the compounds being regioisomers was

confirmed using GCMS and melting point data. They both displayed an m/z of 386 confirming that both compounds contained the same elemental formulas. Boger's compound **65a** melted at 65-66 °C while compound **65** melted between 54-57 °C indicating that these compounds were indeed regioisomers. Finally, both compounds were submitted for X-Ray crystal diffraction, which provided the final evidence that compounds **65** and **65a** were regioisomers (Figures 32 and 33).

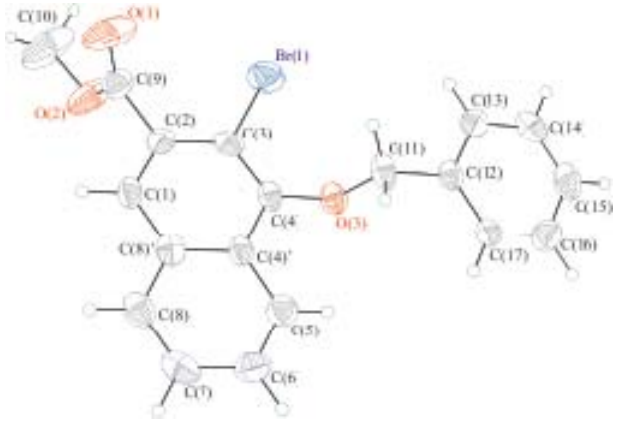

Figure 32: X-Ray Crystal Structure of **65a**

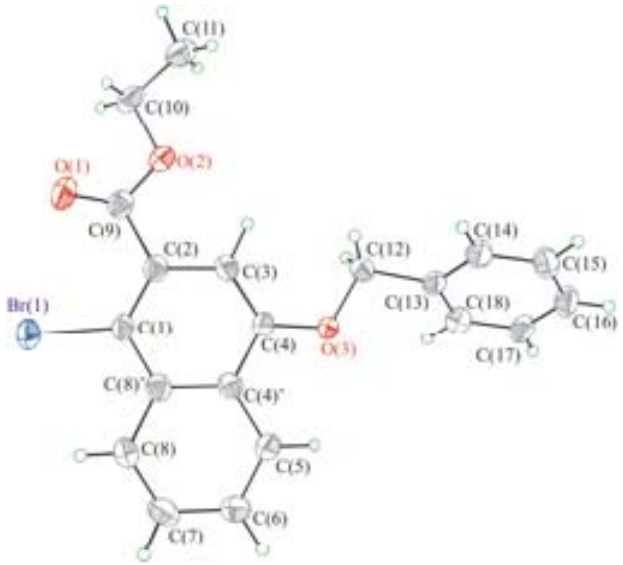

Figure 33: X-Ray Crystal Structure of **65**

With the question of regiochemistry settled, the focus was switched to developing an alternate route into **65** that could give improved yields. Initial ideas involved using the commercially available homophthalic acid (**66**) as the starting material (Scheme 17).

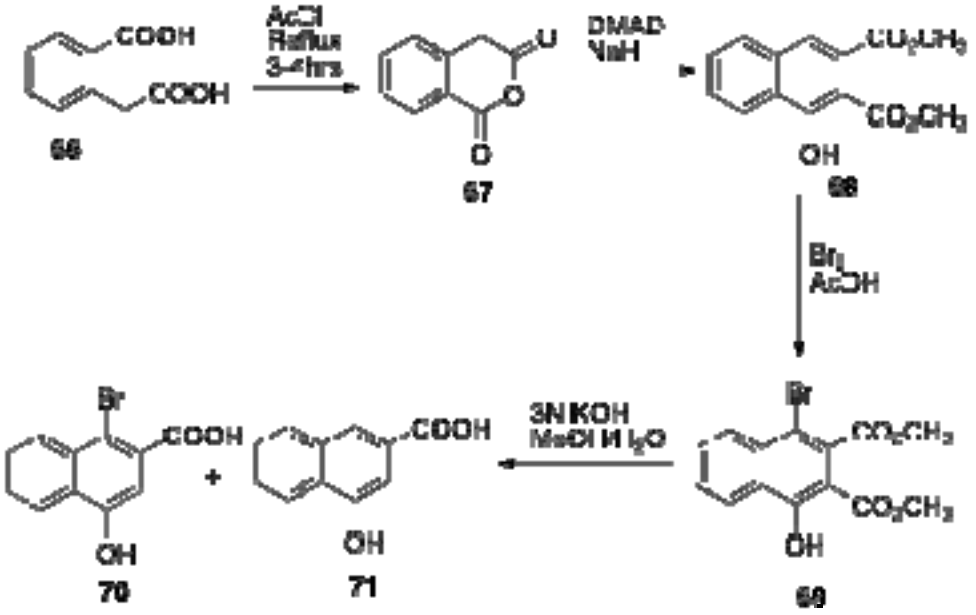

Scheme 17: DMAD Route into Bromo Acid **70**

Following the procedure of Tamura *et al*., the synthesis began by refluxing homophthalic acid (**66**) in acetyl chloride for 3-4 hours to give the anhydride **67** in 95% yield.[53] Compound **67** was then taken up in anhydrous tetrahydrofuran and allowed to stir at room temperature for several hours in the presence of sodium hydride and dimethylacetylene dicarboxylate to afford the dimethyl ester **68** in 54% yield. With the C-3 position blocked, bromination occurred smoothly to give compound **69** in 85% yield. The hydrolysis and decarboxylation presented an unanticipated problem. According to GCMS data roughly a 50:50 ratio of the bromo acid **70** and debrominated acid **71** were found. Since these compounds displayed the same R_f values this route was not pursued further due to the inability to separate them chromatographically.

The investigation focused on the installation of a bulky non-electrophilic group, which could direct the bromination to the C-1 position. The *tert*-butyldimethyl silyl moiety was chosen as a protecting group for the phenol for several reasons. First, the group could withstand the conditions necessary for bromination, and secondly, the large *t*-butyl group could act to block the C-3 position by its steric bulk thus promoting bromination at C-1 (Scheme 18).

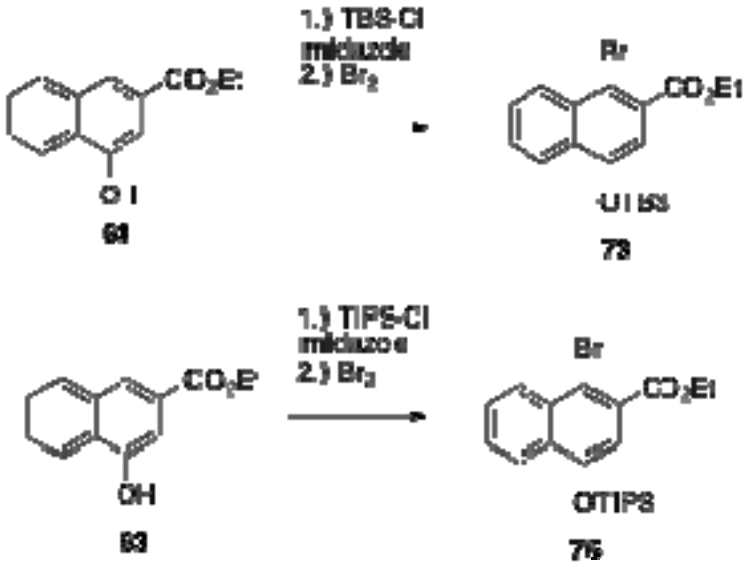

Scheme 18: Installation of Silyl Protecting Groups

The *t*-butyl group proved too labile as it spontaneously decomposed upon standing and, thus, resulted in a mixture of products upon bromination. Tri*iso*propylsilyl chloride was investigated for use as an alternative-protecting agent. Silylation and bromination of compound **62** occurred smoothly to give the desired bromo ester **75** in 82% overall yield. The bromination of **75** was carefully monitored by GCMS in order to monitor the completion of the reaction and also to determine if any dibrominated material was formed. The GCMS showed a m/z of 436/438 in a 50:50 ratio confirming the

appearance of a brominated product. The bromosilyl ester **67** was then submitted for ^{1}H NMR in order to confirm that the correct regioisomer was produced. A singlet for the C-3 proton occurred downfield at 7.11 ppm, which matched the previously reported NMR data. In order to assess the usefulness of this scheme another route was investigated which involved the use of 1, 4-dihydroxy-2-naphthoic acid (**76**).

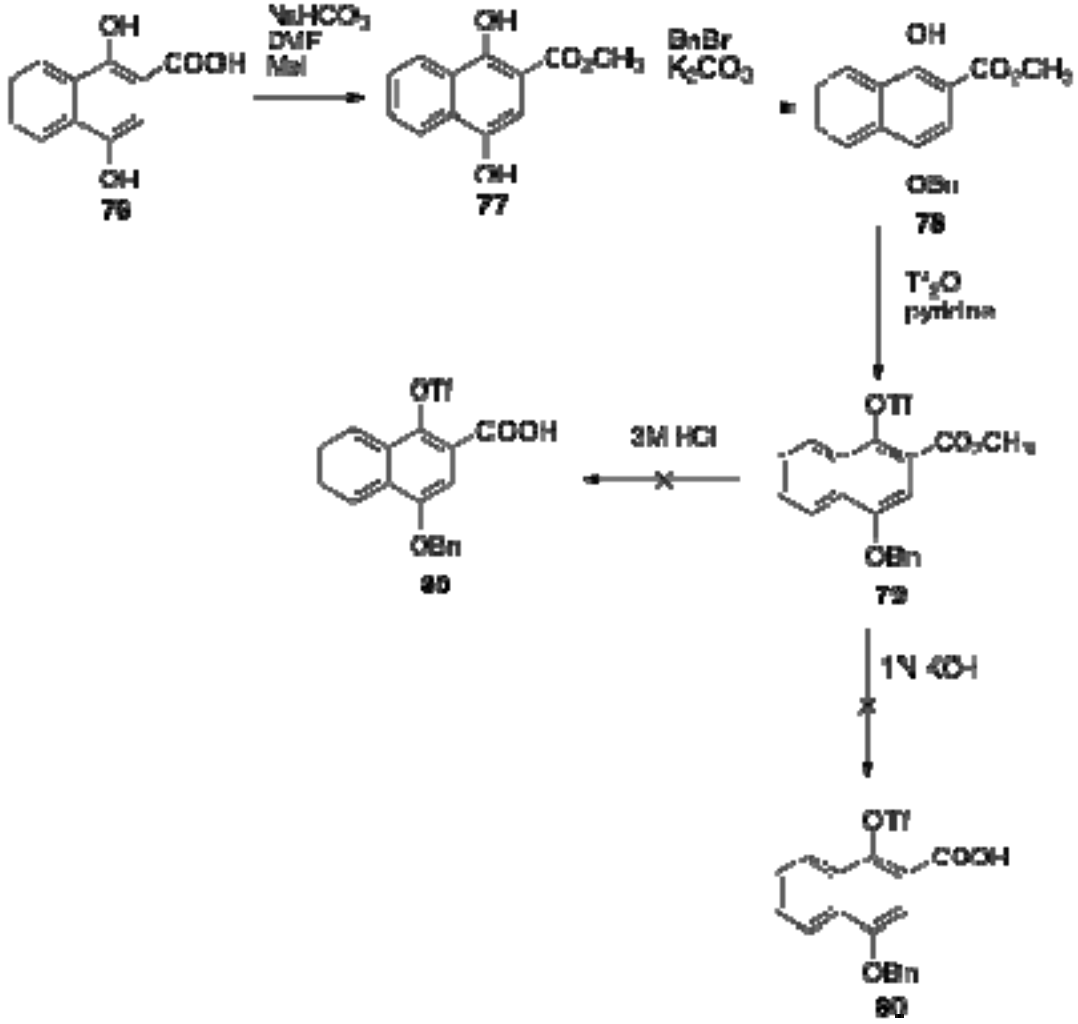

Scheme 19: Attempted Synthesis of Triflate Acid **80**

An alternative route involving 1, 4-dihydroxynaphthoic acid (**76**) was investigated for several reasons. First, the regiochemistry has already been defined eliminating that

aspect of the synthesis. Second, aryl triflates are known to undergo Heck cyclization reactions in an analogous manner to the aromatic halides. Finally, with the pre-defined regiochemistry set the need to build the naphthalene ring system has been eliminated saving not only time but also synthetic steps.

Following the procedure of Hattori *et al.* compound **76** was stirred at room temperature for 3-4 hours in the presence of sodium bicarbonate and methyl iodide to give the ester **77** in 90% yield (Scheme 19).[54] Compound **77** was selectively benzylated at the 4-hydroxy position to furnish compound **78** in 50% overall yield.[53] The ester **78** was dissolved in pyridine and allowed to react with triflic anhydride for 1 hour at room temperature to give the triflate **79** in 90% yield. Several attempts were made to selectively hydrolyze the ester **79** to its corresponding acid **80**.[56] The hydroylsis in acidic conditions failed to occur and the reproducibility of basic hydrolysis was also a problem.

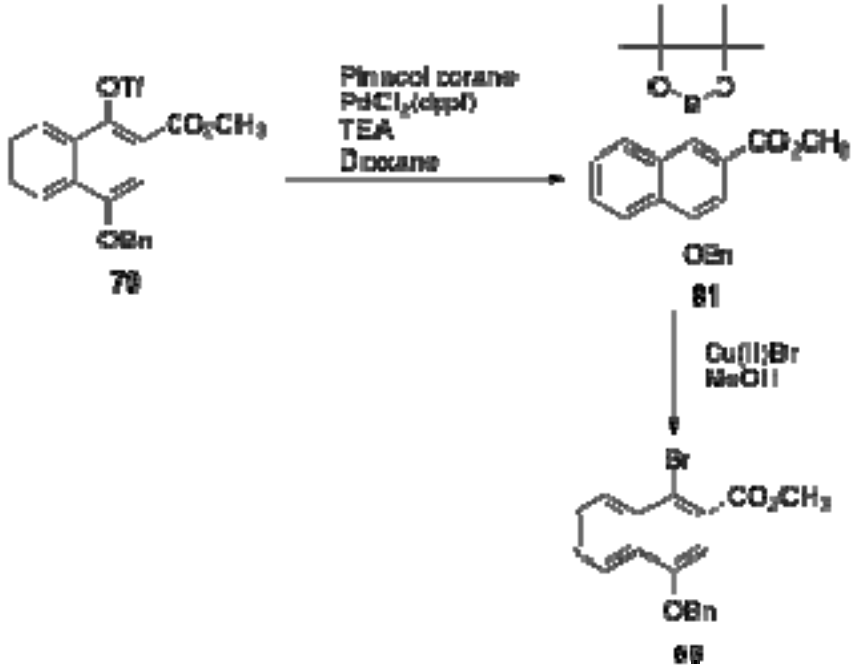

Scheme 20: Conversion of Triflate **79** into Bromo Ester **65**

Murata *et al*. and Thompson *et al*. have reported that aryl triflates could be converted to a boronate ester, which could then be displaced with a bromine atom using copper(II)bromide in methanol and water (Scheme 20).[57,58]

Compound **79** was stirred in dioxane in the presence of pinacol borane to give the desired boronate ester **81** in 85% yield. The ester **81** was then placed in a methanol-water solution to which copper(II)bromide was added and stirred at room temperature for several hours to afford compound **65** in 88% yield. Compound **65** was confirmed using melting point data obtained from the earlier schemes reported as well as with ^{1}H NMR, which showed a singlet for the H-3 proton at 7.1 ppm.

Slight modification of Scheme 17 allowed for the production of compound **63** without incorporating part of Boger's methodology (Scheme 15).

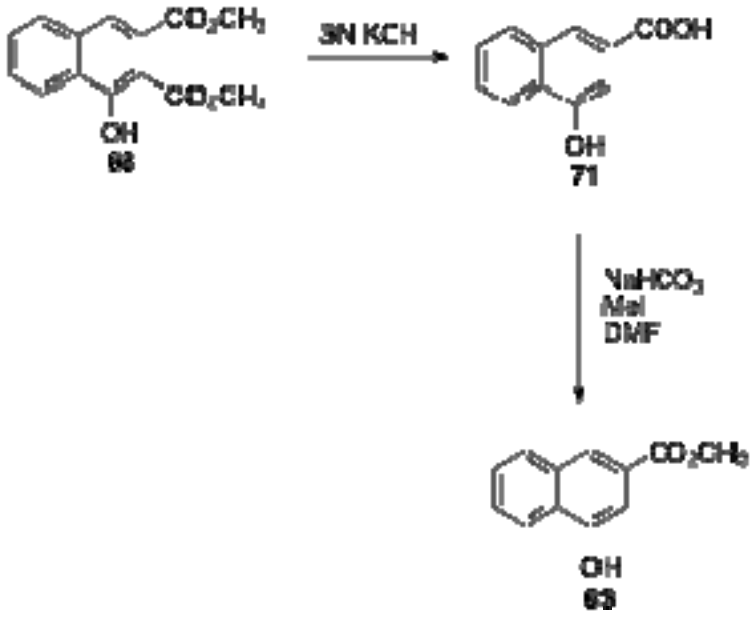

Scheme 21: Synthesis of Mono Ester **63**

Hydrolysis and decarboxylation of compound **68** occurred smoothly to give **71** in quantitative yield, which was subsequently esterified to the desired mono ester **63** in 90%

yield (Scheme 21). The use of the sodium bicarbonate and methyl iodide resulted in quicker product formation (2 hrs vs. 24-48 hrs) with only slightly lower yields (90% vs. 95%) than standard Fischer esterification conditions.

The next step was to develop a synthesis for the production of the propenyl pyrrolidine **87** side chain. Two methods (A and B) were investigated during the course of this study in order to evaluate which would be more facile (Scheme 22).

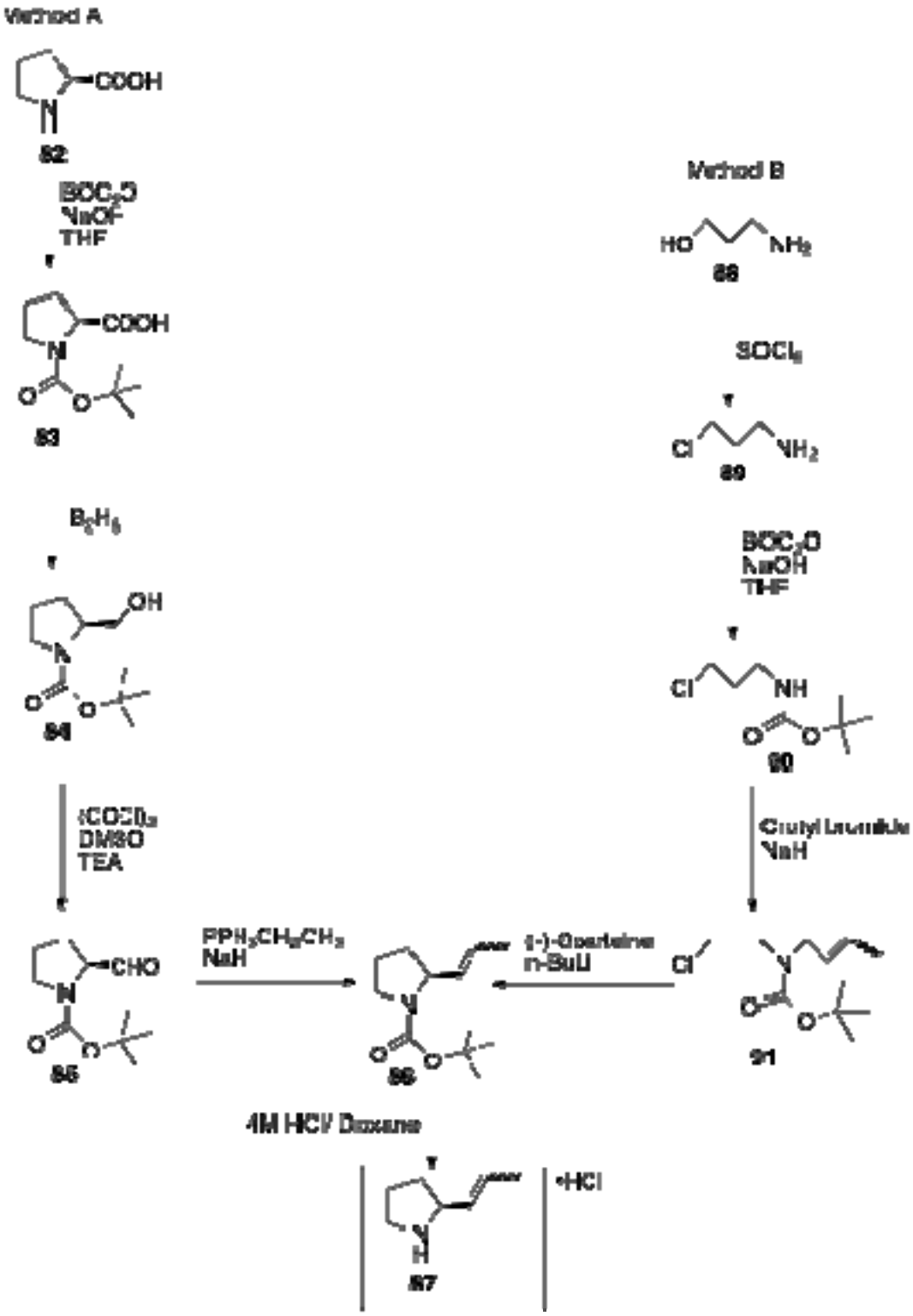

Scheme 22: Synthesis of L-Propenyl pyrrolidine **88**

Method A involved the use of commercially available L-proline (**82**), which was subsequently protected as the *tert*-butyl carbamate under standard conditions to give compound **83** in 95% yield.[59] The Boc-proline (**83**) was then treated with diborane to effect conversion to the alcohol **84** in 85% yield. Swern conditions were used to effect conversion of **84** to its aldehyde **85** in 90% yield.[60] Compound **85** was then stirred at room temperature in the presence of *n*-BuLi and ethyl triphenyl phosphonium bromide for 3-4 hours to afford **86** in 80% yield. Deprotection of the *N*-Boc-propenyl pyrrolidine (**86**) was effected by stirring in 4M HCl, which resulted in the formation of the hydrochloride salt **87** in 95% yield.

Method B began by treating commercially available propanolamine (**88**) with thionyl chloride to give compound **89** in 95% yield.[61] The amine was then protected as the Boc carbamate to give compound **90** in 90% yield. Compound **91** was then allowed to stir at room temperature in the presence of sodium hydride and crotyl bromide to furnish **91** in 80% yield. Finally, **91** underwent intramolecular cyclization using (-)-sparteine and *n*-BuLi to give the propenyl pyrrolidine **86** in 75% yield. Beak *et al*. reported that this cyclization resulted in 85% enantiomeric purity for the *trans* isomer and 51% purity for the *cis* isomer, which was determined by gas chromatography using a Ciclodex-B column.[62,63] Deprotection of **86** was carried out under identical conditions of method A to give **87** in 95% yield.

Evaluations between the two methods led to several conclusions. Method A provided a stereochemically pure material in L-proline (**82**). The Wittig reaction of prolinal **85** has the potential of epimerizing to a mixture of isomers although there is no precedence in the literature for this occurring. Method B does provide easier synthetic

steps and purification procedures of the resulting products. Also, the use of (+)-sparteine could be used to effect the cyclization and give the other isomer. In the end, method A was chosen due to the stereochemical purity of L-proline (**82**).

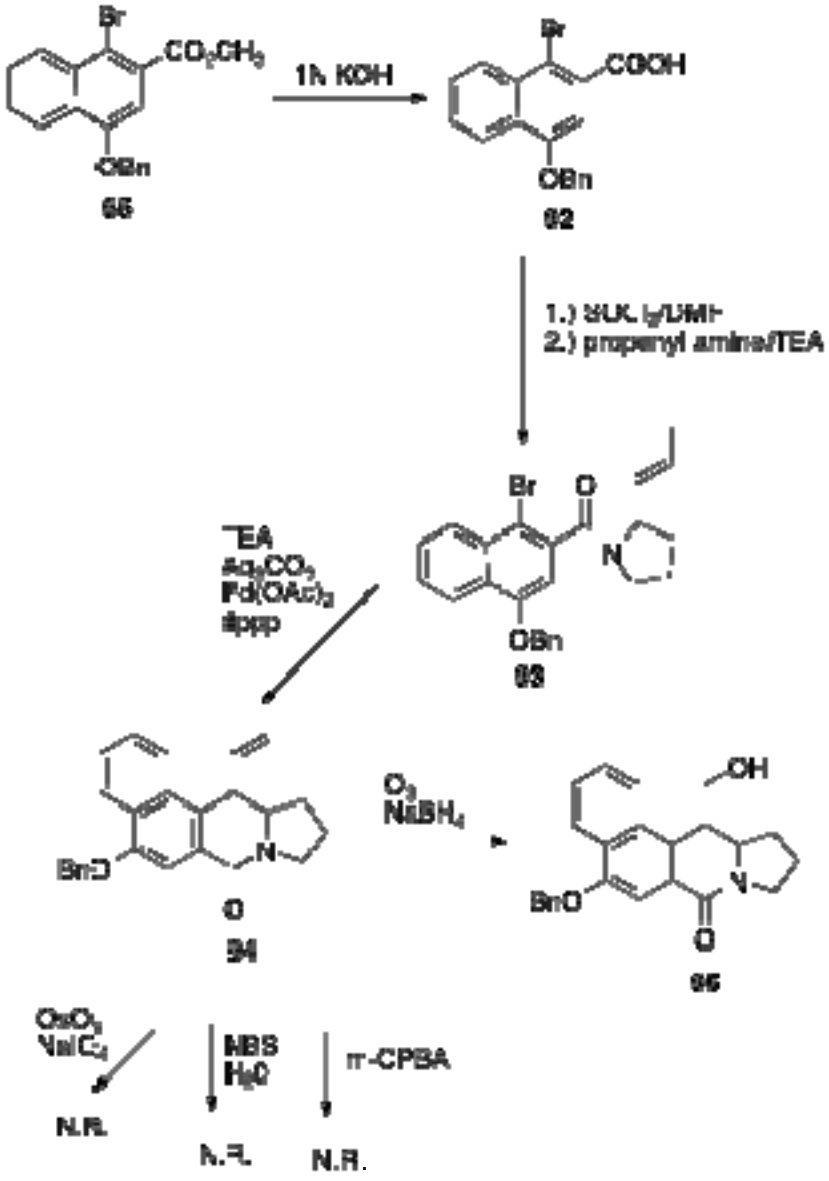

Scheme 23: Synthesis of Key Alcohol Intermediate **95**

The bromo ester **65** was hydrolyzed in 1N potassium hydroxide to give the key bromo acid intermediate **92** in 95% yield. The acid **92** was then coupled to the propenyl

amine **87** in 75% yield. The bromo amide **93** then underwent an intramolecular Heck cyclization reaction to afford the vinyl alkene **94** in 50% yield, which was confirmed using ^{1}H and ^{13}C NMR.[64] The oxidative cleavage of compound **94** proved more difficult than was anticipated. Initially the alkene **94** was treated with osmium tetroxide and sodium periodate, but only starting material was recaptured. Subsequent attempts to cleave the alkene using *m*-chloroperbenzoic acid and *N*-bromosuccinimide/water also resulted in the recapturing of starting material or in some cases complete degradation. The pyrrolidine moiety is a sufficiently bulky group to prevent most of these large electrophiles from approaching the alkene. However, the use of the smaller ozone molecule followed by reductive workup in sodium borohydride resulted in a 50:50 ratio of the *cis* and *trans* alcohols **95** as was confirmed by TLC and ^{1}H NMR.[65]

Synthesis of 2-Methyl-1, 2, 10, 10a tetrahydrobenzo[*f*]cyclopropa[*d*] isoquinoline -3,5-dione (98)

Retrosynthetic analysis of the *N*-methyl cyclopropyl compound **98** proved analogous to that of compound **28**. The target compound **98** was thought to arise from the debenzylation of the mesylate **109** followed by intramolecular cyclization under basic conditions (Scheme 24).

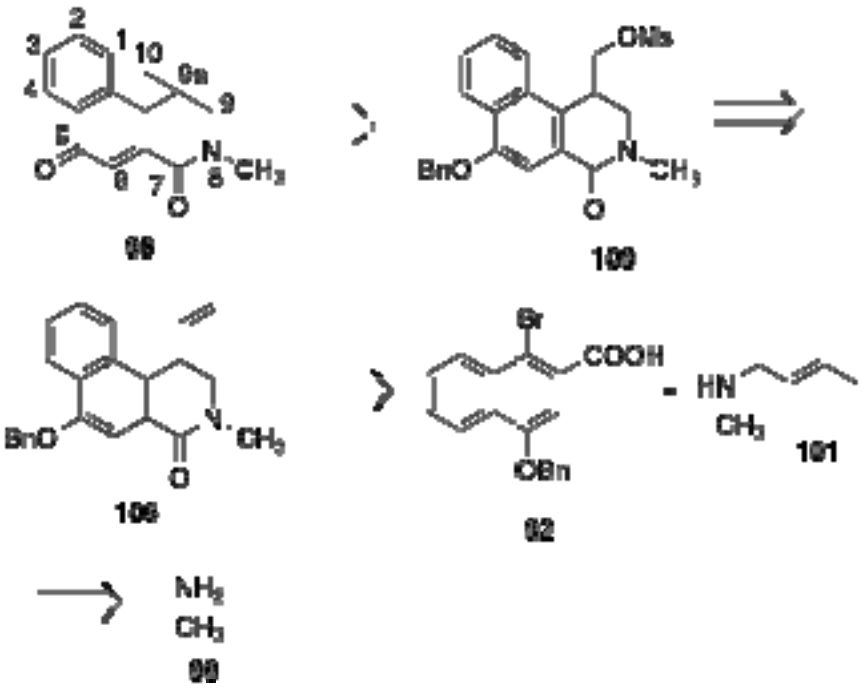

Scheme 24: Retrosynthetic Analysis of Compound **98**

It was thought that the *N*-methyl benzyl mesylate **109** could arise from an oxidative cleavage of *N*-methyl vinyl **106** followed by sodium borohydride reduction of the corresponding aldehyde. Compound **106** was expected to arise from a simple S_N2

displacement of the prepared acid chloride of compound **92** utilizing *N*-methyl crotyl amine **101**, which could then undergo an intramolecular Heck cyclization reaction. The *N*-methyl crotyl amine **101** was envisioned coming from a simple protection of methylamine (**99**) using di-*tert*-butyl dicarbonate, which could then undergo the installation of the crotyl functionality followed by deprotection of the Boc group in mild acid to afford compound **101** (Scheme 25).

Scheme 25: Attempted Synthesis of Compound **101**

N-Methylamine hydrochloride (**99**) was stirred at reflux with crotyl bromide (**100**) for several hours but no product formation was observed (Scheme 25). Before further attempts at producing **101** were investigated it was decided to investigate a synthesis for crotyl bromide (**100**), which would be needed in large quantities for future use. Crotyl alcohol (**102**) was stirred in the presence of phosphorus tribromide for several hours but conversion to compound **100** was not found (Scheme 26).

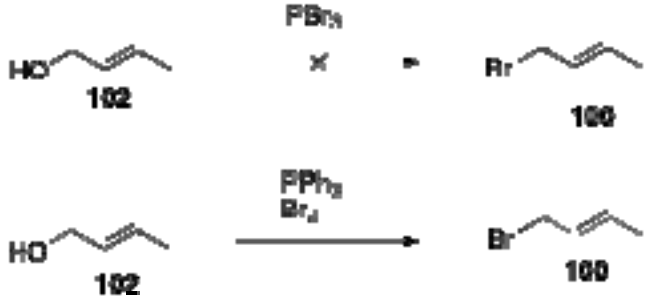

Scheme 26: Routes into Crotyl Bromide **100**

However, by reacting bromine and triphenyl phosphine together then allowing it to react with crotyl alcohol (**102**) the production of compound **100** occurred in 60% yield

after short-path distillation. This allowed for the large-scale production of compound **100** in a facile manner.

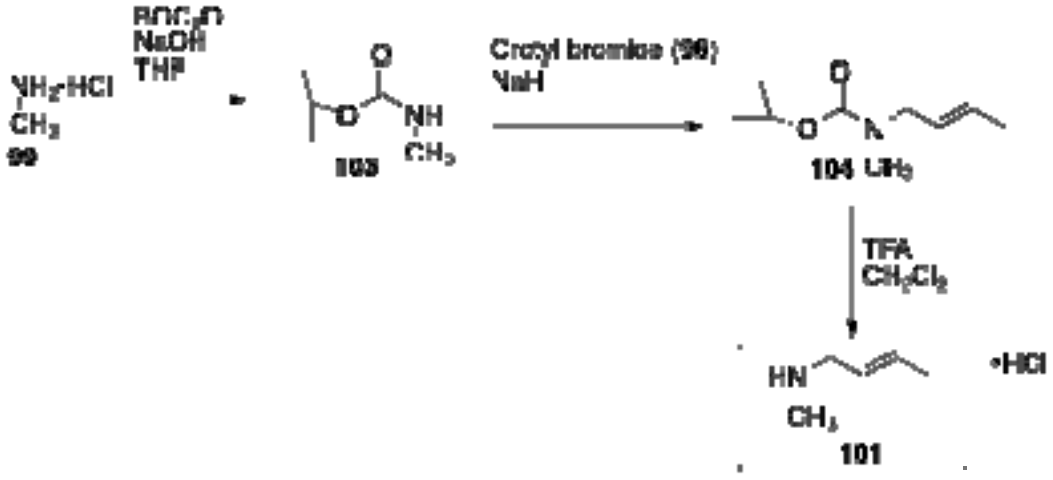

Scheme 27: Synthesis of *N*-Methyl Side Chain (**101**)

During the investigation for methods into compound **101**, it was thought that the procedure utilized for the manipulation of L-proline (**82**) could be adapted and modified as needed for the production of **101**. *N*-Methylamine (**99**) was initially protected using di-*tert*-butyl dicarbonate and purified using kugelrohr distillation, which allowed for preparation of large quantities of compound **103** in 65% yield.[66] The *N*-Boc amine **103** was then allowed to react with crotyl bromide under strongly basic conditions in order to install the butenyl group to give **104** in 80% yield. Deprotection was carried out in dichloromethane using trifluoroacetic acid to effect the removal of the Boc group to give **101** as its hydrochloride salt in 95% yield (Scheme 27).

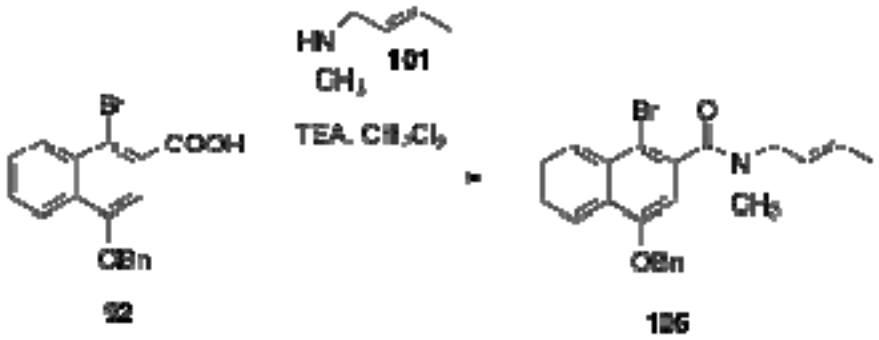

Scheme 28: Condensation of Bromo Acid **92** with *N*-Methyl Side Chain **101**

Coupling of the *N*-methyl crotyl amine (**101**) with the previously prepared bromo acid **92** occurred smoothly in 70% yield to afford compound **105** (Scheme 28).

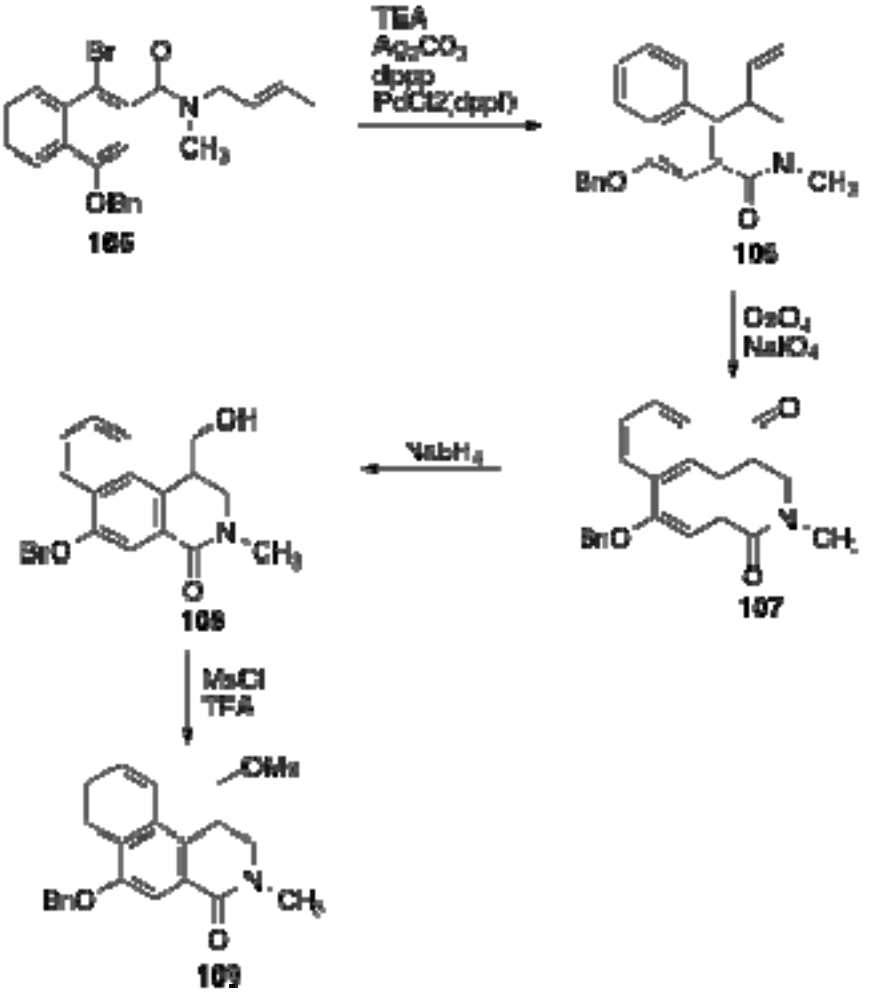

Scheme 29: Synthesis of Benzyl Mesylate **109**

Compound **105** then underwent an intramolecular Heck cyclization to give the vinyl alkene **106** in 45% yield.[64] The vinyl alkene **106** was oxidatively cleaved using osmium tetroxide and sodium periodate to give the aldehyde **107**, which was subsequently reduced using sodium borohydride to afford the alcohol **108** in 75% overall yield. Mesylation of the alcohol **108** proceeded smoothly in 95% yield to give compound **109** (Scheme 29).

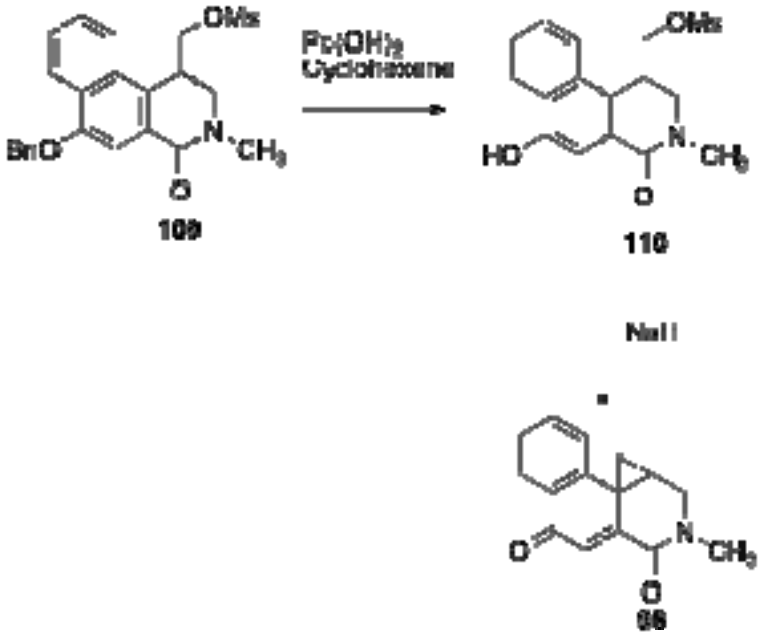

Scheme 30: Synthesis of Final Compound (**98**)

Debenzylation was initially carried out utilizing 10% palladium on carbon under standard hydrogenolysis conditions (Scheme 30). The conditions failed to cleave the benzyl ether **109**. Pearlman's catalyst was then used to successfully effect debenzylation to furnish the phenol mesylate **110** in 70% yield. NMR data confirmed the loss of the benzyl protons at 5.2 ppm and a much simpler aromatic region corresponding to the five aromatic protons. The singlets (3.04 ppm and 3.34 ppm) confirmed that both the *N*-methyl and mesylate protons were still there. The phenol mesylate **110** was then stirred in

the presence of sodium hydride in anhydrous tetrahydrofuran for 30 minutes. The reaction appeared to successfully occur by TLC, but due to the low quantity of material produced an NMR was unable to be procured.

SUMMARY AND CONCLUSION

The objective of this work was to develop novel synthetic methodologies that would allow for the production of agents that could potentially be alkylated by the DNA minor groove in a fashion analogous to the natural products (+)-CC-1065 (**1**), Duocarmycin A (**2**), and Duocarmycin SA (**3**). Initial work focused on the synthesis of 10,11,12,12a,12b,13-hexahydro-5*H*-benzo[*f*]cyclopropa[*d*]pyrido[1,2-*b*]isoquinoline-5,7(9*H*)-dione (**27**), which was based on the work reported by Reddy *et al*.[44] Minor synthetic modifications were made to the syntheses of compound **28**, which involved primarily a ring expansion from the pyrrolidine ring to the piperidine ring. Condensation of the imine **40** with the anhydride **38** led to a 50:50 diastereomeric mixture of the 6 membered acids **41**, which were subsequently reduced to the corresponding alcohols **42** and separated chromatographically to give the pure *cis* and *trans* isomers. The rest of the syntheses were carried out on the individual diastereomers to furnish the desired final compound **27**. Upon completion of the syntheses, the individual isomers were then sent to the National Cancer Institute (NCI) to undergo testing in a 60-cell panel of various cancer lines. The results indicated that the *trans* isomer was the more active compound and was subjected to a hollow fiber assay, which of all compounds tested by the NCI only about 1% are selected for this assay. Results showed a combined ip + sc score of 24,

which met the NCI standards for further testing; however, the *trans* isomer **27** was not chosen.

AutoDock 3.0 was utilized to model possible compounds for future synthetic work. During the course of the modeling studies several key structural modifications were noted. In an AT-rich region, the installation of a methoxy group at the C-6 position resulted in the correct orientation of the cyclopropyl ring towards the floor of the minor groove. The endocyclic analogs although not energetically favored over the exocyclic analogs were found to more consistently orient themselves correctly within the minor groove. Also, NH and O heteroatoms could be used to differentiate between AT and GC-rich regions by forming specific hydrogen bonds and van der Waals interactions with the nucleotide base pairs. The C-11 position was favored over C-10 thus allowing the molecules to bind tighter within the minor groove. During the course of these modeling studies it became apparent that alternate synthetic routes had to be developed in order to add functionality, which was not possible with the synthetic schemes reported for the synthesis of **27**.

The target compounds identified were the stereochemically-controlled synthesis of 9, 10, 11, 11a, 11b, 12-hexahydrobenzo[*f*]cyclopropa[*d*]isoquinoline-5,7-dione (**28**) and 2-methyl-1, 2, 10, 10a-tetrahydrobenzo[*f*]cyclopropa[*d*] isoquinoline- 3,5-dione (**98**). Retrosynthetic analysis of both compounds indicated that the bromo acid **92** was the key intermediate from which both schemes were based. Initial attempts at producing **92** were proven through X-Ray diffraction to contain the wrong bromo regioisomer. An alternate route was identified for the production of compound **92** by utilizing homophthalic acid (**66**) as the starting material. By refluxing **66** in acetyl chloride for several hours then

allowing it to react with dimethylacetylene dicarboxylate, **68** could be prepared in moderate yields. Subsequent hydrolysis/decarboxylation, esterification, and silyl protection reactions afforded compound **74**, which could then be brominated. Deprotection followed by benzylation and hydrolysis furnished the desired bromo acid **92** intermediate.

The development of the key bromo acid intermediate **92** allowed for the installation of either the (*S*)-2-propenyl pyrrolidine (**87**) or the *N*-methyl-*N*-butene (**101**) functional groups. Once at that stage each compound could then undergo similar reaction conditions to afford the desired materials. The development of the *N*-methyl **98** could lead to the linking of Dervan's polyamides by removal of the *N*-methyl moiety and subsequent installation of the desired Im, Py, or Hp polyamide chains.

EXPERIMENTAL SECTION

Materials and Methods

Melting points were recorded on a Thomas-Hoover melting point apparatus and are uncorrected. ^{1}H and ^{13}C NMR spectra were recorded on a Bruker AC 250 Spectrometer (operated at 250 or 62.9 MHz, respectively) or AC 400 Spectrometer (operated at 400 or 100 MHz, respectively). All ^{1}H chemical shifts are reported in δ relative to the internal standard tetramethylsilane (TMS, δ 0.00). ^{13}C chemical shifts are reported in δ relative to $CDCl_3$ (center of triplet, δ 77.23) or relative to DMSO-d_6 (center of septet, δ 39.51). The spin multiplicities are indicated by the symbols s (singlet), d (doublet), t (triplet), q (quartet), m (multiplet), and br (broad). Atlantic Microlabs, Norcross, Georgia, performed elemental analyses. Reactions were monitored by thin-layer chromatography (TLC) using 0.25 mm E. Merck silica gel 60-F_{254} percoated silica gel plates with visualization by the irradiation with Mineralight UVGL-25 lamp or exposure to iodine vapor. Column chromatography was performed on Whatman silica gel (average particle size 2-25 μm, 60Å) and elution with the indicated solvent system. Spinning Band Chromatography was performed on a Chromatotron 8900 using Merck silica gel 7749 with gypsum binder and fluorescent indicator. Yields refer to the

spectroscopically (^{1}H and ^{13}C NMR) and chromatographically homogeneous materials. GC-MS was performed with an HP-5890 GC coupled with an HP-5970 mass selective detector (Hewlett Packard, Palo Alto, CA) using Helium (grade 5.0) as carrier gas. The mass spectrometer was operated on the electron impact (EI) mode using ionization voltage of 70 eV and a source temperature of 230 °C. Samples were dissolved in HPLC grade acetonitrile (Fisher Scientific, NJ, USA) and manually introduced (1 μL) individually.

2-Carboxymethyl-3-carboxy-furan diethylester (31)

Compound **31** was prepared using the procedure of Tada *et al*.[44] Diethyl-1, 3-diethylacetone dicarboxylate **29** (35 g, 0.247 mol) and chloroacetaldehyde **30** (50%) (44 g, 0.283 mol) were added simultaneously at equal rates to anhydrous pyridine (100 mL). The reaction was stirred at 50 °C for 24 h. The reaction mixture was diluted with water (200 mL) and extracted with diethyl ether (3 X 50 mL). The organic layers were combined and washed with 2N HCl, 10% NaOH, and 10% $NaHCO_3$, dried over sodium sulfate and concentrated under reduced pressure to give a dark colored oil. The oil was purified by kugelrohr distillation (86-90 °C at 0.2 mmHg) to give **31** (36g, 64%) as a light colored oil; ^{1}H NMR ($CDCl_3$): δ 7.32 (d, 1H, J=1.9 Hz), 6.69 (d, 1H, J=1.9 Hz), 4.28 (q, 2H, J=7.5 Hz), 4.16 (q, 2H, J=7.5 Hz), 4.05 (s, 2H), 1.33 (t, 3H, J=7.5 Hz), 1.25 (t, 3H, J=7.5 Hz). ^{13}C NMR: δ 168.6 (C), 163.4 (C), 154.2 (C), 141.7 (CH), 115.7 (C), 110.8 (CH), 61.3 (CH_2), 60.4 (CH_2), 33.8 (CH_2), 14.2 (CH_3), 14.1 (CH_3). IR (film): A_{max} 3130, 2983, 1742, 1707, 1614, 1517, 1307, 1261, 1182 cm-1. MS (EI): 226 (m/z), 181, 153, 125, 108.

3-Carboxy-4-carboxymethyl-1-napthol diethylester (35)

Compound **35** was prepared utilizing the procedure of Logullo *et al*.[45] To a solution of anthranilic acid **32** (6.06 g, 74 mmol) in anhydrous THF (100 mL) was added trichloroacetic acid (860 mg, 5.2 mmol) and isoamyl nitrite (6 mL, 74 mmol). The reaction mixture was stirred at room temperature for 1-2 h. A reddish precipitate (**30**) formed during the reaction and was subsequently filtered and washed with cold THF and 1,2-dichloroethane. The precipitate **33** must remain wet to prevent explosion. The solid

(**33**) was taken up in fresh 1,2-dichloroethane (75 mL) to which a solution of **31** (6.6 g, 29 mmol) in 1,2-dichloroethane (15 mL) was added dropwise over 15 min. The reaction was allowed to stir at reflux for 1 h. The solvent was removed *in vacuo* and the residue taken up in $CHCl_3$ (50 mL). To the solution was added BF_3OEt_2 (20 mL, 296 mmol) and the reaction was stirred at room temperature for 30 min. The reaction mixture was quenched with water, extracted with $CHCl_3$ (3 X 20 mL), dried over sodium sulfate and concentrated under reduced pressure. The residue was covered with cold diethyl ether and filtered to give **35** as a light brown solid (4.4 g, 50%), m.p. 105-107 °C; ^{1}H NMR ($CDCl_3$): δ 7.96-7.93 (m, 2H), 7.86-7.83 (m, 2H), 6.9 (s, 1H), 4.46 (s, 2H), 4.21-4.07 (dq, 4H, J=7.5 Hz), 1.23-1.12 (dt, 6H, J=7.5 Hz). ^{13}C NMR: δ 172.9 (C), 167.8 (C), 151.2 (C), 133.62 (CH), 130.2 (CH), 128.5 (CH), 128.37 (CH), 126.8 (C), 126.4 (CH), 124.3 (C), 122.62 (CH), 108.71 (CH), 61.2 ($2CH_2$), 34.3 (CH_2), 14.2 (CH_3), 14.1 (CH_3). IR (KBr): U_{max} 3396, 3074, 2989, 1739, 1679, 1599, 1478, 1433, 1385, 1335, 1259 cm-1. Anal. Calcd for: $C_{17}H_{18}O_5$: C, 67.54; H, 5.96. Found: C, 67.33; H, 6.00.

1-Benzyloxy-3-carboxy-4-carboxymethyl naphthalene diethylester (36)

To a solution of **35** (3 g, 10 mmol) in acetone (10 mL) was added K_2CO_3 (1.38 g, 10 mmol) and benzyl bromide (1.3 mL, 11 mmol). The reaction was stirred at reflux overnight. The suspension was filtered and concentrated under reduced pressure to give a dark colored oil. The oil was crystallized from diethyl ether/petroleum ether to give **36** (3.5 g, 95%) as a light brown solid, m.p. 80-81 °C; ^{1}H NMR ($CDCl_3$): δ 8.42-8.38 (m, 1H), 8.05-8.02 (m, 1H), 7.56-7.53 (m, 4H), 7.39-7.37 (m, 3H), 5.23 (s, 2H), 4.46 (s, 2H), 4.39 (q, 2H, J=7.5 Hz), 4.15 (q, 2H, J=7.5 Hz), 1.4 (t, 3H, J=7.5 Hz), 1.21 (t, 3H, J=7.5

Hz). ^{13}C NMR (CDCl3): δ 171.4 (C), 167.8 (C), 153.4 (C), 136.6 (C), 133.5 (C), 128.4 (CH), 128.3 (CH), 128.2 (C), 128.1 (C), 127.9 (CH), 127.8 (CH), 127.4 (C), 126.8 (2CH), 125.8 (2CH), 124.6 (CH), 122.5 (CH), 105.1 (CH), 69.9 (CH_2), 61.1 (CH_2), 60.6 (CH_2), 34.3 (CH_2), 14.1 (CH_3), 14.0 (CH_3). MS (EI): 392 (m/z), 347, 319, 255, 200, 155, 127, 91. IR (KBr): U_{max} 3436, 2986, 1731, 1708, 1596, 1369, 1242, 1199 cm-1. Anal. Calcd for: $C_{24}H_{24}O_5$: C, 73.46; H, 6.12. Found: C, 73.33; H, 6.19.

1-Benzyloxy-3-carboxy-4-carboxymethyl napthalene (37)

Compound **36** (2.28 g, 6.2 mmol) was refluxed for 6 h in a solution of 3N methanolic KOH. The methanol was removed *in vacuo* and the residue was taken up in water and washed with diethyl ether (3 X 15 mL). The aqueous layer was acidified with 1N HCl and cooled to 0 °C. The precipitate was filtered, washed with water, and dried to give **37** (1.72 g, 91%) as a light brown solid, m.p. 191-193 °C; ^{1}H NMR ($CDCl_3$/DMSO-d_6): δ 8.39-8.36 (m, 1H), 8.15-8.12 (m, 1H), 7.61-7.52 (m, 4H), 7.48 (s, 1H), 7.45-7.38 (m, 3H), 5.08 (s, 2H), 4.3 (s, 2H). ^{13}C NMR: δ 172.6 (C), 169.8 (C), 152.6 (C), 136.0 (C), 132.9 (C), 128.4 (C), 128.3 (CH), 127.9 (CH), 127.3 (C), 126.8 (C), 126.7 (2CH), 126.2 (2CH), 125.5 (CH), 124.4 (CH), 121.8 (CH), 104.8 (CH), 69.4 (CH_2), 34.0 (CH_2). IR (KBr): U_{max} 2953, 2625, 1713, 1679, 1596, 1513, 1411, 1367, 1259, 1096 cm-1. MS (EI): 336 (m/z), 318, 274, 155, 127, 91. Anal. Calcd for: $C_{20}H_{16}O_5$: C, 71.43; H, 4.76. Found: C, 71.21; H, 4.92.

1-Benzyloxy-3-carboxy-4-carboxymethyl naphthalene anhydride (38)

A solution of **37** (1.72 g, 5.7 mmol) in acetyl chloride (30 mL) was refluxed for 12 h. Acetyl chloride was removed under reduced pressure and the residue was washed with benzene (3 X 10 mL). The residue was crystallized from benzene/petroleum ether to give **38** (1.32 g, 73%) as a light green solid, m.p. 204-206 °C; ^{1}H NMR ($CDCl_3$): δ 8.43-8.40 (m, 1H), 7.99-7.98 (m, 1H), 7.76-7.71 (m, 2H), 7.57-7.54 (m, 2H), 7.49-7.37 (m, 4H), 5.34 (s, 2H), 4.50 (s, 2H). IR (KBr): U_{max} 3456, 3107, 1784, 1738, 1659, 1594, 1420, and 1374, cm-1.

α-Tripiperideine (40)

Compound **40** was made using the procedure of Quick and Oterson.[46] A suspension of **39** (3.48 mL, 66 mmol) in diethyl ether (30 mL) was cooled to -10 °C and treated with *N*-chlorosuccinimide (15.92 g, 119 mmol). The suspension was stirred at room temperature for 1 h. The suspension was filtered and the solid was taken up in methanol and treated with 1N KOH (3.69 g, 66 mmol). The reaction mixture was stirred at reflux for 2-3 h. The methanol was removed under reduced pressure and the aqueous layer was extracted with diethyl ether (3 X 10 mL), dried over sodium sulfate, and concentrated *in vacuo* to give a light colored oil. The oil was crystallized from cold acetone to give **40** (2.7 g, 50%) as a light yellow solid, m.p. 58-61 °C (obs. m.p. 59-60 °C); ^{13}C NMR ($CDCl_3$): δ 81.7, 46.1, 28.7, 25.4, 22.0.

1, 2, 3, 4, 13, 13a-hexahydro-13-carboxy-8-benzyloxy-benzo[*f*]pyrido[1,2-*b*] isoquinolin-6-one (41)

To a solution of **38** (100 mg, 0.314 mmol) in anhydrous CH_2Cl_2 (10 mL) was added **40** (26 mg, 0.314 mmol) in anhydrous CH_2Cl_2 (5 mL) and the reaction was allowed to stir at reflux for 1 h. The reaction then stirred for an additional 2 h at room temperature. The reaction was diluted with diethyl ether (40 mL), cooled, and filtered to give **41** (100 mg, 79%) as a brown solid; ^{1}H NMR ($CDCl_3$/DMSO-d_6): δ 8.41 (m, 1H), 8.17 (m, 1H), 7.72 (s, 1H), 7.61 (m, 4H), 7.41 (m, 3H), 5.31 (s, 2H), 4.59 (d, 1H, J= 14 Hz, C13-H), 4.40 (d, 1H, J= 5 Hz, C13-H), 3.87 (m, 1H), 3.46 (br s, 2H, H_2O), 2.86 (ddd, 1H), 2.16 (d, 1H), 1.86-1.24 (m, 6H, C1-H, C2-H, C3-H). ^{13}C NMR: δ 172.0, 153.8, 136.6, 130.8, 128.3, 127.8, 127.3, 126.8, 125.0, 123.8, 122.6, 103.2 (C6-*trans*), 102.7 (C6-*cis*), 69.9, 60.1, 45.6, 42.2, 24.9, 23.6, 22.4, 20.8. EILRMS : 401.1 (m/z), 357.1, 318, 264.

1, 2, 3, 4, 13, 13a-hexahydro-13-hydroxymethyl-8-benzyloxy-benzo[*f*]pyrido[1,2-*b*] isoquinoline-6-one (42)

Diborane (.283 g, 0.372 mmol) was added by syringe to a cooled solution (0 °C) of **41** (50 mg, 0.124 mmol) in anhydrous THF (15 mL) and the reaction was brought to room temperature and stirred for 12 h. The reaction was cooled to 0 °C, quenched, and diluted with water (50 mL). The reaction mixture was extracted with EtOAc (3 X 25 mL), dried over sodium sulfate, and concentrated under reduced pressure to give a light colored oil. Spinning band chromatography (silica gel, 1mm plate, 50% petroleum ether-chloroform) afforded pure **42** as separate diastereomers (30 mg, 69%); *Cis* isomer: ^{1}H

NMR ($CDCl_3$): δ 8.43-8.40 (m, 1H), 8.11-8.07 (m, 1H), 7.66 (s, 1H, C6-H), 7.59-7.55 (m, 4H), 7.45-7.34 (m, 3H), 5.27 (s, 2H), 4.48-4.43 (m, 1H, C4-H), 4.14-4.11 (m, 1H, C13b-H), 3.88-3.84 (m, 1H, C13b-H), 3.78-3.76 (m, 1H, C13a-H), 3.65-3.63 (m, 1H, C13-H), 2.92-2.91 (m, 1H, C4-H), 2.02-1.87 (m, 3H), 1.56-1.52 (m, 1H), 1.37-1.35 (m, 1H), 1.25-1.21 (m, 1H). ^{13}C NMR: δ 166.9 (C), 153.5 (C), 136.8 (C), 130.9 (C), 130.3 (C), 128.5 (CH), 127.9 (CH), 127.7 (CH), 127.4 (C), 127.1 (2CH), 126.8 (2CH), 126.3 (C), 124.4 (CH), 122.7 (CH), 102.9 (CH), 70.0 (CH_2), 61.8 (CH_2), 56.7 (CH), 42.5 (CH_2), 40.3 (CH), 28.5 (CH_2), 24.0 (CH_2), 22.7 (CH_2). This isomer was a light-yellow solid (m.p. 186-196ºC). *Trans* isomer: ^1H NMR ($CDCl_3$): δ 8.44-8.40 (m, 1H), 8.09-8.06 (m, 1H), 7.74 (s, 1H, C6-H), 7.61-7.56 (m, 4H), 7.46-7.38 (m, 3H), 5.30 (s, 2H), 4.85-4.80 (m, 1H, C4-H), 4.08-4.02 (m, 1H, C13a-H), 3.78-3.75 (m, 2H, 2 C13b-H), 3.55-3.53 (m, 1H, C13-H), 2.83-2.79 (m, 1H, C4-H), 1.88-1.61 (m, 7H, C1-H; C2-H; C3-H). ^{13}C NMR: δ 163.4 (C), 154.1 (C), 137.1 (C), 131.9 (C), 128.8 (CH), 128.2 (CH), 128.0 (CH), 127.8 (C), 127.6 (2CH), 127.1 (2CH), 126.3 (C), 126.1 (C), 123.7 (CH), 123.4 (CH), 103.2 (CH), 70.4 (CH_2), 64.2 (CH_2), 58.5 (CH), 46.9 (CH_2), 41.3 (CH), 32.3 (CH_2), 25.9 (CH_2), 25.5 (CH_2). This isomer was a light-yellow solid (m.p. 60-70ºC).

1, 2, 3, 4, 13, 13a-hexahydro-13-(methanesulfonyloxymethyl)-8-benzyloxy-benzo[*f*] pyrido[1,2-*b*]isoquinoline-6-one (43)

Compound **42** (100 mg, 0.258 mmol) was taken up in anhydrous CH_2Cl_2 (20 mL) and treated with TEA (70 μL, 0.516 mmol) and methanesulfonyl chloride (30 μL, 0.388 mmol). The reaction was stirred at room temperature overnight. The reaction was diluted with CH_2Cl_2 (30 mL), washed with 1N HCl, saturated $NaHCO_3$, water, dried over sodium

sulfate and concentrated under reduced pressure. Flash chromatography (silica gel, 100% $CHCl_3$) afforded **43** (115 mg, 92%) as a white solid; *Cis* isomer: ^{1}H NMR ($CDCl_3$): δ 8.45-8.42 (m, 1H), 8.11-8.08 (m, 1H), 7.66 (s, 1H), 7.63-7.60 (m, 4H), 7.45-7.38 (m, 3H), 5.31 (s, 2H), 4.70-4.65 (m, 1H), 4.47-4.42 (m, 1H), 4.32-4.26 (m, 1H), 3.93-3.86 (m, 2H), 2.99-2.95 (m, 1H), 2.82 (s, 3H), 1.96-1.90 (m, 4H), 1.66-1.60 (m, 1H), 1.38-1.36 (m, 1H). ^{13}C NMR: δ 166.7 (C), 154.5 (C), 136.8 (C), 130.7 (C), 128.8 (CH), 128.2 (CH), 128.0 (CH), 127.7 (2CH), 127.5 (2CH), 127.3 (C), 127.2 (C), 123.9 (CH),123.4 (CH), 103.2 (CH), 70.4 (CH_2), 68.1 (CH_2), 56.4 (CH_3), 42.8 (CH_2), 38.1 (CH), 37.3 (CH), 31.7 (CH_2), 28.8 (CH_2), 24.1 (CH_2), 22.7 (CH_2).

Trans isomer: ^{1}H NMR ($CDCl_3$): δ 8.46-8.42 (m,1H), 8.11-8.08 (m, 1H), 7.74 (s, 1H), 7.67-7.60 (m, 4H), 7.46-7.40 (m, 3H), 5.32 (s, 2H), 4.85-4.80 (m, 1H), 4.30-4.28 (m, 2H), 3.97-3.95 (m, 1H), 3.85-3.82 (m, 1H), 2.99 (s, 3H), 2.85-2.82 (m, 1H), 1.90-1.86 (m, 2H), 1.72-1.59 (m, 4H). ^{13}C NMR: δ 163.1 (C), 154.7 (C), 136.8 (C), 131.6 (C), 128.8 (CH), 128.2 (CH), 128.0 (C), 127.9 (C) 127.7 (2CH), 127.4 (2CH), 126.7 (C), 123.5 (CH), 123.2 (CH), 103.2 (CH), 70.4 (CH_2), 69.3 (CH_2), 58.0 (CH_3), 52.6 (CH), 46.9 (CH_2), 38.7 (CH), 37.6 (CH), 31.6 (CH_2), 25.6 (CH_2), 25.2 (CH_2). This isomer was a white crystalline solid (m.p. 55-65ºC).

1, 2, 3, 4, 13, 13a-hexahydro-13-(methanesulfonyloxymethyl)-8-hydroxybenzo[*f*] pyrido[1,2-*b*]isoquinolin-6-one (44)

In a glove box, compound **43** (49 mg, 0.105 mmol) was placed in a parr flask and charged with anhydrous THF (20 mL) and 10% Pd/C (30 mg). The suspension was shaken under H_2(g) for 12 h. The suspension was filtered thru a celite plug and

concentrated under reduced pressure. Flash chromatography (silica gel, 100% $CHCl_3$) gave pure **44** (33 mg, 88%); *Cis* isomer: ^{1}H NMR ($CDCl_3$): δ 8.536-8.530 (m, 1H), 8.32-8.29 (m, 1H), 7.97 (s, 1H), 7.86-7.77 (m, 2H), 4.85-4.83 (m, 1H), 4.53-4.49 (m, 2H), 4.04-4.00 (m, 1H), 3.25-3.23 (m, 1H), 3.00 (s, 3 H), 2.17-2.12 (m, 5H), 1.65-1.58 (m, 2H), 1.49 (s, 1H).

Trans isomer: ^{1}H NMR ($CDCl_3$): δ 8.43-8.40 (m, 1H), 8.27 (s, 1H), 8.08-8.05 (m, 1H), 7.65-7.59 (m, 2H), 4.86-4.84 (m, 1H), 4.32-4.28 (m, 2H), 4.04-4.01 (m, 1H), 3.84-3.74 (m, 2H), 2.99 (s, 3H), 1.92-1.61 (m, 6H). ^{13}C NMR: δ 163.8 (C), 153.9 (C), 131.8 (C), 128.0 (CH), 127.5 (C), 127.0 (CH), 126.3 (C), 123.7 (CH), 123.2 (CH), 121.9 (C), 107.0 (CH), 69.4 (CH_2), 58.4 (CH_3), 47.2 (CH_2), 38.7 (CH), 37.6 (CH), 31.7 (CH_2), 25.8 (CH_2), 25.1 (CH_2).

10, 11, 12, 12a, 12b, 13-hexahydro-5*H*- benzo[*f*]cyclopropa[*d*]pyrido[1,2-*b*] isoquinoline-5,7(9*H*)-dione (27)

A solution of **44** (45 mg, 0.12 mmol) in anhydrous THF (5 mL) was cooled to 0 °C and treated with NaH (60%) (5.2 mg, 0.154 mmol). The ice bath was removed and the reaction stirred at room temperature for 30 min. The reaction was cooled to 0 °C and a phosphate buffer solution (pH 7.0, 5 mL) was added to the reaction mixture. The mixture was extracted with EtOAc (3 X 10 mL), dried over sodium sulfate, and concentrated under reduced pressure. The residue was crystallized from cold diethyl ether to give **27** (20 mg, 61%) as a white solid; *Cis* isomer: ^{1}H NMR ($CDCl_3$): δ 8.28-8.24 (m, 1H), 7.63-7.57 (m, 1H), 7.46-7.40 (m, 1H), 7.32 (s, 1H), 7.01-6.98 (m, 1H), 4.71-4.66 (m, 1H), 3.72-3.68 (m, 1H), 2.58-2.55 (m, 2H), 2.08-2.00 (m, 1H), 1.98-1.96 (m, 2H), 1.84-1.82

(m, 2H) 1.45-1.43 (m, 2H), 1.25 (s, 1H). ^{13}C NMR: δ 185.4, 163.5, 147.6, 143.7, 133.2, 130.4, 127.0, 126.9, 121.4, 52.4, 42.5, 33.4, 32.7, 26.9, 24.7, 24.4, 23.0, 19.7. EIHRMS: m/e 279.12046 ($C_{18}H_{17}NO_2$ requires 279.3378). Anal. Calcd for $C_{18}H_{17}NO_2$: C, 77.39; H, 6.13; N, 5.01. Found: C, 77.10; H, 6.36; N, 4.97.

Trans isomer: ^{1}H NMR ($CDCl_3$): δ 8.29-8.26 (m, 1H), 7.64-7.61 (m, 1H), 7.47-7.44 (m, 1H), 7.36 (s, 1H), 7.01-6.98 (m, 1H), 4.80-4.78 (m, 1H), 3.90-3.85 (m, 1H), 2.65-2.64 (m, 1H), 2.50-2.47 (m, 1H), 2.04-2.02 (m, 2H), 1.87-1.83 (m, 2H), 1.66-1.60 (m, 2H), 1.32-1.25 (m, 2H). ^{13}C NMR: δ 185.4 (C), 161.4 (C), 146.9 (C), 143.9 (C), 133.2 (CH), 132.8 (C), 130.3 (CH), 127.0 (CH), 126.9 (CH), 121.1 (CH), 57.8 (CH), 46.3 (CH_2), 34.9 (CH_2), 31.2 (CH), 29.8 (CH_2), 26.8 (CH_2), 25.7 (CH_2), 25.1 (CH_2). EILRMS: 279.4 (m/z), 140.2, 77.1, 28.0. EIHRMS: m/e 279.12644 ($C_{18}H_{17}NO_2$ requires 279.3378). Anal. Calcd for $C_{18}H_{17}NO_2$: C, 77.39; H, 6.13; N, 5.01. Found: C, 77.10; H, 6.36; N, 4.97.

Dimethyl-1-hydroxynaphthalene-2, 3-dicarboxylate (68)

Compound **68** was made using the procedure of Tamura *et al*.[52] A solution of homophthalic anhydride **67** (7.92 g, 49 mmol) in anhydrous THF (100 mL) was cooled to 0 °C and treated with NaH (60%) (1.96 g, 49 mmol), which was allowed to stir at 0 °C for 5 min. Dimethyl acetylene dicarboxylate (6.4 mL, 49 mmol) was added by syringe and the reaction stirred at 0 °C for 20 min. The ice bath was removed and the reaction was allowed to continue to stir for an additional 30 min. The reaction was cooled to 0 °C and was slowly quenched with water, acidified with 1N HCl until slightly acidic, extracted with CH_2Cl_2 (3 X 20 mL), dried over sodium sulfate, and removed under reduced pressure to give a dark colored oil. The oil was crystallized from cold methanol

to give **68** (7.27 g, 57%) as a light colored solid, lit. m.p. 104-105 °C (obs m.p. 102-108 °C); ^{1}H NMR ($CDCl_3$): δ 11.89 (s, 1H), 8.37-8.36 (m, 1H), 7.73-7.62 (m, 1H), 7.59-7.56 (m, 2H), 7.42 (s, 1H), 3.94 (s, 3H), 3.91 (s, 3H). ^{13}C NMR: δ 170.4 (C), 169.8 (C), 161.0 (C), 135.3 (C), 130.3 (CH), 130.2 (C), 128.1 (CH), 127.4 (CH), 125.5 (C), 124.2 (CH), 119.8 (CH), 103.2 (C), 52.9 (CH_3), 52.7 (CH_3).

4-Hydroxy-2-naphthoic acid (71)

Compound **71** was made by the procedure of Adcock *et al*.[66] A solution of **68** (6.5 g, 25 mmol) in 3N KOH (3:1 methanol-water) was refluxed overnight. The methanol was removed and the resulting residue taken up in water and washed with diethyl ether (3 X 10 mL). The aqueous layer was acidified with 1N HCl to a pH of 4-5, cooled, and filtered to give **71** (4.22 g, 95%) as a brown solid, lit. m.p. 224-226 °C (obs m.p. 218-220 °C); ^{1}H NMR ($CDCl_3$/DMSO-d_6): δ 9.91 (br s, 1H), 8.25-8.21 (m, 1H), 8.07 (s, 1H), 7.81-7.78 (m, 1H), 7.43 (m, 3H), 7.42 (s, 1H). ^{13}C NMR: δ 167.6 (C), 152.5 (C), 132.8 (C), 128.0 (C), 127.9 (CH), 126.3 (C), 125.9 (CH), 122.8 (CH), 121.5 (CH), 120.9 (CH), 106.6 (CH).

Ethyl 4-Hydroxy-2-naphthalene carboxylate (63)

Compound **63** was made by a modified procedure of Hattori *et al*.[53] The acid **71** (5.1 g, 27 mmol) was taken up in anhydrous DMF (50 mL) to which $NaHCO_3$ (2.27 g, 27 mmol) was added. The reaction was stirred at reflux for 30 min., cooled to room temperature and EtI (1.67 mL, 27 mmol) was added and the reaction was allowed to stir 4-5 h. The reaction mixture was diluted with water, extracted with EtOAc (3 X 20 mL).

The combined organic layers were dried over sodium sulfate and concentrated under reduced pressure. The oil was crystallized from methanol-water to give **63** (4.95 g, 90%) as a light colored solid, lit. m.p. 139-141 °C (obs m.p. 140-142 °C); ^{1}H NMR ($CDCl_3$): δ 8.27 (d, 1H, J=2.5 Hz), 8.24 (s, 1H), 7.89 (d, 1H, J=5 Hz), 7.63 (s, 1H), 7.56 (m, 2H), 4.44 (q, 2H, J=7.5 Hz), 1.44 (t, 3H, J=7.5 Hz). ^{13}C NMR: δ 167.6 (C), 152.4 (C), 134.0 (C), 129.3 (CH), 127.7 (CH), 127.3 (CH), 127.1 (C), 127.0 (C), 123.5 (CH), 122.2 (CH), 107.6 (CH), 61.7 (CH_2), 14.5 (CH_3).

Methyl 4-Tri*iso*propylsiloxy-2-naphthalene carboxylate (74)

To a solution of **63** (3.26 g, 16 mmol) in anhydrous DMF (50 mL) was added imidazole (2.83 g, 42 mmol) and the reaction was allowed to stir at room temperature for 20 min. Tri*iso*propylsilyl chloride (4.04 mL, 19 mmol) was added by syringe and the reaction continued to stir at room temperature for 5-6 h. The reaction was diluted with water and extracted with EtOAc (3 X 20 mL). The combined organic layers were washed with water, dried over sodium sulfate, and concentrated under reduced pressure to give **74** (5.44 g, 95%) as a light colored oil; ^{1}H NMR ($CDCl_3$): δ 8.32-8.30 (m, 1H), 8.25 (m, 1H), 7.97 (m, 1H), 7.90-7.86 (m, 1H), 7.54-7.52 (m, 1H), 7.06 (s, 1H), 3.95 (s, 3H), 2.88 (ds, 3H), 1.18 (s, 18H). ^{13}C NMR: δ 167.38, 162.65, 152.24, 135.07, 134.01, 130.02, 129.20, 127.61, 127.54, 126.95, 123.77, 122.78, 121.64, 110.92, 52.23, 36.45, 31.44, 18.12, 17.82, 13.03, 12.48. GCMS (EI): 358 (m/z), 315, 283, 185.

Methyl 1-Bromo-4-tri*iso*propylsiloxy-2-naphthalene carboxylate (75)

A solution of **74** (5.44 g, 15 mmol) in $CHCl_3$ (30 mL) was treated portionwise with liquid bromine (77 μL, 15 mmol) over 15 min. The reaction was monitored by GCMS to completion. The reaction mixture was diluted with water and extracted with $CHCl_3$ (3 X 15 mL). The combined organic layers were dried over sodium sulfate and concentrated under reduced pressure to give a reddish oil **75** and was used without further purification in the next step; ^{1}H NMR ($CDCl_3$): δ 8.41-8.40 (m, 1H), 8.29-8.27 (m, 1H) 8.26-8.25 (m, 1H), 7.62-7.59 (m, 1H), 7.12 (s, 1H), 3.98 (s, 3H), 3.03 (s, 3H), 1.16 (s, 18H). GCMS (EI): 436/438 (m/z), 314, 271, 243, 137.

1-Bromo-4-hydroxy-2-naphthalene carboxylate (64)

The TIPS ester **75** (3.0 g, 6.88 mmol) was taken up in THF and treated with TBAF (10 mL) and allowed to stir at room temperature for 20 min. The reaction mixture was acidified with 1N HCl, and extracted with EtOAc (3 X 10 mL). The combined organic layers were washed with water, dried over sodium sulfate and concentrated under reduced pressure to give **64** (1.90 g, 98%) as a red oil, which was used in the next step without further purification. ^{1}H NMR ($CDCl_3$): δ 8.33-8.29 (m, 2H), 7.61-7.55 (m, 2H), 7.20 (s, 1H), 3.93 (s, 3H). ^{13}C NMR: δ 167.99, 153.25, 132.76, 131.04, 128.09, 127.86, 127.83, 127.24, 127.13, 125.98, 108.23, 52.40.

1,4-Dihydroxy-2-methyl naphthoic carboxylate (77)

Compound **77** was prepared using the procedure of Miyano *et al*.[67] Compound **76** (10 g, 49 mmol) was dissolved in anhydrous DMF (75 mL) and treated with $NaHCO_3$

(4.1 g, 49 mmol). The suspension was heated to 50 °C for 30 min. The reaction mixture was cooled to room temperature and treated with MeI (3.03 mL, 49 mmol) and the reaction stirred at room temperature overnight. The reaction was diluted with water and extracted with EtOAc (3 X 25 mL). The combined organic layers were washed with water (3 X 100 mL), dried over sodium sulfate, and concentrated *in vacuo*. The residue was crystallized from methanol-water to give **77** (8.5 g, 80%) as a light colored solid, lit. m.p. 180-183 °C (obs m.p. 185-188 °C); ^{1}H NMR ($CDCl_3$): δ 11.4 (s, 1H), 8.35-8.32 (m, 1H), 8.21-8.18 (m, 1H), 7.60-7.52 (m, 2H), 7.14 (s, 1H), 3.95 (s, 3H). ^{13}C NMR: δ 171.1 (C), 154.1 (C), 144.8 (C), 129.5 (C), 128.3 (CH), 125.8 (C), 125.2 (CH), 123.4 (CH), 122.1 (CH), 104.5 (CH), 52.0 (CH_3).

4-Benzyloxy-1-hydroxy-2-methyl naphthoic carboxylate (78)

Compound **78** was prepared utilizing the procedure of Diez-Martin *et al*.[54] The ester **77** (840 mg, 3.85 mmol) was dissolved in acetone (20 mL) and treated with K_2CO_3 (1.6 g, 11.55 mmol) and benzyl bromide (46 μL, 3.85 mmol) and stirred at reflux for 3-4 h. The reaction mixture was filtered and the mother liquor was concentrated to give a dark colored oil. The oil was dissolved in EtOAc (50 mL) and washed with 1N HCl, saturated $NaHCO_3$, water, dried over sodium sulfate, and concentrated under reduced pressure. The residue was crystallized from cold $CHCl_3$ to give **78** (726 mg, 61%) as a yellow solid, m.p. 159-160 °C; ^{1}H NMR ($CDCl_3$): δ 11.64 (s, 1H), 8.37-8.35 (m, 1H), 8.25-8.21 (m, 1H), 7.60-7.55 (m, 4H), 7.52-7.43 (m, 3H), 7.11 (s, 1H), 5.16 (s, 2H), 3.98 (s, 3H). ^{13}C NMR: δ 170.8 (C), 155.1 (C), 146.2 (C), 136.6 (C), 129.5 (C), 128.7 (C),

128.2 (CH), 127.6 (CH), 127.1 (CH), 126.1 (CH), 125.0 (C), 123.3 (CH), 121.6 (CH), 103.9 (CH), 69.9 (CH_2), 52.0 (CH_3).

4-Benzyloxy-1-trifluoromethanesulfonyloxy naphthalene-2-carboxylic acid methyl ester (79)

The benzyl phenol **78** (1.56 g, 5.06 mmol) was taken up in anhydrous pyridine (10 mL) and cooled to 0 °C. The solution was then treated with trifluoromethanesulfonic anhydride (2.56 mL, 15.12 mmol). The reaction was stirred at room temperature overnight. The reaction mixture was cooled to 0 °C and quenched with water and extracted with diethyl ether (3 X 10 mL), washed with 10% HCl, saturated NaCl, dried over sodium sulfate, and concentrated under reduced pressure to give a dark colored solid. The solid was crystallized from petroleum ether-diethyl ether to give pure **79** (1.58 g, 71%) as a yellow solid, m.p. 93-95 °C; ^{1}H NMR ($CDCl_3$): δ 8.376-8.374 (m, 1H), 8.123-8.103 (m, 1H), 7.707-7.689 (m, 2H), 7.536-7.532 (m, 2H), 7.463-7.427 (m, 4H), 5.282 (s, 2H), 4.011 (s, 3H). ^{13}C NMR: δ 165.66 (C), 153.92 (C), 138.67 (C), 136.10 (C), 128.93 (CH), 128.83 (CH), 128.67 (CH), 128.59 (CH), 128.57 (CH), 127.86 (CH), 127.31 (CH), 126.95 (C), 122.87 (CH), 122.21 (C), 121.65 (C), 118.5 (C), 104.76 (CH), 70.69 (CH_2), 53.04 (CH_3). Anal Calcd for $C_{20}H_{14}F_3O_6S$; C, 54.54; H, 3.43. Found; C, 54.43; H, 3.44

4-Benzyloxy-1-(4, 4, 5, 5-tetramethyl-[1,2,3]dioxaborolan-2-yl)-naphthalene-2-carboxylic acid methyl ester (81)

The triflate **79** (1.48 g, 3.36 mmol) was taken up in anhydrous dioxane (25 mL) and treated with $PdCl_2$(dppf) (82 mg, 0.1008 mmol) and pinacol borane (2.17 g, 15.12 mmol). The suspension was stirred at reflux for 2-3 h under nitrogen. The reaction was quenched with water, extracted with CH_2Cl_2 (3 X 10 mL), dried over sodium sulfate, and concentrated under reduced pressure to give a dark colored oil. The oil was taken up in petroleum ether (15 mL) and filtered thru a plug of $MgSO_4$. Partial concentration of the mother liquor led to crystallization to give pure **81** (1.13 g, 81%) as a white solid; ^{1}H NMR ($CDCl_3$): δ 8.46-8.45 (m, 1H), 8.03-8.02 (m, 1H), 7.55-7.54 (m, 4H), 7.41 (s, 1H), 7.39-7.35 (m, 3H), 5.28 (s, 2H), 3.97 (s, 3H), 1.53 (s, 12H). ^{13}C NMR: δ 168.9, 155.38, 136.93, 136.51, 131.96, 128.99, 128.24, 127.75, 127.68, 127.37, 127.26, 122.66, 103.84, 84.35, 70.34, 52.70, 25.76 ($4CH_3$).

4-Benzyloxy-1-bromo-naphthalene-2-carboxylic acid methyl ester (65)

Compound **65** was prepared by two different procedures. Method A: In a glove box, the boronate ester **81** (50 mg, 1.19 mmol) was taken up in methanol (10 mL) and was subsequently treated with Cu(II)Br (800 mg, 3.59 mmol) in water (10 mL). The reaction mixture was stirred at reflux for 3-4 h. The reaction was diluted with water and extracted with diethyl ether (3 X 10 mL). The combined organic layers were washed with 1N HCl, saturated $NaHCO_3$, dried over sodium sulfate, and concentrated under reduced pressure to give a dark colored residue. The residue was crystallized from 3:1 petroleum ether-diethyl ether to give pure **65** (390 mg, 88%) as a light brown solid. Method B: A

solution of **64** (1.0 g, 3.56 mmol) in acetone (20 mL) was treated with K_2CO_3 (1.23 g, 8.9 mmol), benzyl bromide (46 μL, 3.92 mmol), and stirred at reflux for 5 h. The reaction mixture was filtered thru a plug of silica and the mother liquor was concentrated under reduced pressure to give a dark colored oil. The oil was crystallized from petroleum ether-diethyl ether to give **65** (1.25 g, 95%) as a brown solid; ^{1}H NMR ($CDCl_3$): δ 8.39-8.37 (m, 1H), 8.32-8.30 (m, 1H), 7.62-7.56 (m, 4H), 7.47-7.41 (m, 3H), 7.11 (s, 1H), 5.21 (s, 2H), 3.97 (s, 3H). ^{13}C NMR: δ 168.18, 154.20, 136.43, 133.08, 131.08, 128.88, 128.75, 128.60, 128.46, 127.93, 127.77, 127.74, 122.71, 113.75, 105.60, 70.72, 52.91.

4-Benzyloxy-1-bromo-naphthalene-2-carboxylic acid (92)

A solution of **65** (221 mg, 0.649 mmol) in 1.5 M methanolic KOH (25 mL) was refluxed for 6 h. The methanol was removed *in vacuo* and the residue taken up in water, washed with diethyl ether (3 X 5 mL), acidified with 1N HCl, cooled, and filtered to give **92** (195 mg, 95%) as a white solid, m.p. 211-213 °C; ^{1}H NMR ($CDCl_3$/DMSO-d_6): δ 8.31 (t, 2H), 7.60 (m, 4H), 7.36 (m, 3H), 7.20 (s, 1H), 5.26 (s, 2H). ^{13}C NMR: δ 167.5 (C), 152.4 (C), 135.0 (C), 131.4 (C), 131.2 (C), 127.3 (CH), 126.9 (CH), 126.7 (CH), 126.3 (CH), 126.1 (CH), 125.9 (C), 121.1 (CH), 110.6 (CH), 104.4 (CH), 69.0 (CH_2). Anal. Calcd for $C_{18}H_{13}BrO_3$: C, 60.52; H, 3.67. Found: C, 60.48; H, 3.76.

***N*-(*tert*-Butoxycarbonyl)-(*S*)-proline (83)**

Compound **83** was prepared utilizing the procedure of Ragnarsson and Karlsson.[58] L-Proline **82** (5 g, 43 mmol) was taken up in THF (100 mL) and was treated with NaOH (3.48 g, 86 mmol) in water (75 mL). To this solution was added Boc anhydride (10.4 g,

47 mmol) and the reaction stirred at room temperature overnight. The reaction mixture was diluted with diethyl ether (100 mL) and the biphasic solution was made mildly acidic with 2N HCl (pH 6.0). The layers were separated and the aqueous layer extracted with EtOAc (3 X 25 mL), dried over sodium sulfate, and concentrated under reduced pressure to give a light colored oil. The oil was triturated with petroleum ether, cooled, and filtered to give **83** (8.7 g, 95%) as a white solid, m.p. 133-134 °C (obs m.p. 133 °C); ^{1}H NMR ($CDCl_3$): δ 10.34 (bs, 1H), 4.36-4.21 (m, 1H), 3.54-3.35 (m, 2H), 2.27-1.91 (m, 4H), 1.47 (s, 9H). ^{13}C NMR: δ 177.6, 154.2, 80.5, 59.0, 46.7, 29.4 (3C), 28.3, 23.6.

***N*-(*tert*-Butoxycarbonyl)-(*S*)-prolinol (84)**

Compound **84** was prepared using the procedure of Katzenellenbogen.[59] A solution of **83** (10 g, 46.5 mmol) in anhydrous THF (250 mL) was cooled to 0 °C and treated with diborane (51 mL, 51 mmol). The reaction was stirred at room temperature for 3-4 h, cooled to 0 °C, and quenched with water. The aqueous layer was extracted with EtOAc (3 X 25 mL). The combined organic layers were washed with saturated $NaHCO_3$, brine, water, dried over sodium sulfate, and concentrated under reduced pressure to give **84** (8.5 g, 91%) as a light colored oil, which was used without further purification in the next step; ^{1}H NMR ($CDCl_3$): δ 4.19-4.17 (m, 1H), 3.92 (m, 1H), 3.57 (m, 2H), 3.42 (m, 1H), 3.27 (m, 1H), 1.96 (m, 1H), 1.73 (m, 2H), 1.56 (m, 1H), 1.44 (s, 9H). ^{13}C NMR: δ 154.5, 78.2, 64.6, 58.2, 57.6, 46.1, 26.9(3C), 22.6.

***N*-(*tert*-Butoxycarbonyl)-(*S*)-prolinal (85)**

Compound **85** was prepared by the method of Katzenellenbogen.[59] To a cooled solution (-60 °C) of oxalyl chloride (13 μL, 1.49 mmol) in anhydrous CH_2Cl_2 (5 mL) was added anhydrous DMSO (19 μL, 2.61 mmol) dropwise over 5 min. A solution of **84** (250 mg, 1.24 mmol) in anhydrous CH_2Cl_2 (5 mL) was added and the reaction stirred at -60 °C for 30 min. A solution of TEA (69 μL, 4.98 mmol) was added dropwise and the reaction was allowed to warm to room temperature over 30 min. The reaction was quenched with water and extracted with CH_2Cl_2 (3 X10 mL). The combined organic layers were washed with 1N HCl, saturated $NaHCO_3$, dried over sodium sulfate and concentrated under reduced pressure to give a green oil. The oil was purified by kugelrohr distillation (145 °C at 0.2 mmHg) to give **85** (4.5 g, 91%), which crystallized upon standing to give a light-colored solid, m.p. 26-32 °C (obs m.p. 26-32 °C); ^{1}H NMR ($CDCl_3$): δ 9.45-9.38 (m, 1H), 4.18-4.03 (m, 1H), 3.48 (m, 2H), 2.2-1.8 (m, 4H), 1.40 (d, 9H). ^{13}C NMR: δ 200.3, 153.9, 80.5, 65.0, 46.8, 28.2, 26.7 (3C), 24.6.

3-Chloropropane-1-amine hydrochloride (89)

Compound **89** was prepared using the procedure of Geneste and Hesse.[60] Propanolamine **88** (10 g, 13 mmol) was taken up in diethyl ether (50 mL) with a small amount of ethanol (1-2 drops) to help solubilize the salt. Hydrochloride gas was bubbled into the solution resulting in a yellow oil, which oiled out of the solution. The solvent was decanted and the yellow oil was taken up in thionyl chloride (96 mL, 1.33 mmol). The reaction mixture was then stirred at room temperature for 3 h. The thionyl chloride was removed under reduced pressure and the residue was washed with benzene (3 X 10 mL).

The oily residue was crystallized from diethyl ether-ethanol to give pure **89** (15.54 g, 90%) as a white solid, m.p. 142-144 °C (obs m.p. 144-146 °C); ^{1}H NMR ($CDCl_3$): δ 2.2-2.4 (m, 2H), 3.1-3.3 (m, 2H), 3.7-3.9 (m, 2H). ^{13}C NMR: δ 29.58, 36.92, 41.47.

_N_-Boc-3-chloropropylamine (90)

Compound **90** was prepared utilizing the procedure of Beak *et al*.[62] To a solution of di-*tert*-butyldicarbonate (15.2 g, 69 mmol) and TEA (16 mL, 116 mmol) in THF (100 mL) was added **89** (10 g, 77.5 mmol) at 0 °C. The reaction mixture was stirred for 20 min at 0 °C, warmed to room temperature and stirred for an additional 18 h. The reaction mixture was diluted with 10% $NaHCO_3$ solution and extracted with diethyl ether (3 X 25 mL). The combined organic layers were washed with brine, dried over sodium sulfate, and concentrated under reduced pressure. The oil was purified by distillation to give pure **90** (12.7 g, 85%) as a colorless oil; ^{1}H NMR ($CDCl_3$): δ 1.44 (s, 9H), 1.94 (m, 2H), 3.28 (m, 2H), 3.61 (t, 2H, J=6.33 Hz). ^{13}C NMR: δ 28.43(3C), 32.70, 37.95, 42.43, 67.97, 79.31, 156.13.

_N_-(*tert*-Butoxycarbonyl)-_N_-(2-butenyl)-3-chloropropylamine (91)

Compound **91** was prepared using the procedure of Beak *et al*.[62] Sodium hydride (60%, 414 mg, 10.36 mmol) was taken up in anhydrous THF (20 mL) and cooled to 0 °C. Compound **90** (1.0 g, 5.18 mmol) dissolved in anhydrous THF (10 mL) was added dropwise and stirred for 5 min. Crotyl bromide (64 μL, 6.21 mmol) was added by syringe to the reaction mixture. The ice bath was removed and the reaction continued to stir at room temperature overnight. The reaction was cooled to 0 °C and quenched with water,

extracted with EtOAc (3 X 20 mL), dried over sodium sulfate, and concentrated under reduced pressure, and purified by flash chromatography (silica gel, 100% petroleum ether) to give **91** (998 mg, 78%) as a yellow oil; ^{1}H NMR ($CDCl_3$): δ 1.42 (s, 9H), 1.65 (m, 3H), 1.96 (m, 2H), 3.26 (m, 2H), 3.50 (m, 2H), 3.71 (m, 2H), 5.38 (m, 1H), 5.55 (m, 1H). ^{13}C NMR: δ 17.8, 28.6 (3C), 32.1, 42.7, 79.7, 126.7, 128.3, 155.6.

(*S*)-*N*-(*tert*-Butoxycarbonyl)-2-(1-propenyl)pyrrolidine (86)

Compound **86** was prepared by 2 different methods. Method A: This compound was made by the procedure of Serino *et al*.[61] Ethyl triphenylphosphonium bromide (2.33 g, 6.28 mmol) was taken up in anhydrous THF (50 mL) cooled to 0 °C and treated with n-BuLi (1.6 M, 3.93 mL, 6.28 mmol). The reaction was allowed to stir at 0 °C for 15 min. A solution of **85** (500 mg, 2.5 mmol) in anhydrous THF (30 mL) was added dropwise and the reaction proceeded to stir at 0 °C for 1 h. The ice bath was removed and the reaction continued to stir for 3-4 h. The reaction was diluted with pentane, cooled, and filtered thru a plug of silica, and purified by flash chromatography (silica gel, 9:1 petroleum ether-diethyl ether) to give **86** (400 mg, 75%) as a light colored oil. Method B: The procedure of Beak *et al*. was utilized.[62] A solution of (-)-sparteine (78 μL, 3.38 mmol) was dissolved in anhydrous THF (20 mL) and cooled to -78 °C, which was treated with n-BuLi (1.6 M, 35 μL, 3.38 mmol) and the reaction was stirred for 30 min at 0 °C. A solution of **91** (570 mg, 2.3 mmol) in anhydrous THF (20 mL) was added dropwise. The reaction was stirred for 4 h at-78 °C. The reaction was quenched with water, extracted with diethyl ether (3 X 20 mL), dried over sodium sulfate, and concentrated under reduced pressure to give a light colored oil. Flash chromatography (silica gel, 3:1

petroleum ether-ethyl acetate) gave pure **86** (339 mg, 70%) as a light colored oil; ^{1}H NMR ($CDCl_3$): δ 5.34-5.18 (m, 2H), 4.43 (m, 1H), 3.31-3.26 (m, 2H), 1.69-2.0 (m, 4H), 1.65-1.67 (m, 3H), 1.97-1.34 (m, 9H). ^{13}C NMR: δ 154.3, 131.9, 124.6, 78.5, 53.8, 46.1, 32.9, 28.3 (3C), 23.5, 17.3.

_S_-(2)-Propenyl pyrrolidine (87)

Compound **87** was prepared using the procedure of Tietze *et al*.[63] A solution of **86** (210 mg, 1.10 mmol) in CH_2Cl_2 (10 mL) was treated with 4N HCl (2.0 mL) and the reaction stirred at reflux for 30 min. The solvent was removed under reduced pressure and **87** was used in the next step without further purification.

4-Benzyloxy-1-bromo-2-(2-propenyl pyrrolidine) carboxylic acid amide (93)

The bromo acid **92** (120 mg, 0.336 mmol) was taken up in acetyl chloride (10 mL) and treated with DMF (3-4 drops). The reaction mixture was stirred at reflux for 3 h. The acetyl chloride was removed *in vacuo* and the residue was taken up in benzene (3 X 5 mL), which was subsequently removed under reduced pressure to remove traces of acetyl chloride. The residue was taken up in EtOAc (20 mL) and a solution of the propenyl pyrrolidine **87** (37 mg, 0.336 mmol) and TEA (15 μL, 0.72 mmol) in EtOAc (10 mL) was added dropwise and the reaction stirred at room temperature for 1-2 h. The reaction was diluted with water, extracted with EtOAc (3 X 10 mL), and the combined organic layers were washed with 1N HCl, saturated $NaHCO_3$, dried over sodium sulfate and concentrated under reduced pressure to give a brown oil. The oil was purified by spinning band chromatography (silica gel, 1 mm plate, 50% petroleum ether-diethyl

ether) to give **93** (113 mg, 75%) as a light colored oil; ^{1}H NMR ($CDCl_3$): δ 8.34 (m, 1H), 8.23 (m, 1H), 7.61 (m, 4H), 7.41 (m, 3H), 6.72 (m, 1H), 5.64 (m, 1H), 5.22 (s, 2H), 5.08, 4.93, 4.52, 3.83, 3.69, 2.16-1.65, 1.25, 0.57. ^{13}C NMR: δ 169.4 (C), 154.2 (C), 136.6 (C), 130.8 (CH), 130.3 (CH), 129.8 (C), 128.8 (C), 128.6 (CH), 128.4 (CH), 128.3 (CH), 127.7 (C), 127.5 (C), 127.3 (CH), 127.0 (CH), 125.2 (CH), 122.6 (CH), 105.6 (CH), 103.9 (CH), 70.6 (CH_2), 55.5 (CH_3), 46.3 (CH_2), 31.4 (CH_2), 23.2 (CH_2).

5-Benzyloxy-12-vinyl-10, 11, 11a, 12-tetrahydro-9*H*-benzo[*f*]pyrrolo[1,2-*b*] isoquinoline-7-one (94)

In a glove box, the bromo amide **93** (100 mg, 0.227 mmol) was placed in a sealed tube and charged with anhydrous acetonitrile (10 mL). To this solution was added TEA (47 μL, 0.34 mmol), Ag_2CO_3 (69 mg, 0.249 mmol), dppp (23 mg, 0.057 mmol), and $Pd(OAc)_2$ (6.4 mg, 0.028 mmol) in order. The tube was sealed and stirred at 100 °C for 1 h. The reaction mixture was filtered thru a plug of celite and the mother liquor concentrated under reduced pressure. Spinning band chromatography (silica gel, 1mm plate, 50% petroleum ether-diethyl ether) afforded **94** (65 mg, 80%) as a light colored oil; ^{1}H NMR ($CDCl_3$): δ 8.44 (m, 1H), 8.02 (m, 1H), 7.66 (s, 1H), 7.57 (m, 4H), 7.45 (m, 3H), 5.78 (ddd, 1H), 5.32 (d, 2H), 5.12 (ddd, 1H), 4.21 (m, 1H), 4.17 (m, 1H), 3.84 (m, 1H), 3.63 (m, 1H), 2.12 (m, 5H), 1.87 (m, 1H), 1.25 (s, 1H). ^{13}C NMR: δ 163.6 (C), 154.1 (C), 137.2 (C), 134.6 (CH), 130.2 (C), 128.7 (CH), 128.2 (C), 127.8 (CH), 127.4 (C), 126.9 (C), 124.1 (CH), 123.3 (CH), 119.1 (CH), 103.0 (CH), 70.4 (CH_2), 59.7 (CH), 45.5 (CH_2), 42.2 (CH), 29.2 (CH_2), 23.4 (CH_2).

1, 2, 3, 12, 12a-Tetrahydro-12-(hydroxymethyl)-7-benzyloxy benzo[*f*]pyrrolo [1,2-*b*]isoquinoline-5-one (95)

Compound **94** (100 mg, 0.27 mmol) was placed in a three necked round bottom flask to which methanol was added. The solution was cooled to 0 °C and O_3 was bubbled through. To effect addition of ozone, the exit port of the ozone generator was connected with a piece of Tygon tubing that terminated in a glass frit. The fritted end was submerged in the solvent. The reaction stirred at 0 °C for 1-2 hours, after which the ozone generation was terminated and $NaBH_4$ (20 mg, 0.54 mmol) was added and the reaction proceeded to stir overnight while slowly warming to room temperature. The reaction was placed under a slightly positive pressure of N_2(g) and stirred overnight. The methanol was removed *in vacuo*, and the residue taken up in H_2O and extracted with EtOAc (3 X 10 mL), dried over Na_2SO_4, and concentrated to give a yellow oil. Spinning band chromatography (1 mm plate, silica gel, 100% $CHCl_3$) gave the pure diastereomers **95** (30 mg, 60%) as a light colored oils.

Cis isomer: ^{1}H NMR ($CDCl_3$): δ 8.39-8.37 (m, 1H), 8.11-8.09 (m, 1H), 7.55-7.51 (m, 5H), 7.41-7.38 (m, 3H), 5.21 (s, 2H), 4.04-4.02 (m, 1H), 3.85-3.83 (m, 3H), 3.70-3.68 (m, 1H), 3.5-3.48 (m, 1H), 2.75 (br s, 1H), 2.38-2.35 (m, 1H), 2.18-2.15 (m, 1H), 2.05-2.01 (m, 1H), 1.8-1.77 (m, 1H). ^{13}C NMR: δ 163.4, 153.8, 136.8, 131.1, 129.0, 128.5, 127.8, 127.6, 127.5, 127.3, 126.6, 124.0, 123.0, 102.4, 70.1, 61.3, 58.7, 45.2, 39.0, 29.1, 23.3. *Trans* isomer: ^{1}H NMR ($CDCl_3$): δ 8.41-8.40 (m, 1H), 8.15-8.13 (m, 1H), 7.74 (s, 1H), 7.55-7.53 (m, 4H), 7.37-7.35 (m, 3H), 5.29 (s, 2H), 4.24-4.22 (m, 1H), 4.05-4.02 (m, 1H), 3.90-3.88 (m, 2H), 3.68-3.66 (m, 1H), 3.35-3.32 (m, 1H), 2.5 (br s, 1H), 2.08-2.05 (m, 1H), 1.90-1.88 (m, 2H), 1.52-1.49 (m, 1H). ^{13}C NMR: δ 163.7, 153.4, 136.6,

131.5, 128.3, 127.7, 127.3, 126.7, 126.5, 126.3, 126.2, 123.9, 122.7, 102.5, 69.9, 65.9, 58.3, 44.5, 39.0, 30.8, 21.5.

Methylcarbamic acid *tert*-butyl ester (103)

Compound **103** was prepared using the procedure of Lee *et al.*[65] To a stirred solution of methylamine hydrochloride **99** (2.0 g, 30 mmol) in THF (25 mL) was added TEA (8.3 mL, 60 mmol) and the solution stirred for 5 minutes at room temperature. The mixture was cooled to 0°C and a solution of di-*tert*-butyl dicarbonate (6.54 g, 27 mmol) in THF (20 mL) was added. The ice bath was removed and the reaction mixture was stirred at room temperature overnight. The reaction was diluted with water and extracted with diethyl ether (3 X 20 mL). The combined organic layers were washed with saturated $NaHCO_3$, brine, dried over sodium sulfate, and concentrated under reduced pressure to give 103 as a yellow oil. Kugelrohr distillation (110 °C at 2-4 mmHg) gave **75** (2.43 g, 62%) as a clear oil; ^{1}H NMR ($CDCl_3$): δ 1.44 (s, 9H), 2.72 (s, 3H), 4.84 (br s, 1H). ^{13}C NMR: δ 27.22, 28.40 (3C), 78.99, 156.79. GCMS (EI): 131 (m/z), 116, 57, 41.

But-2-enyl-methyl carbamic acid *tert*-butyl ester (104)

A solution of **103** (500 mg, 3.82 mmol) was dissolved in anhydrous THF (20 mL) and cooled to 0 °C. Sodium hydride (60%, 306 mg, 7.64 mmol) was added and the suspension stirred for 5 min. To the suspension was added crotyl bromide (47 μL, 4.58 mmol) by syringe and the reaction was allowed to stir at room temperature overnight. The reaction was cooled to 0 °C, quenched with water, and extracted with diethyl ether (3 X 10 mL). The combined organic layers were washed with saturated NaCl, dried over

sodium sulfate, and concentrated *in vacuo* to give **104** as a yellow oil. Flash chromatography (silica gel, 100% petroleum ether) afforded **76** (550 mg, 85%) as a clear oil; ^{1}H NMR ($CDCl_3$): δ 1.44 (s, 9H), 1.69 (m, 3H), 2.77 (m, 3H), 3.71 (m, 2H), 5.38 (m, 1H), 5.58 (m, 1H). ^{13}C NMR: δ 17.78, 22.87, 28.59 (3C), 33.52, 79.38, 127.12, 128.09, 155.82. GCMS (EI): 185 (m/z), 170, 85.

_N_-methyl-2-butene (101)

To a solution of **104** (350 mg, 1.89 mmol) in CH_2Cl_2 (10 mL) was added TFA (21 μL, 2.83 mmol) and the reaction stirred at room temperature for 30 min. The reaction mixture was poured into diethyl ether (25 mL) and washed with 10% NaOH, brine, dried over sodium sulfate, concentrated under reduced pressure to give **101**, and used without further purification in the next step; ^{1}H NMR ($CDCl_3$): δ 5.95-5.89 (m, 1H), 5.61-5.55 (m, 1H), 3.76 (d, 2H), 2.75 (s, 3H), 1.72 (d, 3H). ^{13}C NMR: δ 132.95, 121.9, 50.26, 32.24, 18.32.

4-Benzyloxy-1-bromo-naphthalene-2-carboxylic acid but-2-enyl-methyl-amide (105)

Bromo acid **92** (80 mg, 1.07 mmol) was taken up in thionyl chloride (30 mL) and DMF (3-4 drops) was added and the reaction was refluxed for 3-4 h. The thionyl chloride was removed under reduced pressure and the residue washed with benzene (3 X 5 mL) to give light colored yellow oil. The oil was taken up in EtOAc (20 mL) and cooled to 0 °C. TEA (45 μL, 3.21 mmol) was added and the reaction proceeded to stir at room temperature for 2-3 h. The reaction mixture was diluted with EtOAc, washed with 1N

HCl, saturated $NaHCO_3$, water, dried over sodium sulfate, and concentrated *in vacuo*. Spinning band chromatography (silica gel, 1 mm plate, 3:1 petroleum ether-diethyl ether) afforded **105** (348 mg, 80%) as a dark colored oil; ^{1}H NMR ($CDCl_3$): δ 8.36-8.32 (m, 1H), 8.25-8.21 (m, 1H), 7.63-7.53 (m, 4H), 7.49-7.40 (m, 3H), 6.75 (s, 1H), 5.8-5.71 (m, 2H), 5.21 (s, 2H), 4.12-4.09 (m, 1H), 3.67-3.63 (m, 1H), 3.08 (s, 3H), 2.75 (s, 3H), 1.77 (d, 3H), 1.65 (d, 3H). ^{13}C NMR: δ 169.66, 154.88, 136.36, 132.64, 130.04, 129.91, 128.82, 128.34, 127.66, 127.24, 126.75, 125.63, 125.28, 122.72, 110.32, 104.15, 70.66, 52.97, 48.83, 35.32, 31.88, 17.95.

6-Benzyloxy-3-methyl-1-vinyl-2, 3-dihydro-1*H*-benzo[*f*]isoquinolin-4-one (106)

In a glove box, the bromo amide **105** (620 mg, 1.47 mmol) was taken up in anhydrous acetonitrile (15 mL) and placed in a sealed tube. To the solution was added TEA (31 μL, 2.20 mmol), Ag_2CO_3 (446 mg, 1.62 mmol), dppp (151 mg, 0.367 mmol), and $PdCl_2$(dppf) (150 mg, 0.183 mmol). The sealed tube was then stirred at 100 °C for 1 h, filtered thru a plug of celite and concentrated under reduced pressure to give a dark colored oil. Spinning band chromatography (silica gel, 2 mm plate, 3:1 petroleum ether-diethyl ether) gave **106** (200 mg, 40%) as a light colored oil; ^{1}H NMR ($CDCl_3$): δ 8.43-8.41 (m, 1H), 7.95-7.94 (m, 1H), 7.68 (s, 1H), 7.56-7.53 (m, 4H), 7.42-7.39 (m, 3H), 6.081-6.070 (m, 2H), 5.13 (s, 2H), 4.93 (m, 2H), 4.13 (m, 2H), 3.013 (s, 3H). ^{13}C NMR: δ 165.09, 154.15, 137.72, 131.31, 129.33, 128.82, 128.77, 127.79, 127.57, 127.04, 124.24, 123.21, 117.52, 103.25, 70.44, 53.38, 38.60, 29.89.

6-Benzyloxy-3-methyl-4-oxo-1, 2, 3, 4-tetrahydro-benzo[*f*]isoquinoline-1-carbaldehyde (107)

Compound **106** (150 mg, 0.437 mmol) was placed in a 3:1 dioxane-water solution (20 mL) and OsO_4 (4%, 2.77g, 0.0437 mmol) was added and the reaction was allowed to stir at room temperature for 5 min. $NaIO_4$ (280 mg, 1.31 mmol) was added and the reaction stirred at room temperature overnight. The reaction was diluted with water, extracted with diethyl ether (3 X 10 mL), dried over sodium sulfate, and concentrated under reduced pressure to give a dark colored oil. Spinning band chromatography (silica gel, 2 mm plate, 3:1 petroleum ether-ethyl acetate) afforded **107** (100 mg, 65%) as a light colored oil; ^{1}H NMR ($CDCl_3$): δ 9.7 (s, 1H), 7.96-7.95 (m, 1H), 7.65-7.63 (m, 1H), 7.57 (s, 1H), 7.54-7.46 (m, 4H), 7.41-7.37 (m, 3H), 5.32 (s, 2H), 4.22-4.20 (m, 1H), 4.10-4.05 (m, 1H), 3.97-3.95 (m, 1H), 3.2 (s, 3H). ^{13}C NMR: δ 197.9, 164.07, 155.08, 136.80, 131.52, 128.83, 128.22, 127.98, 127.80, 127.50, 123.71, 123.48, 122.40, 103.58, 70.56, 47.34, 46.11, 35.53. MS (EI): 345 (m/z), 316, 224, 91.

6-Benzyloxy-1-hydroxymethyl-3-methyl-2, 3-dihydro-1*H*-benzo[*f*]isoquinoline-4-one (108)

To a solution of **107** (100 mg, 0.29 mmol) in THF (15 mL) was added $NaBH_4$ (44 mg, 1.16 mmol) and the reaction stirred for 1 h at room temperature. The reaction was cooled to 0 °C, diluted with water, extracted with EtOAc (3 X 10 mL), dried over sodium sulfate, and concentrated under reduced pressure. Spinning band chromatography (silica gel, 1 mm plate, 3:1 petroleum ether-diethyl ether) afforded pure **108** (95 mg, 95%) as a light colored oil; ^{1}H NMR ($CDCl_3$): δ 8.34-8.32 (m, 1H), 7.98-7.97 (m, 1H), 7.57 (s, 1H),

7.49-7.46 (m, 4H), 7.35-7.33 (m, 3H), 5.2 (s, 2H), 3.77-3.61 (m, 5H), 3.19 (s, 3H). ^{13}C NMR: δ 164.9, 154.17, 137.02, 131.31, 128.76, 128.18, 127.75, 127.62, 127.23, 127.10, 123.84, 123.32, 103.19, 70.39, 62.52, 48.57, 36.42, 35.71.

Methanesulfonic acid-6-benzyloxy-3-methyl-4-oxo-1, 2, 3, 4-tetrahydro-benzo[*f*] isoquinolin-1-ylmethyl ester (109)

A solution of **108** (95 mg, 0.288 mmol) in anhydrous CH_2Cl_2 (15 mL) was treated with TEA (7.9 μL, 0.576 mmol) and methanesulfonyl chloride (3.3 μL, 0.432 mmol) and the reaction was stirred at room temperature under nitrogen for 3-4 h. The reaction was diluted with CH_2Cl_2, washed with 1N HCl, saturated $NaHCO_3$, water, dried over sodium sulfate, and concentrated under reduced pressure. Spinning band chromatography (silica gel, 1 mm plate, 3:1 petroleum ether-diethyl ether) gave pure **109** (110 mg, 91%) as a pale yellow oil; ^1H NMR ($CDCl_3$): δ 8.46-8.42 (m, 1H), 8.09-8.06 (m, 1H), 7.66 (s, 1H), 7.56-7.53 (m, 4H), 7.43-7.40 (m, 3H), 5.31 (s, 2H), 4.35 (m, 3H), 3.95-3.90 (m, 2H), 3.24 (s, 3H), 3.02 (s, 3H). ^{13}C NMR: δ 164.49, 154.87, 136.82, 131.02, 128.81, 128.28, 127.97, 127.76, 127.43, 125.03, 123.52, 123.35, 103.29, 70.50, 67.82, 48.23, 37.79, 35.61, 34.22.

Methanesulfonic acid 6-hydroxy-3-methyl-4-oxo-1, 2, 3, 4-tetrahydro-benzo[*f*] isoquinolin-1-ylmethyl ester (110)

In a glove box, compound **109** (40 mg, 0.094 mmol) was dissolved in ethanol (8 mL) to which cyclohexene (4 mL) and $Pd(OH)_2$ (18 mg, 0.0235 mmol) were added and the reaction was refluxed under nitrogen for 2-3 h. The reaction was filtered and the

mother liquor concentrated under reduced pressure to give **110** (29 mg, 91%) as a light colored oil. ^{1}H NMR ($CDCl_3$): δ 8.43-8.40 (m, 1H), 8.08-8.04 (m, 1H), 7.88 (s, 1H), 7.64-7.60 (m, 1H), 6.91-6.89 (m, 1H), 3.98-3.94 (m, 5H), 3.30 (s, 3H), 3.04 (s, 3H).

REFERENCES

1.) http://www.cdc.gov

2.) Elledge, S. **Science** 1996, 274, 1664

3.) Kumar, V.; Fausto, N.; Abba, A. Basis of Disease 2004, Elsevier Science, New York

4.) Weinberg, Robert A. The Biology of Cancer. 2007, Garland Science, New York.

5.) Brune, B. **Cell Death Differ**. 2003, 10, 864

6.) Mattson, M.; Chan, S. **Nature Cell Biol**. 2003, 5, 1041

7.) Chiarugi, A. Moskowitz, M. **Science** 2002, 297, 259

8.) Takaoka, A. *et al*. **Nature** 2003, 424, 516

9.) Yoshida, B. *et al*. **J. Natl. Canc. Inst.** 2000, 92, 1717

10.) Lemke, Thomas; Williams, David. Foye's Principle's of Medicinal Chemistry. 2002, Lippincott, Williams, and Wilkins, Philadelphia, p. 924-951.

11.) Saenger, W. Principles of Nucleic Acid Structure Ed, Springer-Verlag, New York, NY, 1981, 229.

12.) Lee, M. *et al*. **J. Med. Chem**. 1993, 36, 863

13.) Barton, Jacqueline K. **Science** 1986, 233, 727-734

14.) Bailly, Christian; Chaires, Jonathan. **Bioconjugate Chem**. 1998, 9, 513-538.

15.) Hanka *et al*. **J. Antibiotics** 1978, 1211-1217.

16.) Hurley, Laurence; Reynolds, Vincent. **Science** 1984, 226, 843.

17.) Boger, Dale; Mesini, Phillipe. **JACS** 1994, 116, 11335-11348.

18.) Bhuyan, Roy *et al*. **Cancer Research** 1983, 43, 4227-4232.

19.) Li, L. H. *et al*. **Cancer Research** 1982, 42, 999-1004.

20.) Swenson, David *et al*. **Cancer Research** 1982, 42, 2821.

21.) Lin, Chin Hsiung; Hurley, Laurence. **Biochem.** 1990, 29, 9503.

22.) Boger, D. *et al*. **JACS** 1998, 120, 11554-11557.

23.) Boger, D. *et al*. **JOC** 1996, 61, 4894.

24.) Boger, Dale; Yun, Weiya. **JACS** 1994, 116, 5523-5524.

25.) Kopka, Mary *et al*. **Research Article** 1997, 1033-1046.

26.) Kopka, Mary *et al*. **PNAS** 1985, 82, 1376-1380.

27.) Fregeau, N.L. *et al*. **JACS** 1995, 117, 8917-8925.

28.) Hurley, L. **J. Antibiotics** 1977, 30, 349-370.

29.) Petrusek, R. *et al*. **J. Biol. Chem**. 1982, 257, 6207-6216.

30.) Petrusek, Ruby *et al*. **Biochem**. 1981, 20, 1111-1119.

31.) Kopka, Mary *et al*. **Biochem**. 1994, 33, 13593-13610.

32.) Rao, Shashidhar *et al*. **J. Med. Chem**. 1986, 29, 2484-2492.

33.) Kohn, K.; Spears, C. **J. Mol. Bio**. 1970, 51, 551-572.

34.) Marques, Michael *et al*. **Helv. Chim. Acta** 2002, 85, 4485-4517.

35.) Pilch, Daniel *et al*. **Biochem**. 1999, 38, 2143-2151.

36.) Urbach, Adam *et al*. **JACS** 1999, 121, 11621-11629.

37.) Urbach, Adam; Dervan, Peter. **PNAS**, 2001, 98, 4343-4348.

38.) White, S. *et al*. **JACS** 1999, 121, 260-261.

39.) Morris *et al*. **J. of Comp. Chem**. 1998, 19, 1639-1662.

40.) Bursulaya, Badry *et al*. **J. Comp.-Aided Molec. Des**. 2004, 17, 755-763.

41.) Rosenfield, Robin *et al*. **J. Comp.-Aided Molec. Des**. 2003, 17, 525-536.

42.) Osterberg, Fredrik *et al*. **Proteins: Structure, Function, and Genetics** 2002, 46, 34-40.

43.) Sobhani, A.M. *et al*. **J. Molecular Graphics and Modeling** 2006, 25, 459-469

44.) Venkatram, Atigadda *et al*. **J. Heterocyclic Chem**. 2005, 42, 297-301.

45.) Tada, M. *et al*. **Chem. Pharm. Bull**. 1994, 42, 2167-2169.

46.) Logullo, F.; Seitz, A.; Friedman, L. **Org. Synthesis** Vol. 5, 54-59.

47.) Quick, J.; Oterson, R. **Synthesis** 1976, 745-746.

48.) Boyd, M.; Paull, K. **Drug Development Research** 1995, 34, 91-109.

49.) Yang, B.; Buchwald, S. **J. Organometallic Chem**. 1999, 125-146.

50.) Gaertzen, O.; Buchwald, S. **JOC** 2002, 67, 465-475.

51.) Wheeler, A. **Org. and Biol**. 1909, 565-569.

52.) Boger, D.; Turnbull, P. **JOC** 1998, 63, 8004-8011.

53.) Tamura, Y. *et al*. **JOC** 1984, 49, 473-478.

54.) Hattori, T. *et al*. **Tetrahedron: Asymmetry** 1995, 6, 1043-1046.

55.) Diez-Martin, D. *et al*. **Tetrahedron** 1992, 48, 7899-7938.

56.) Hosoya, T. *et al*. **Heterocycles** 1996, 42, 397-414.

57.) Murata, Miki *et al*. **JOC** 2000, 65, 164-168.

58.) Thompson, A. *et al*. **Synthesis** 2005, 4, 547-550.

59.) Ragnarsson, U.; Karlsson, S. **Org. Synthesis** 1973, 53, 203-207.

60.) Reed, P.; Katzenellenbogen, J. **JOC** 1991, 56, 2624-2634.

61.) Geneste, H.; Hesse, M. **Tetrahedron** 1998, 54, 15199-15214.

62.) Serino, C. *et al*. **JOC** 1999, 64, 1160-1165.

63.) Wu, S.; Lee, S.; Beak, P. **JACS** 1996, 118, 715-721.

64.) Tietze, L.; Burkhardt, O. **Liebigs Ann**. 1995, 1153-1157.

65.) Sponholtz, D. *et al*. **J. Chem. Ed**. 1999, 76, 1712-1713.

66.) Lee, S. J. *et al*. **JACS** 2003, 125, 7307-7312.

67.) Adcock *et al*. **Australian Journal of Chem**. 1965, 18, 1365.

68.) Miyano *et al*. **JOC** 1981, 46, 3474.